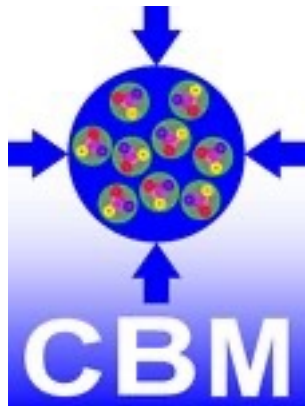


# Probing Quark-Gluon Plasma at the Large Hadron Collider in the Charmonia sector using Machine Learning



**Raghunath Sahoo**

**Indian Institute of Technology Indore, India**



*CBM Juniors' Meeting*

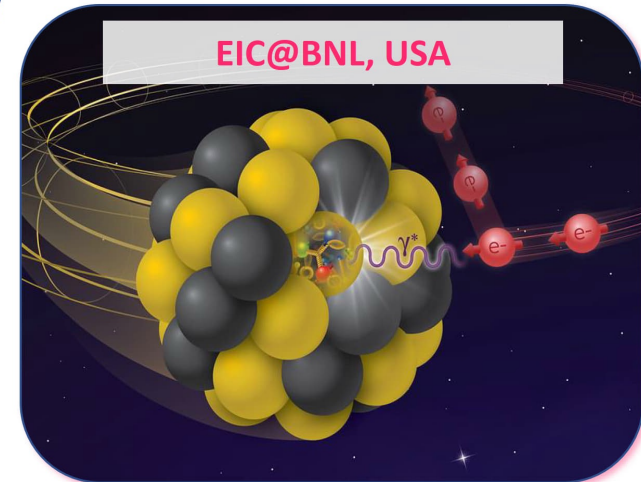


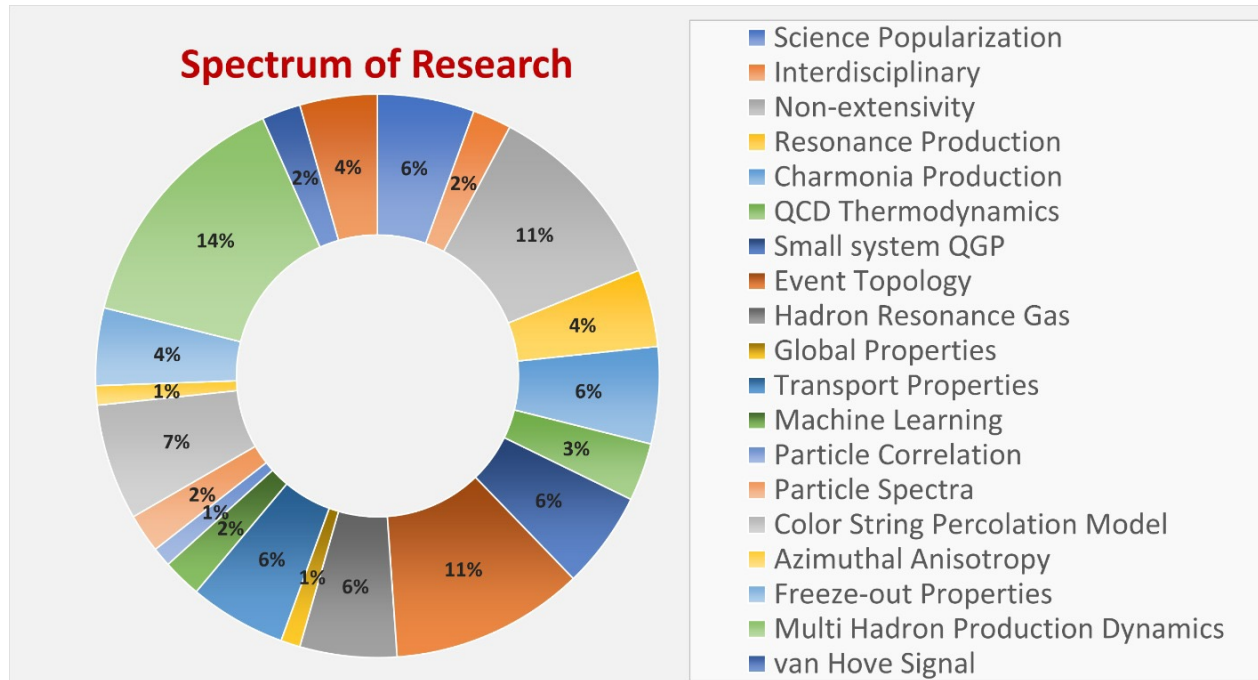
[Raghunath.Sahoo@cern.ch](mailto:Raghunath.Sahoo@cern.ch), [raghunath@iiti.ac.in](mailto:raghunath@iiti.ac.in)

# Experimental High-Energy Physics Group

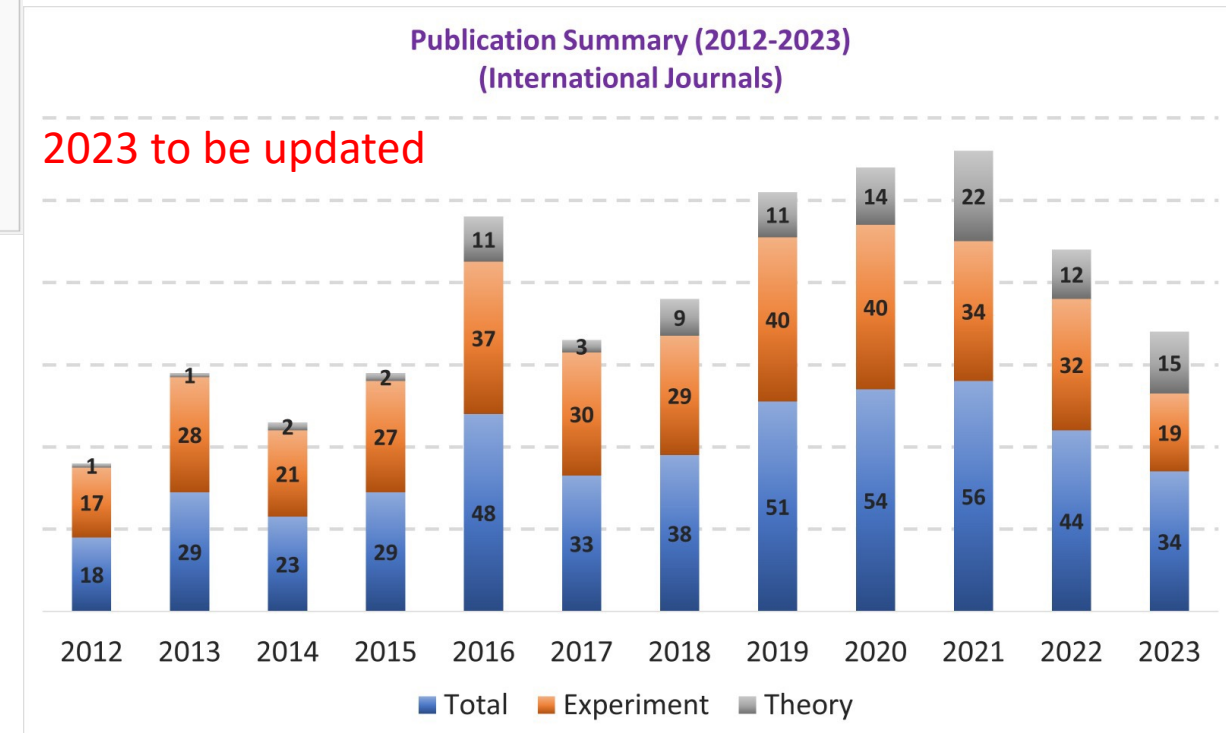


Contact: Prof. Raghunath Sahoo, FlntP  
e-mail: [raghunath@iiti.ac.in](mailto:raghunath@iiti.ac.in)  
Web: [www.iiti.ac.in/~raghunath](http://www.iiti.ac.in/~raghunath)





Details: [www.iiti.ac.in/~raghunath](http://www.iiti.ac.in/~raghunath)





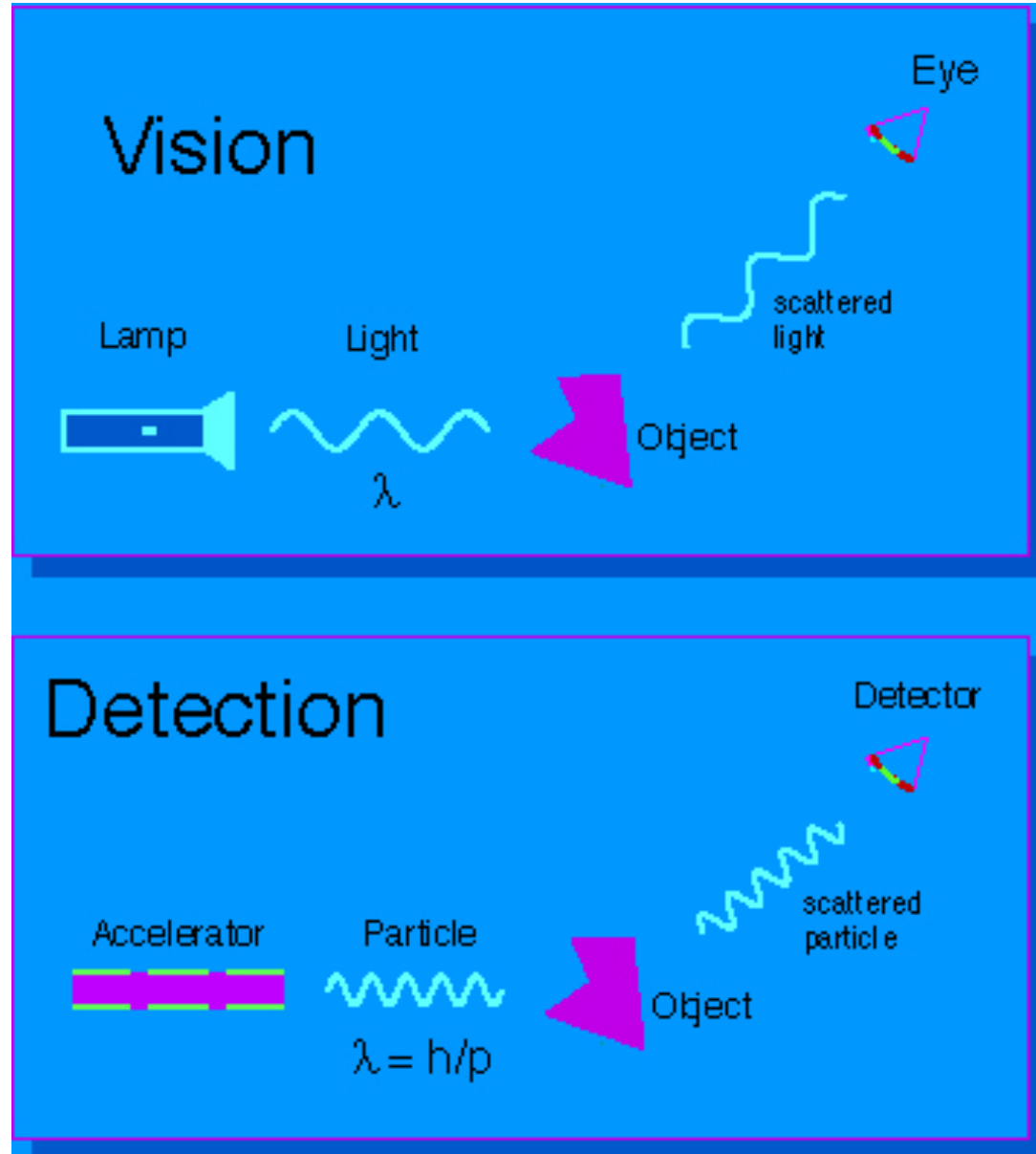
# The Right Light to Look Inside

Vision works by  
scattering of  
'visible' light

$$\lambda = 400\text{-}700 \text{ nm}$$

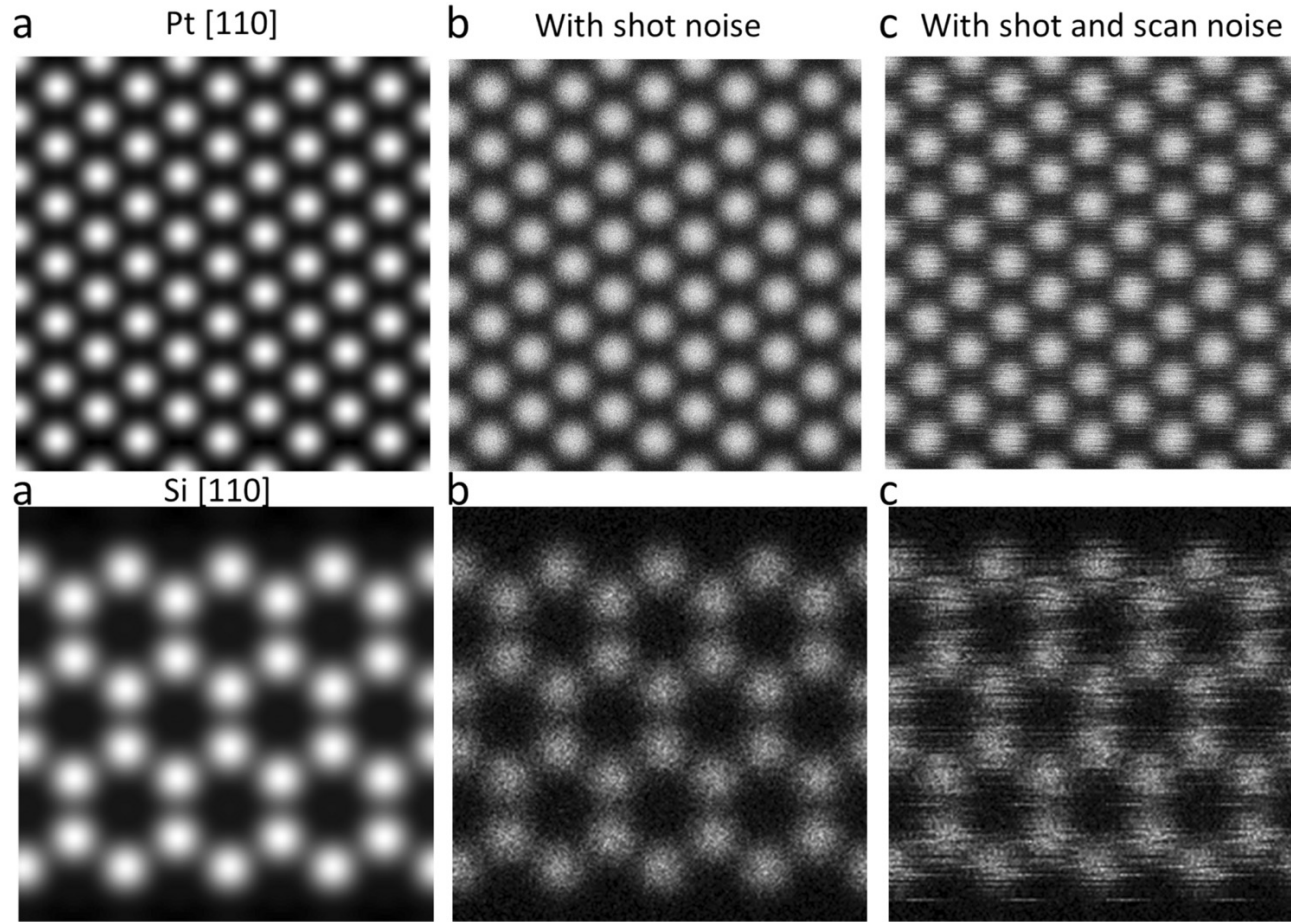
"Vision" of even  
smaller structures via  
scattering of particles

$$\lambda = h/p$$

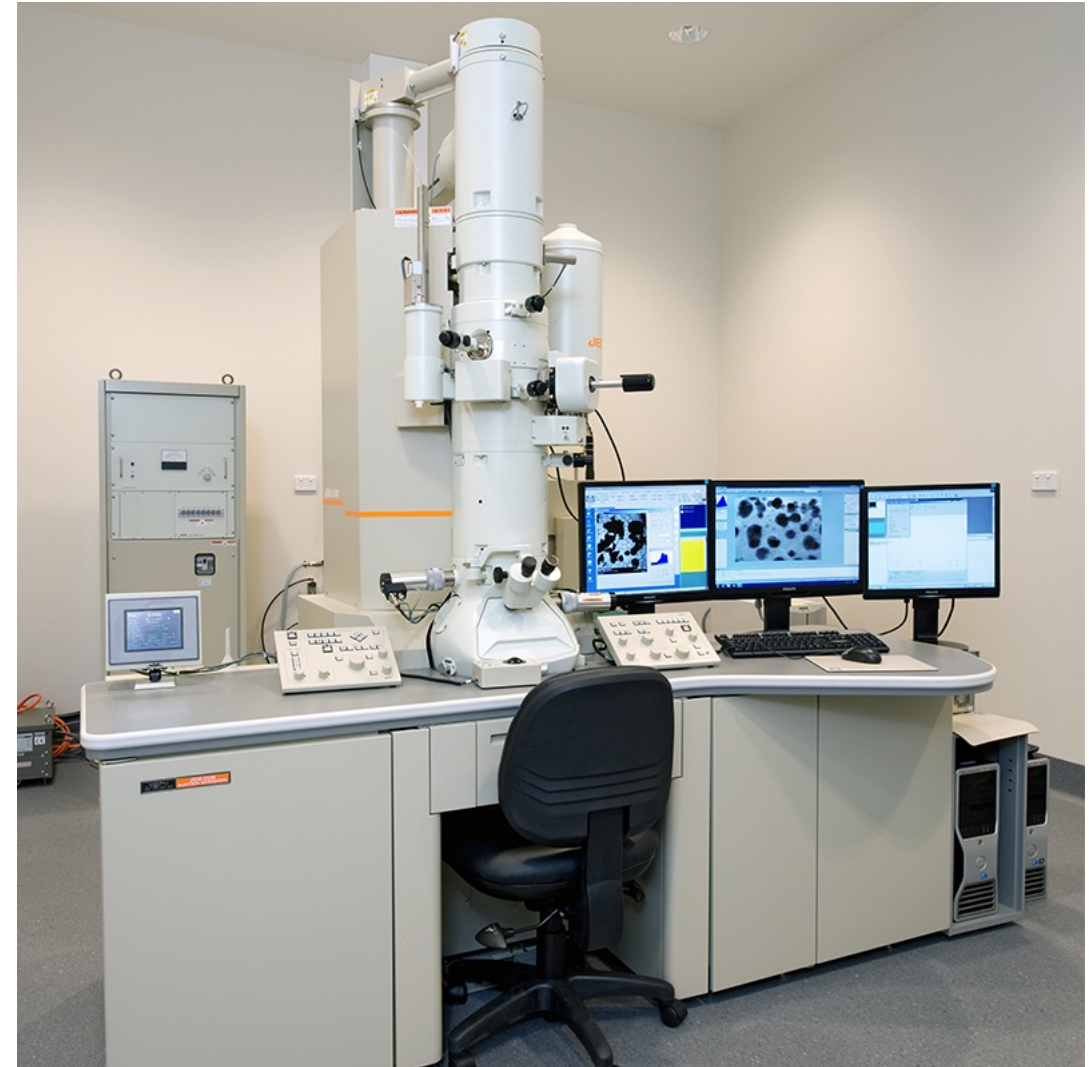




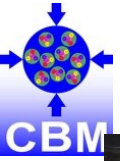
# Seeing the Atoms



(for demonstration purpose)



Transmission Electron Microscope



# A Journey from Electrons to Quarks



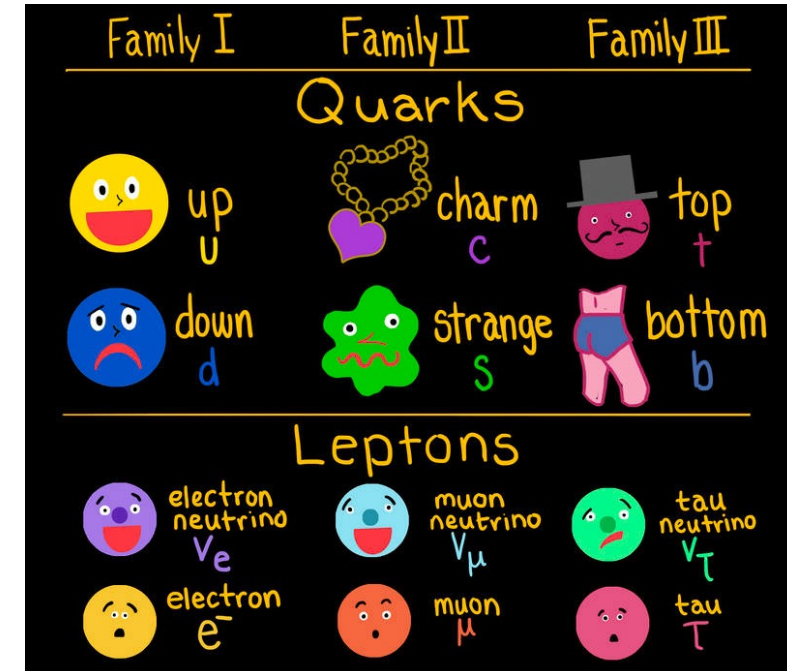
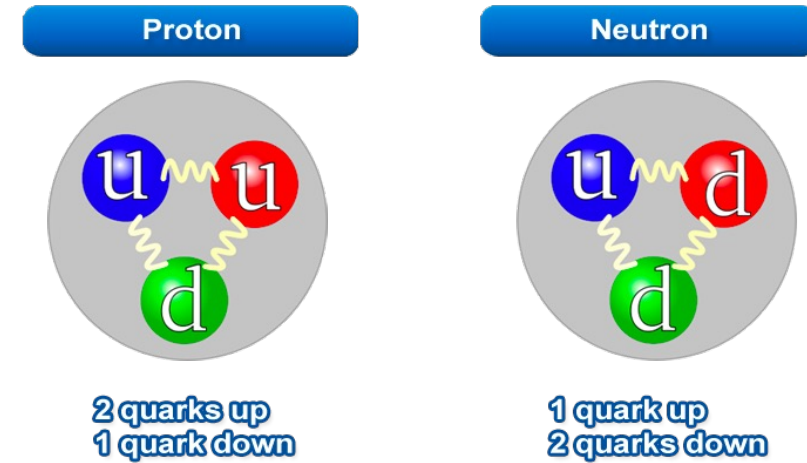
SLAC: Stanford Linear Accelerator Center (3.2 Kms)

Electron-positron energy  $\sim 50$  GeV

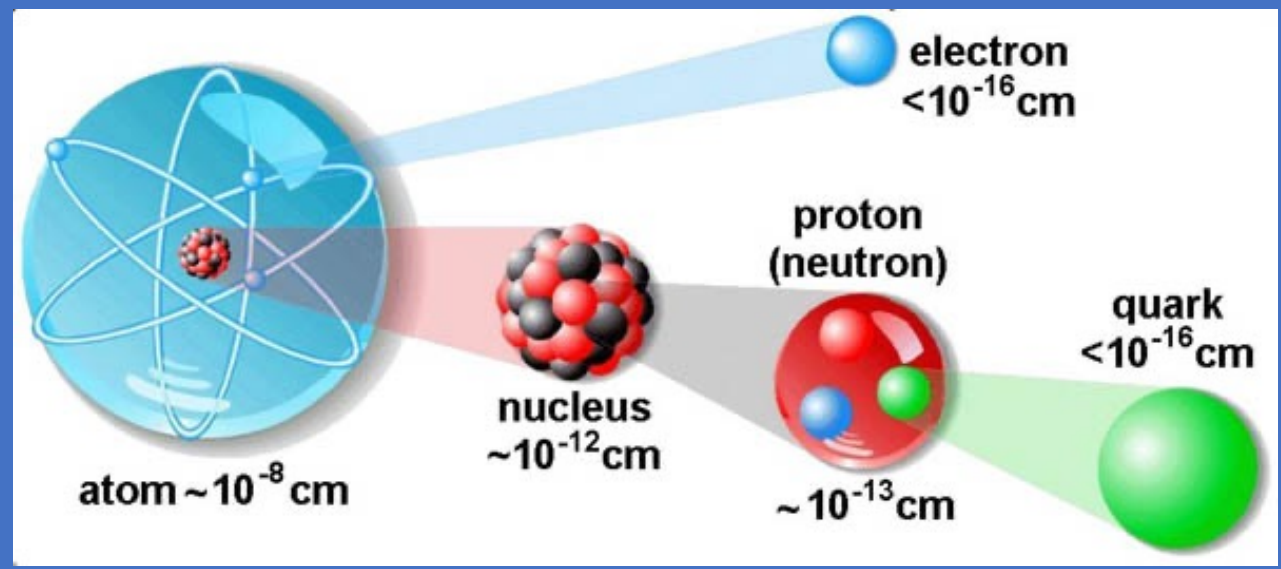
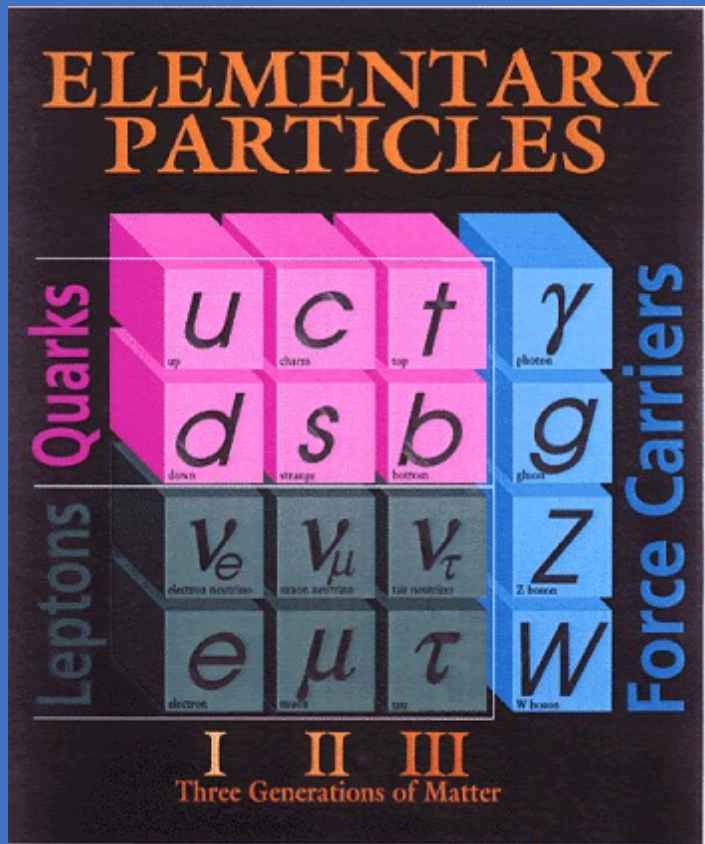
$$\lambda = h / p : \propto 1/E$$

This universal formula of de Broglie helps in deciding the energy of the probe.

Proton charge radius  $\sim 0.843$  fermi.  
(1 fermi =  $10^{-15}$  meter)

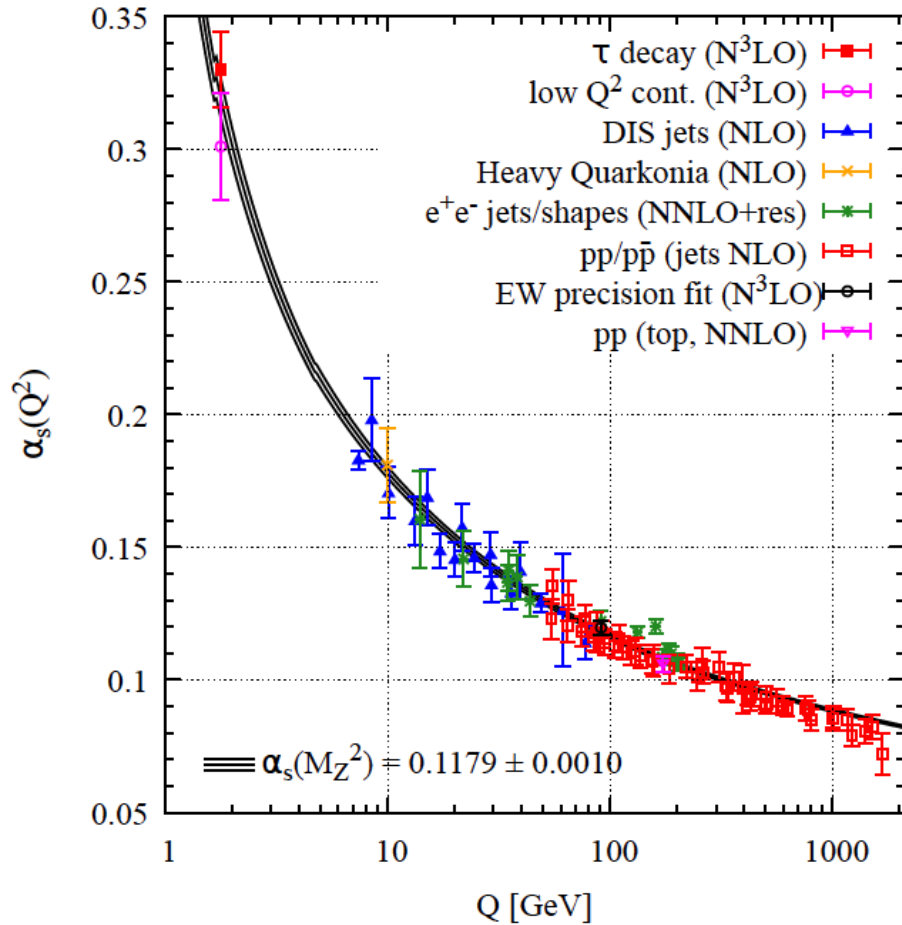








# Can we find free quarks?



To the leading order:

$$\alpha_s(Q^2) = \frac{4\pi}{(33-2n_f)\ln(Q^2/\Lambda^2)}$$

$n_f$  is the no. of quark flavors, with a mass less than  $Q/2$ ,  
 $\Lambda$  is the QCD scale parameter, obtained experimentally  
 $\sim 200$  MeV

☞ Coupling becomes weaker as the momentum transfer increases,

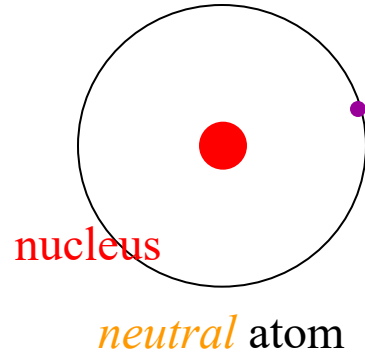
Or as we go smaller in the length-scale → small distance, partons move freely (asymptotic freedom of QCD)

☞ As the inter-quark distance increases, strong coupling grows faster making the quarks confined inside the cage of the hadrons → Quark confinement

Asymptotic freedom and infrared slavery is an inbuilt property of QCD (Strong interaction) →  
No free quarks in nature!

# Analogies and differences between QED and QCD

to study structure of an atom...

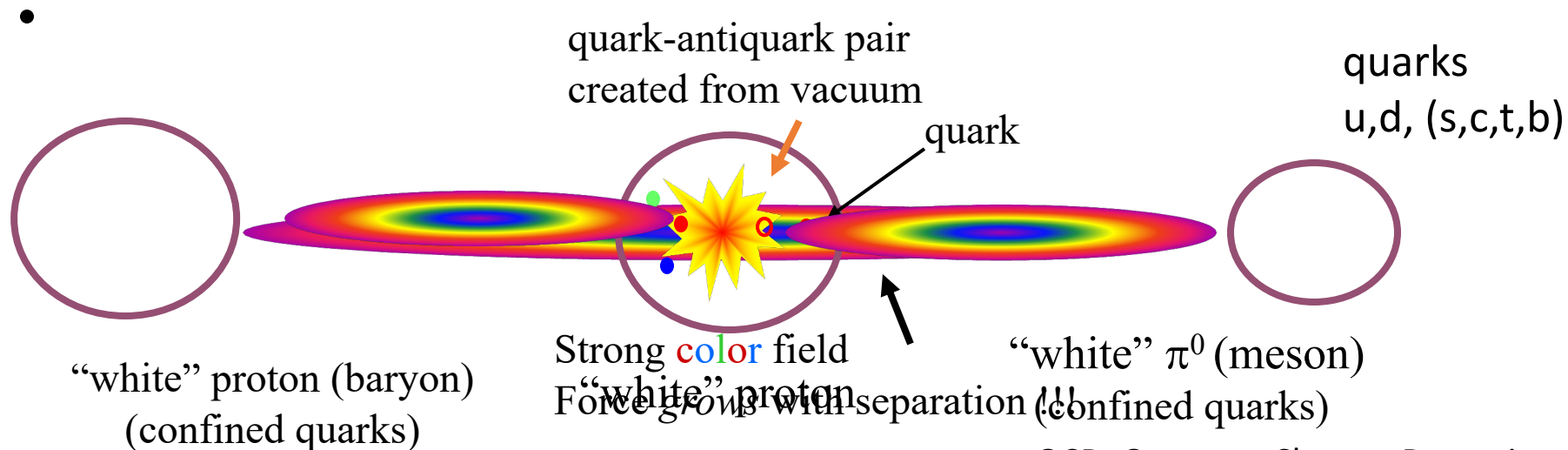


electron

...separate constituents

QED Quantum Electro Dynamics

**Confinement:** fundamental & crucial (but *not* understood!) feature of strong force  
- colored objects (quarks) have  $\infty$  energy in normal vacuum



QCD: Quantum Chromo Dynamics

# Can we find free quarks?

1973: Asymptotic freedom

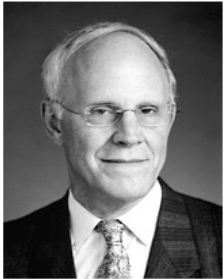
D.J. Gross, F. Wilczek, H.D. Politzer

1975: Asymptotic QCD & deconfinement:

N. Cabibbo and G. Parisi;

J. Collins and M. Perry

2004: Nobel Prize



David J. Gross



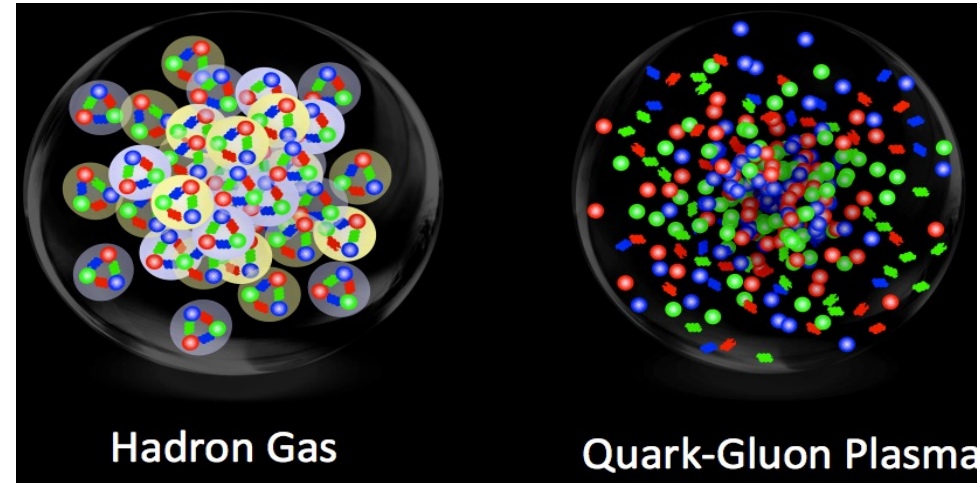
H. David Politzer



Frank Wilczek

**QCD predicts that** normal nuclear matter undergoes a phase transition to quark-gluon plasma (QGP) under extreme temperatures and energy densities.

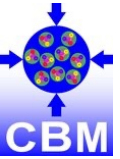
Quark Gluon Plasma



**Quark Gluon Plasma (QGP):** (locally) thermally equilibrated state of matter in which quarks and gluons are deconfined from hadrons, so that color degrees of freedom become manifest over nuclear, rather than merely nucleonic, volumes.

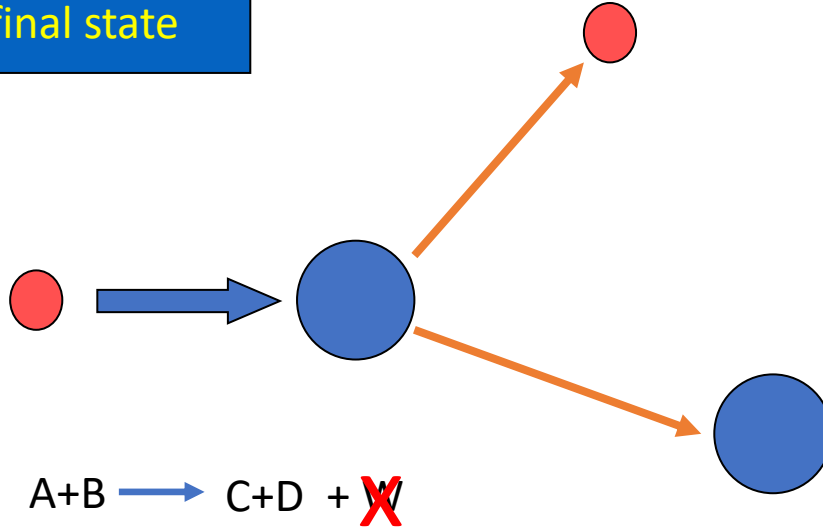
A journey to the beginning of the universe....





# Collisions: Classical vs Relativistic

Two-particle final state

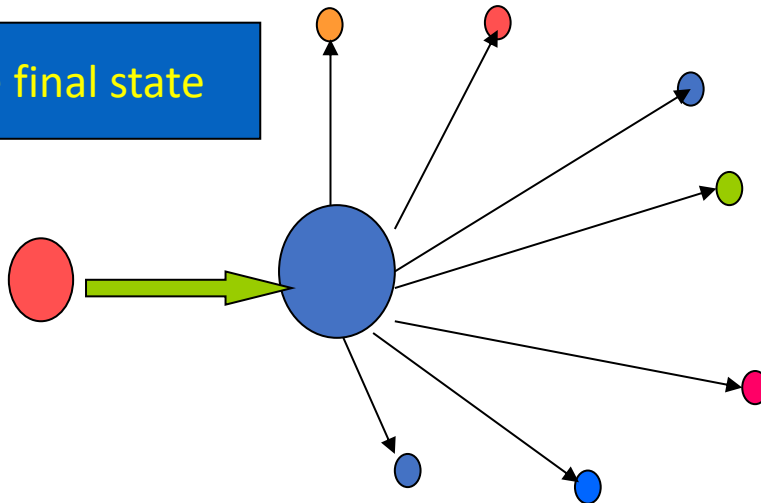


Classical collisions:

- a) Mass is conserved:  $m_A + m_B = m_C + m_D$
- b) Momentum is conserved:  $p_A + p_B = p_C + p_D$
- c) Kinetic energy may(not) be conserved

- i. **Sticky**- K.E. decreases:  $T_A + T_B > T_C + T_D$
- ii. **Explosive**- K.E. increases:  $T_A + T_B < T_C + T_D$
- iii. **Elastic**- K.E. is conserved:  $T_A + T_B = T_C + T_D$

Multi-particle final state



Relativistic collisions:

- a) Energy is conserved:  $E_A + E_B = E_C + E_D$
- b) Momentum is conserved:  $p_A + p_B = p_C + p_D$
- c) Kinetic energy may(not) be conserved

Mass-energy conversions in “explosive collisions” !

If mass is conserved: collision is elastic.

# Why Collider Experiments?



The severity of damage is less.

Energy available for particle production:

In laboratory frame (fixed target):

$$E_{cm} = \sqrt{2m_t E_{beam}}$$

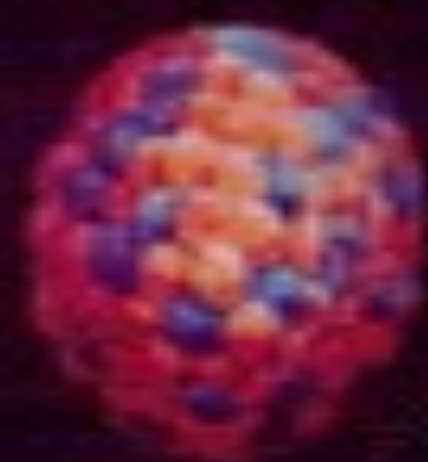
In CM frame (collider):

$$E_{cm} = (2E_{beam})$$



The damage is much higher !



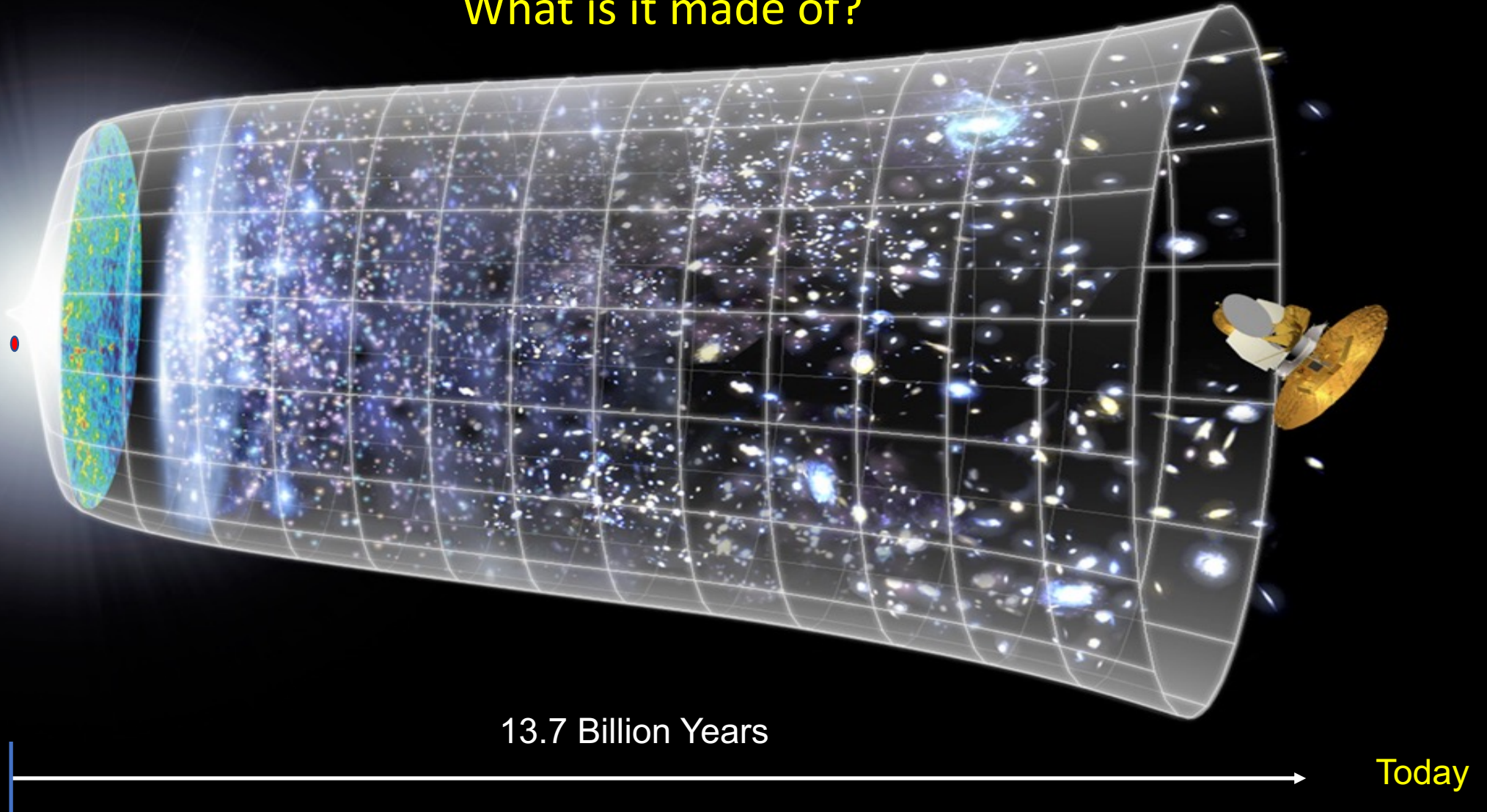




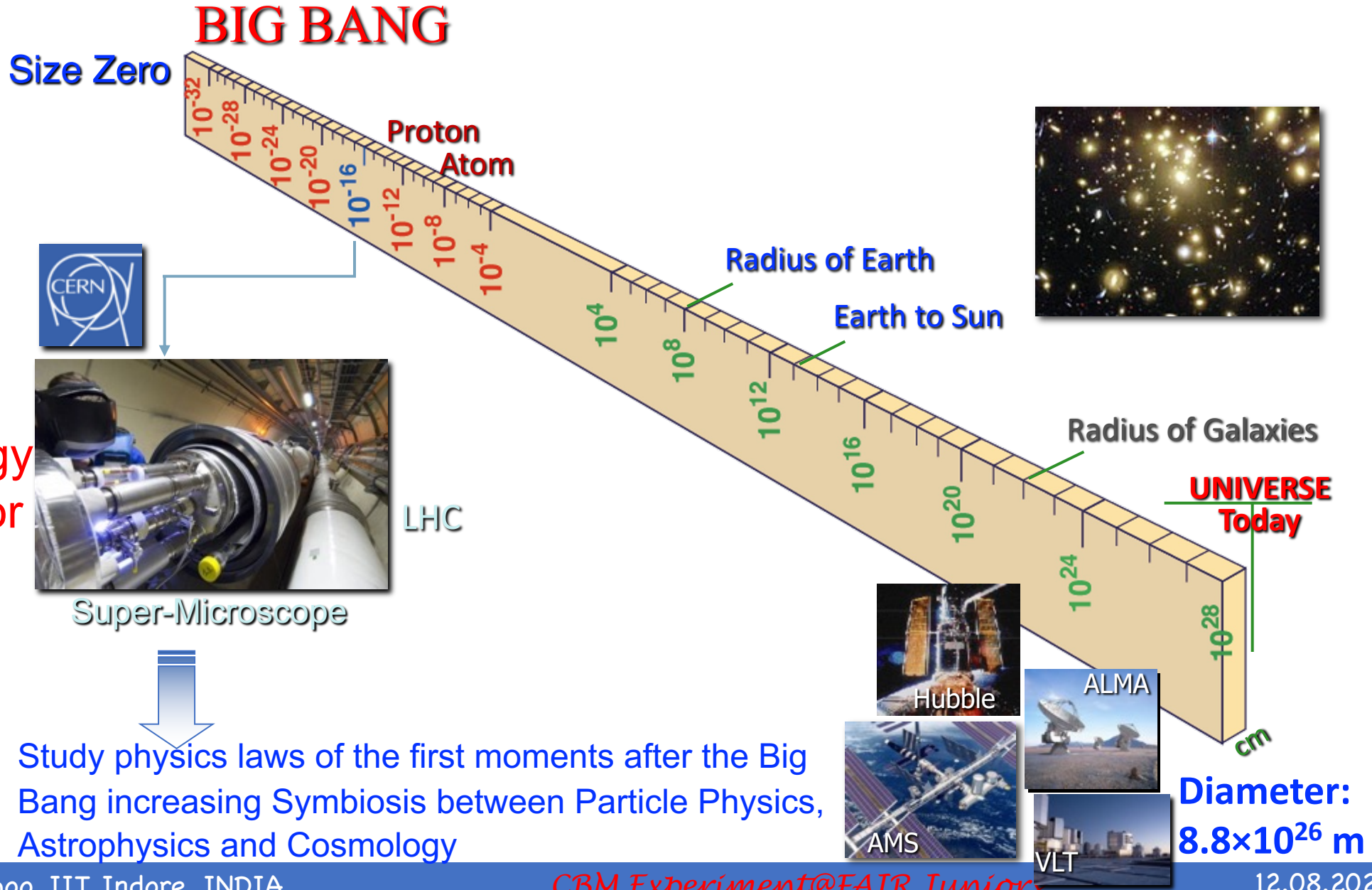
# Our Universe ..... How did it start?

## What is it made of?

**Big Bang**



# Accessing Big Bang conditions

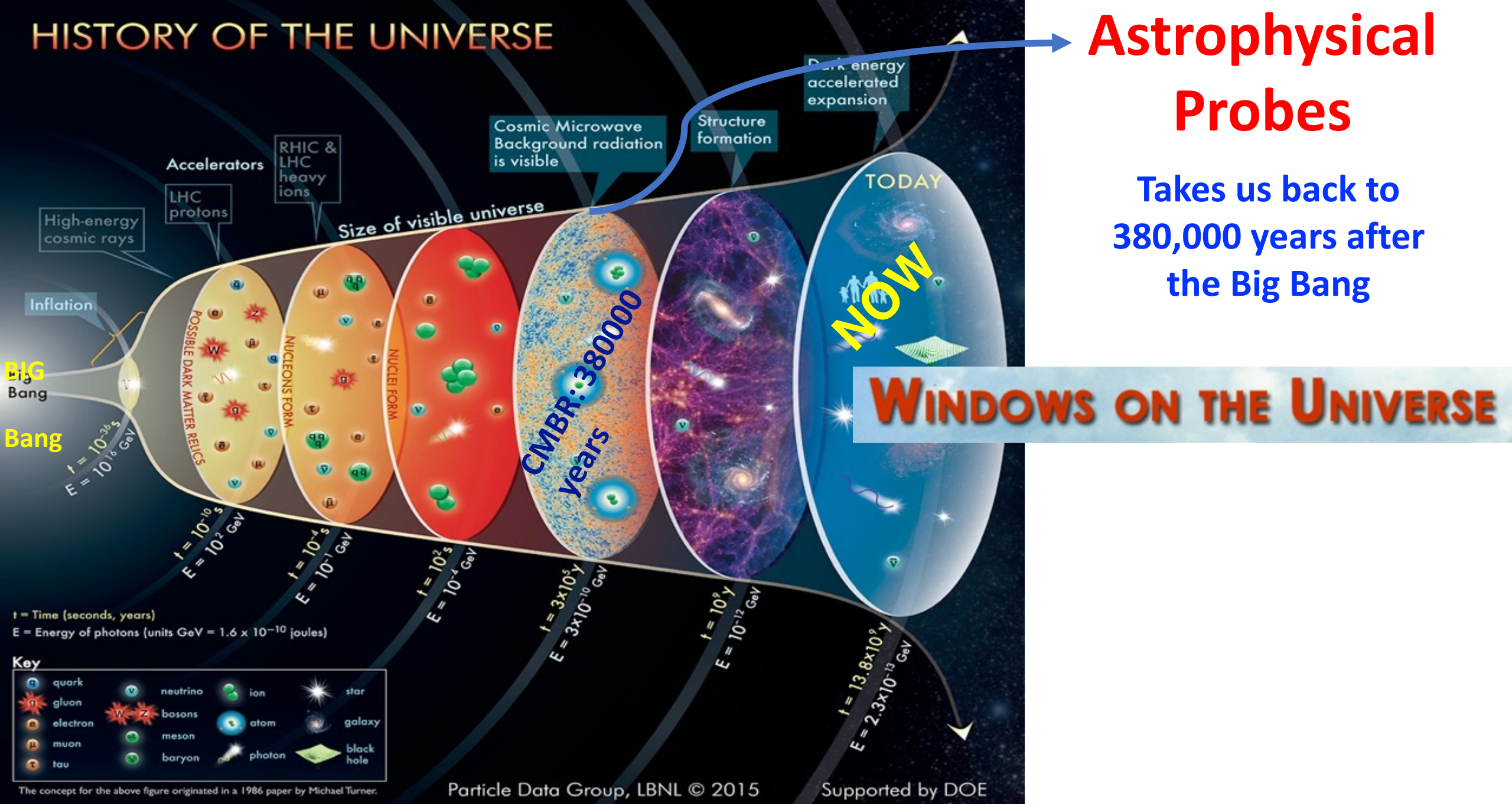




# HISTORY OF THE UNIVERSE

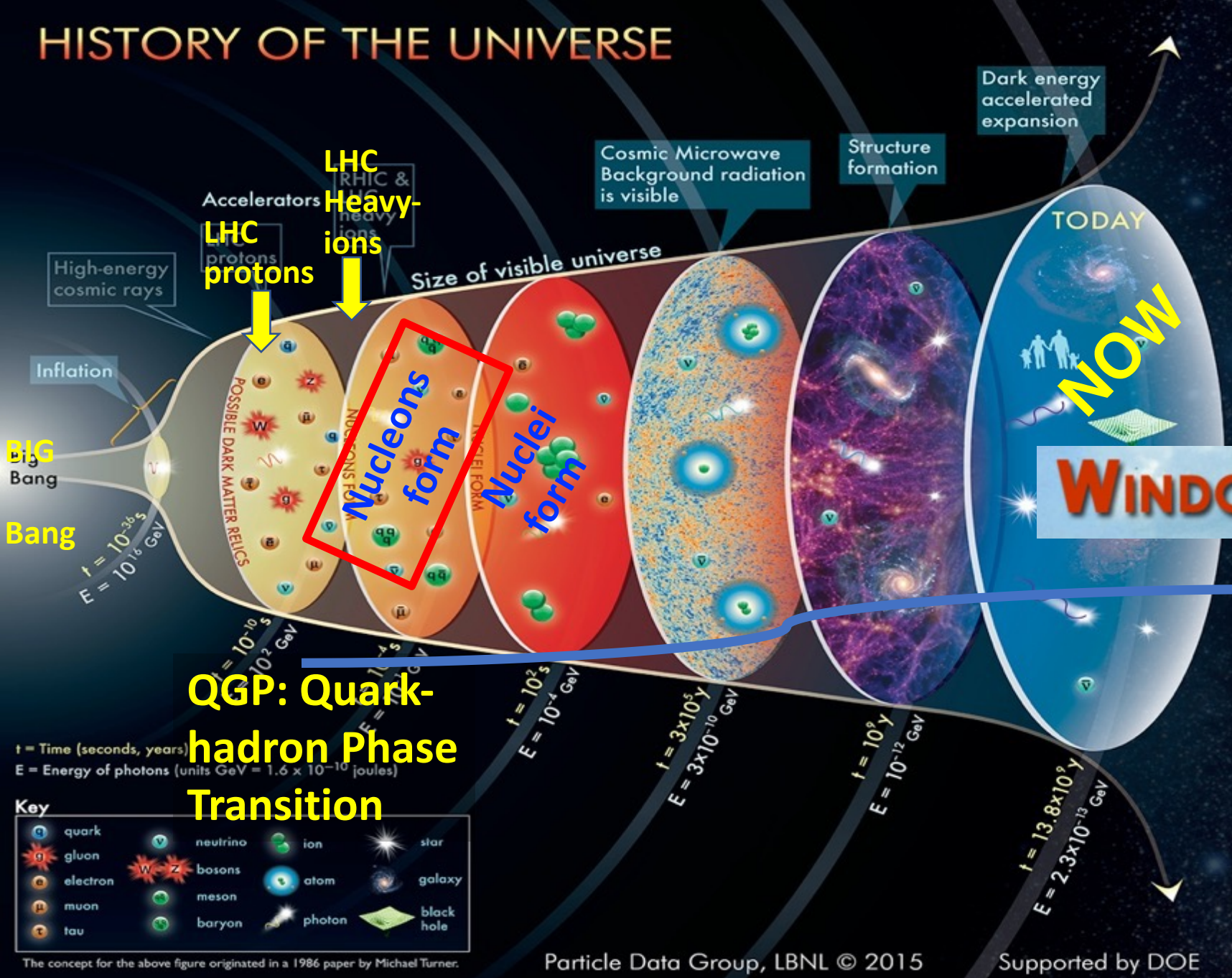
## Astrophysical Probes

Takes us back to  
380,000 years after  
the Big Bang





# HISTORY OF THE UNIVERSE



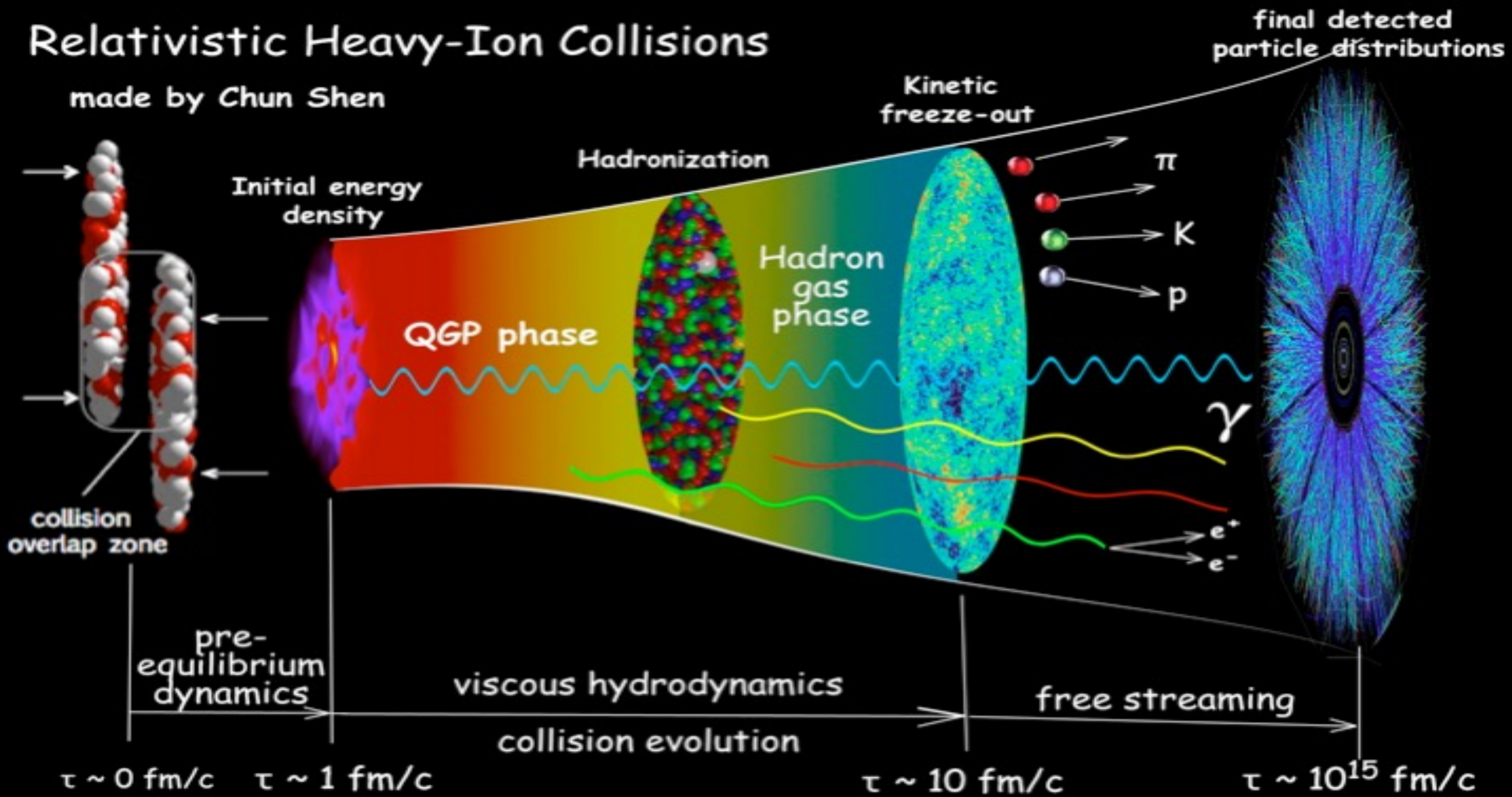
## WINDOWS ON THE UNIVERSE

### Accelerators (LHC)

Takes us back to within  
few Microseconds of  
the Big Bang

# Relativistic Heavy-Ion Collisions

made by Chun Shen





# How much high is high-energy?

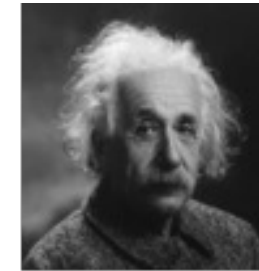
## High energies allow us:

To look deeper into Nature ( $E \propto 1/\text{size}$ ),  
("powerful microscopes")



de Broglie

To discover new particles with  
high(er) mass ( $E = mc^2$ )



Einstein

To study the early universe ( $E = kT$ )



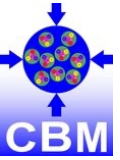
Boltzmann

**Lesson:** To probe the subatomic universe, we need very high energies, which could produce many particles in the final state with very high temperature system.

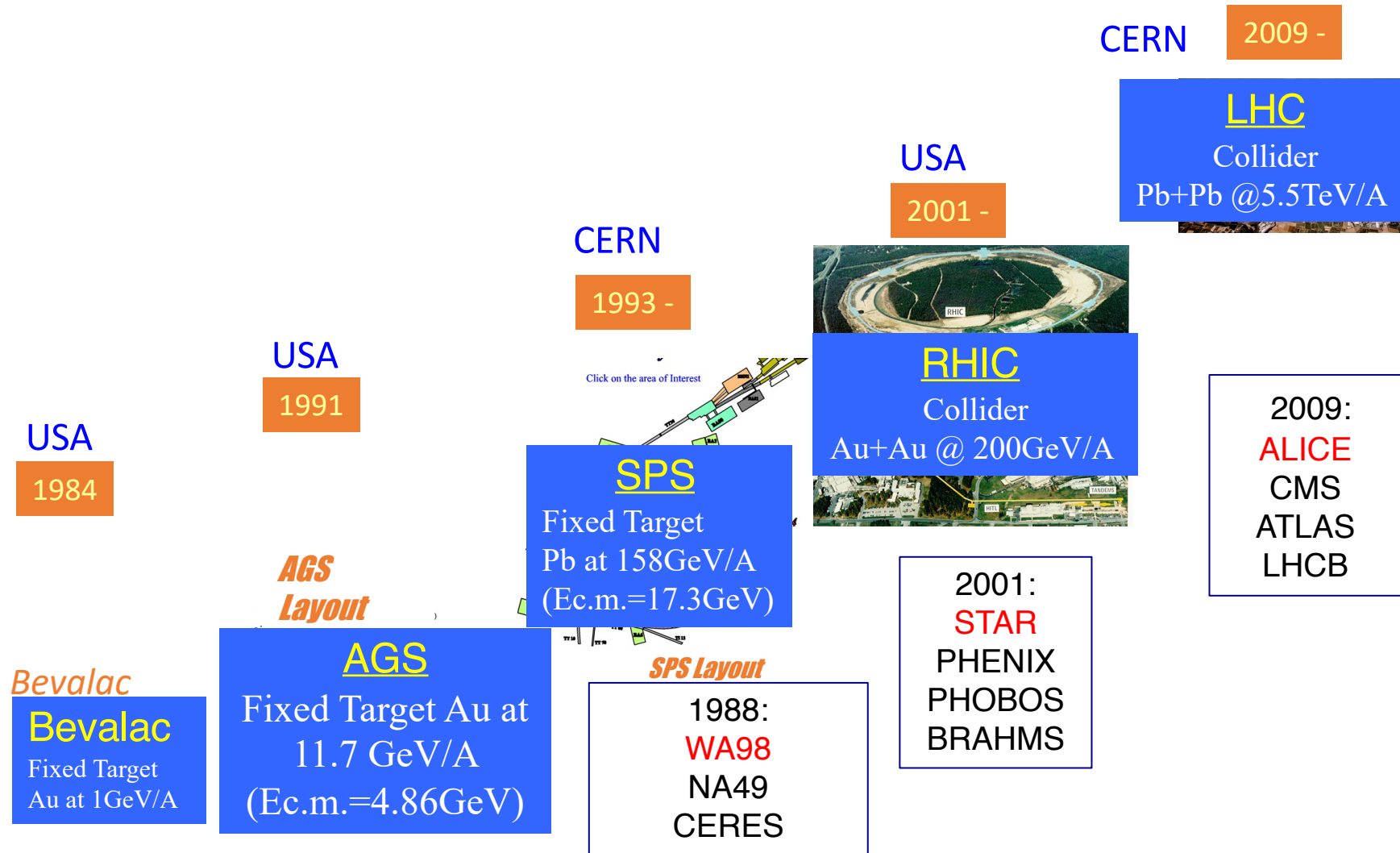
How do we do that?







# Accelerator facilities for heavy-ions





Geneva, Switzerland





# CERN









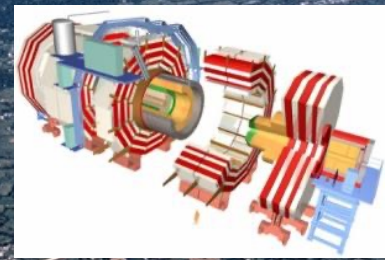
27 km circumference  
~ 100 m underground  
Design Energy:  
14 TeV (pp), 5.5 TeV (Pb-Pb)



# World's Most Powerful Accelerator: The Large Hadron Collider

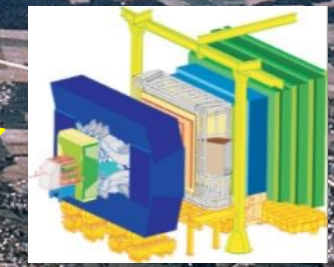
Lake Geneva

CMS

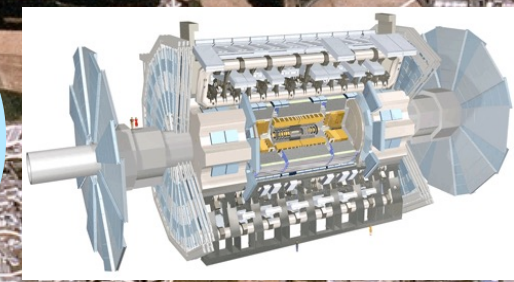


Studying Heavy Ions

LHCb



ATLAS



ALICE



Jura mountains



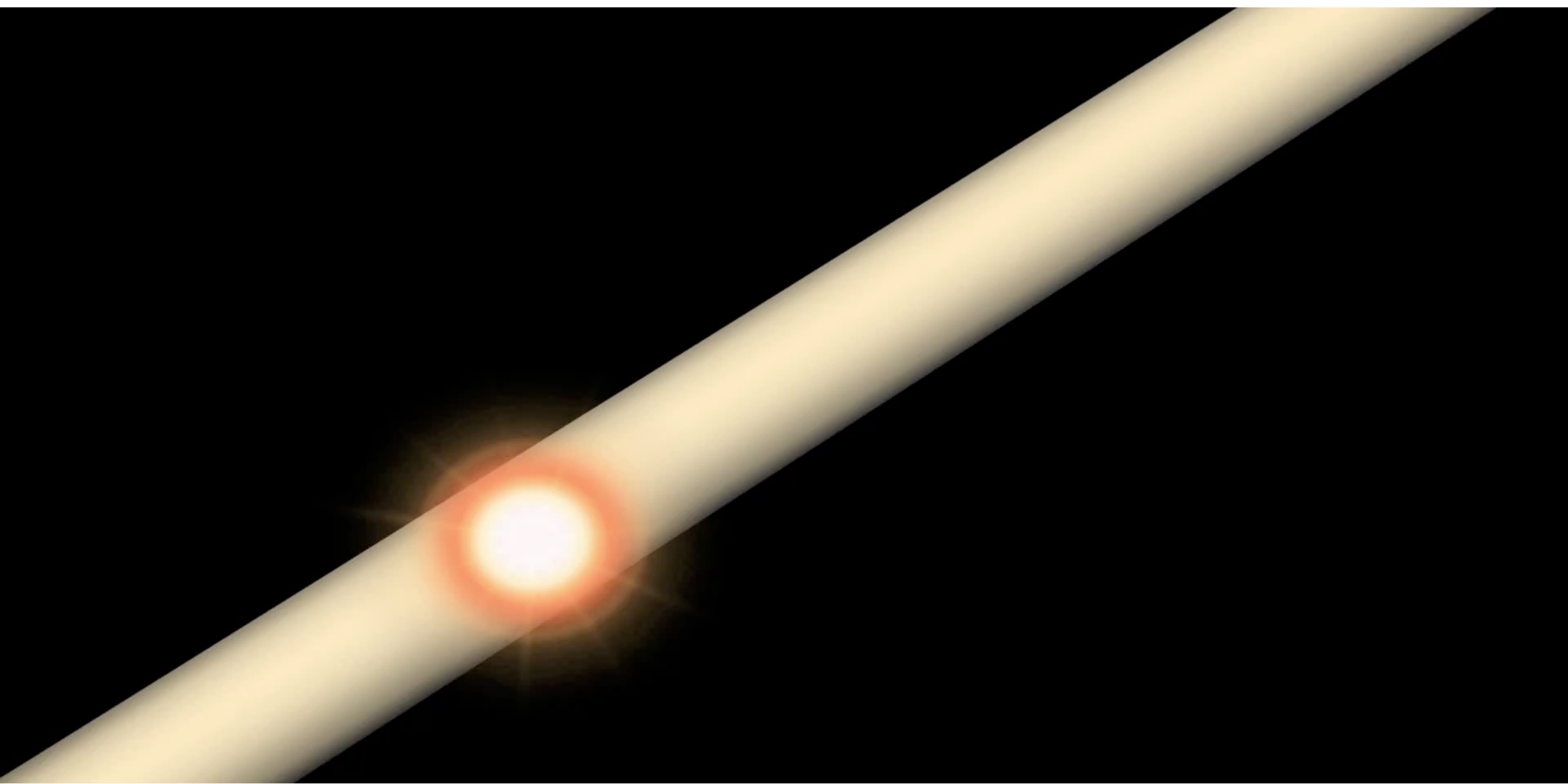
# Large Hadron Collider (LHC)

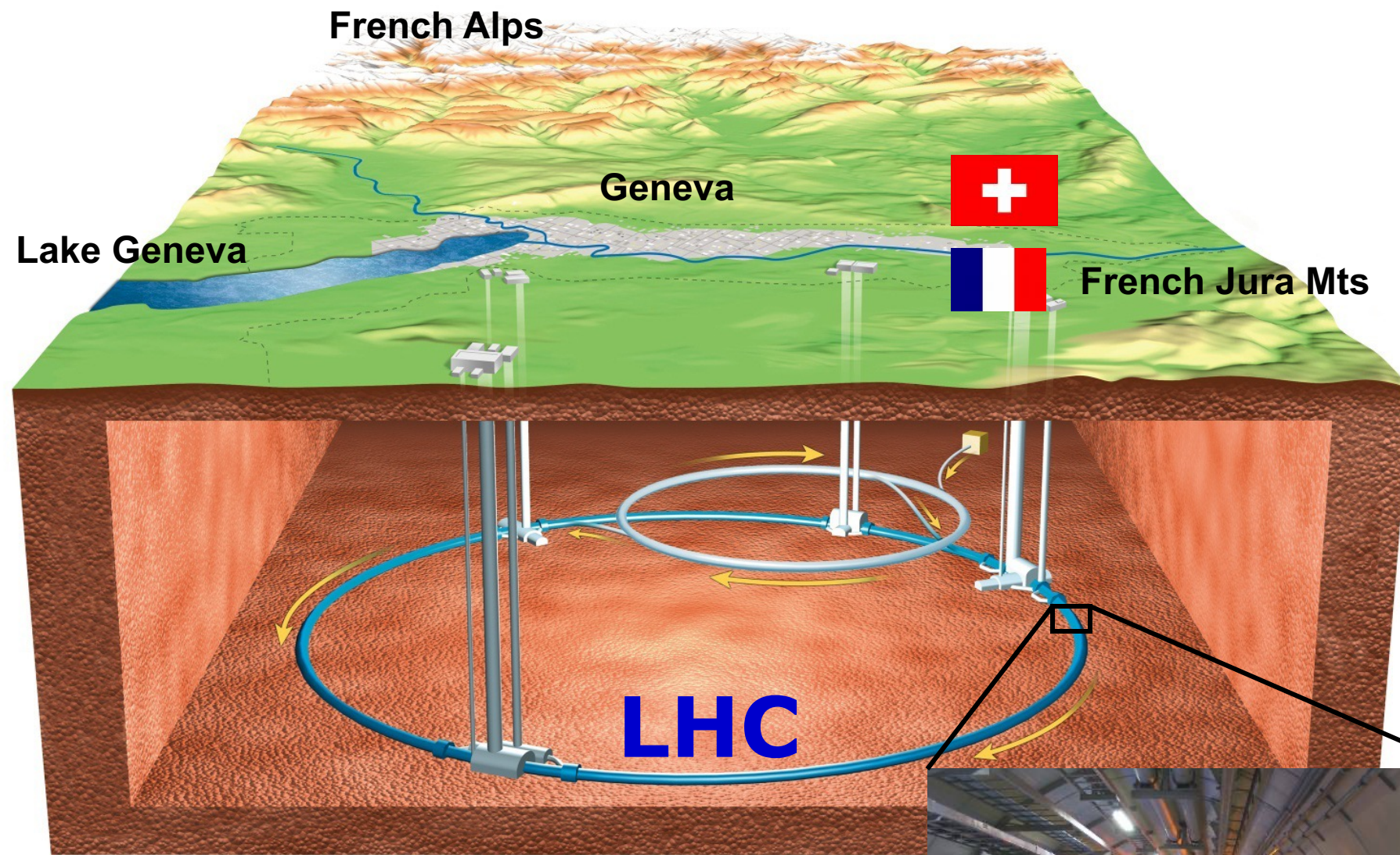


## 27km tunnel:

- 50-150m below ground
- Two beams circulating in opposite directions
- Total of 9300 magnets: beams controlled by 1800 superconducting magnets (up to 8T)







- Electric waves speed particles up
- Magnets bend them in a circle



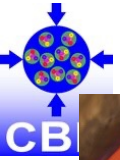




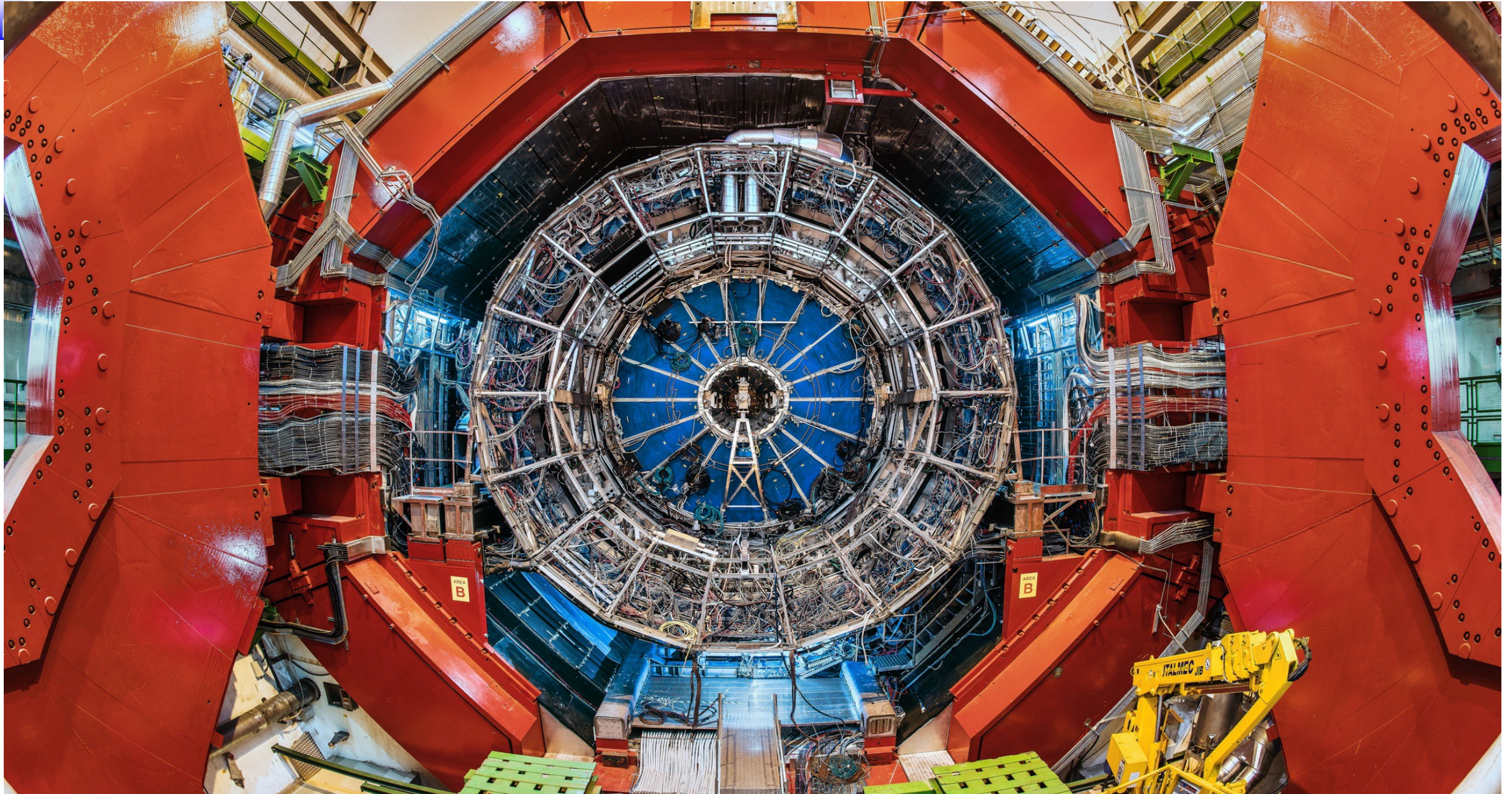
**CMS**

Concentrate energy to create  
new particles (Higgs, SUSY)





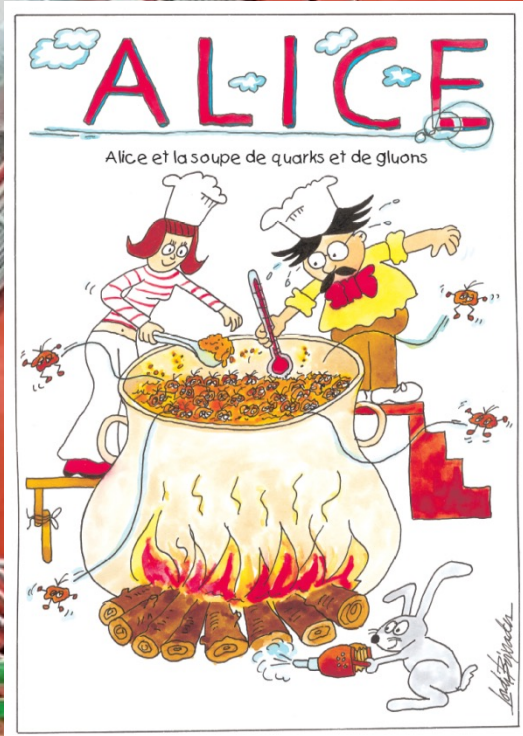
# ALICE at Point-2 of the LHC





# ALICE

## Dedicated experiment to study QGP Matter



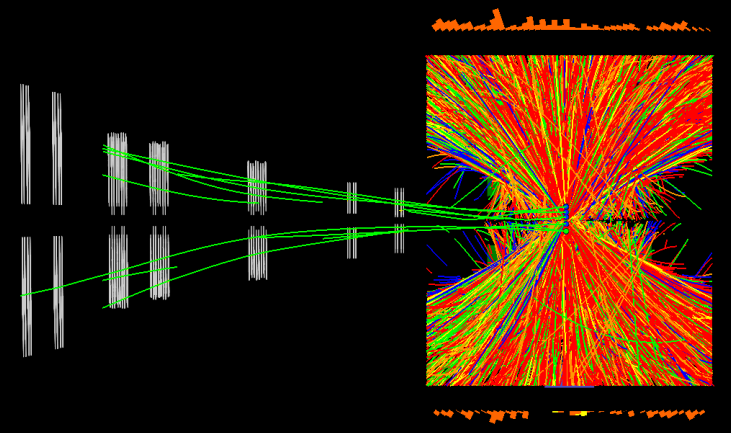
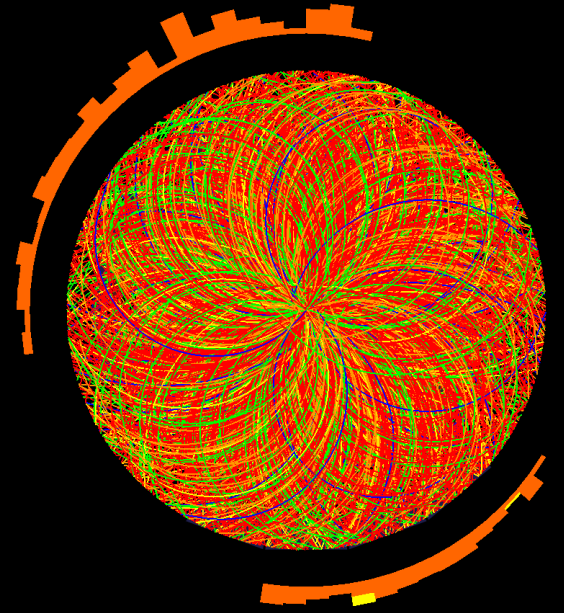
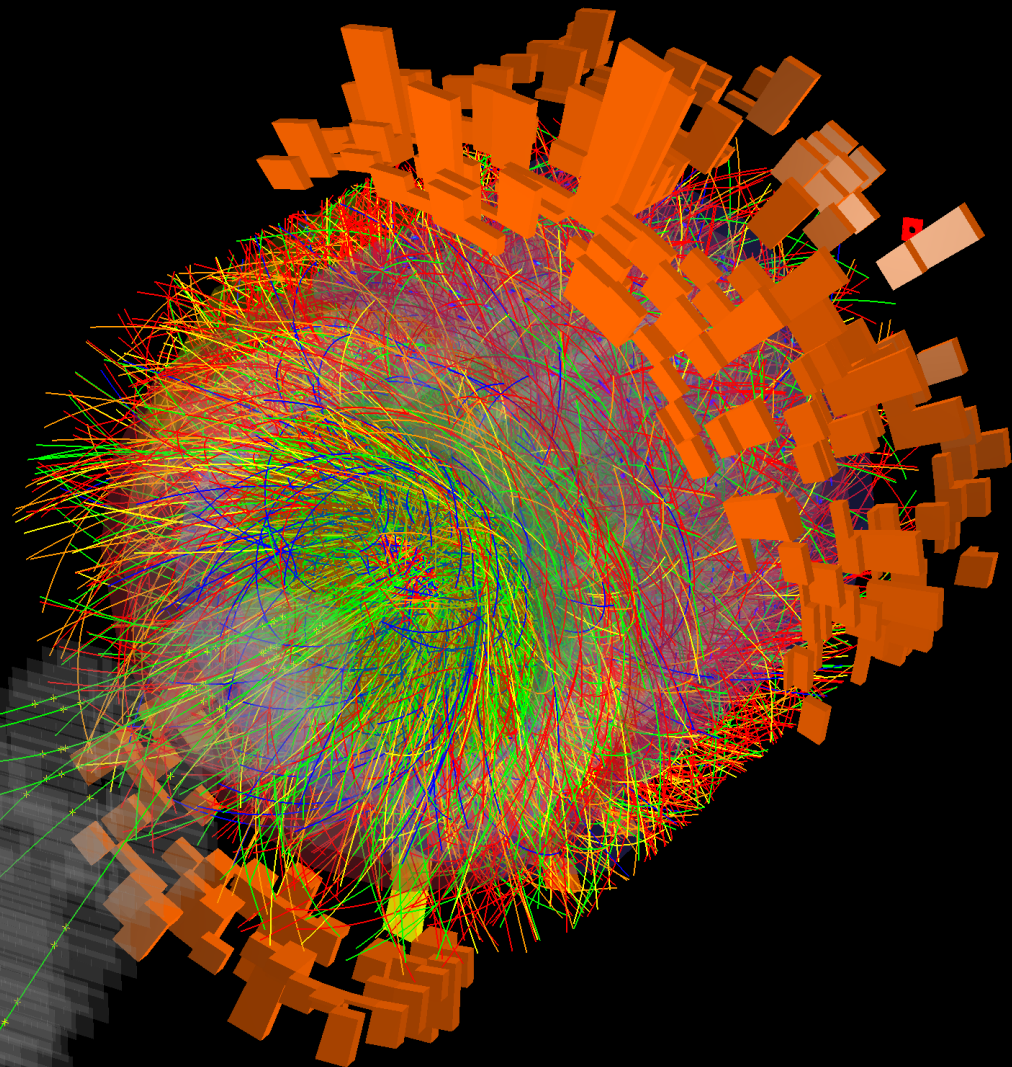
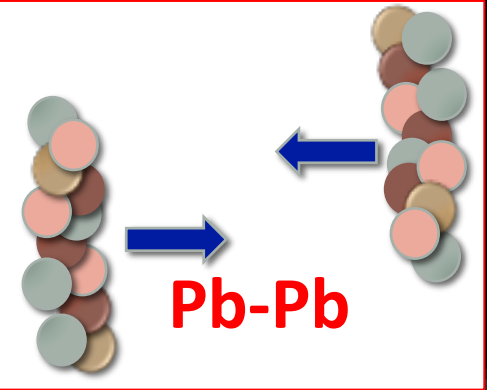
**Size: 16 x 26 meters**

**Weight: 10,000 tonnes**





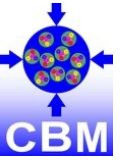
ALICE



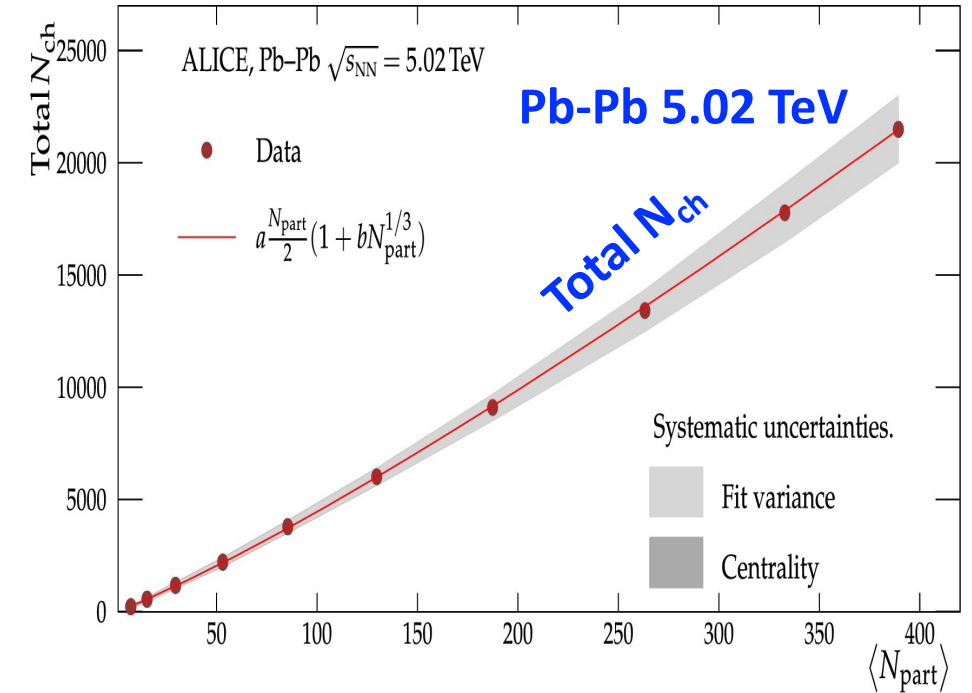
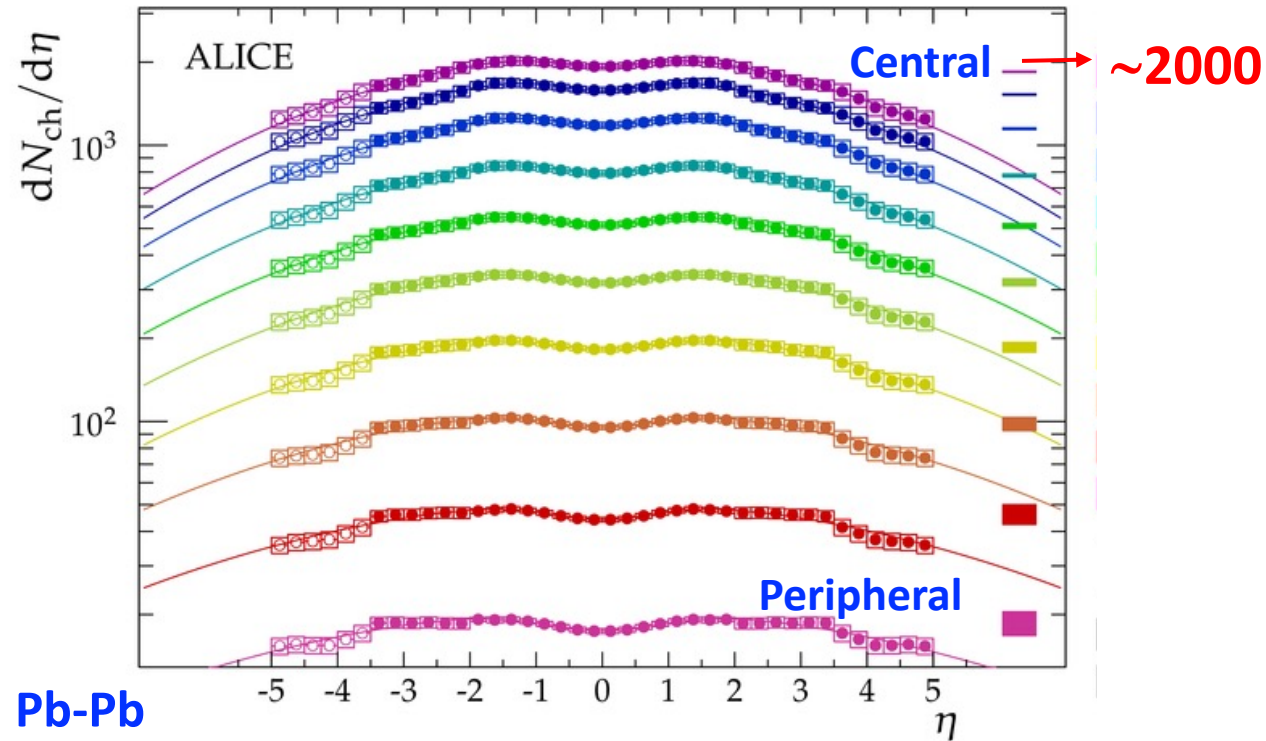
Run:244918  
Timestamp:2015-11-25 11:25:36(UTC)  
System: Pb-Pb  
Energy: 5.02 TeV







# Charged particle multiplicity



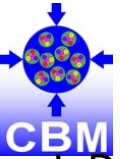
Number of charged particles in one collision:

- Central collisions:  $21400 \pm 1300$
- Peripheral collisions:  $230 \pm 38$

Phys.Lett. B 772 (2017) 567577  
Phys. Rev. Lett. 116 (2016) 222302

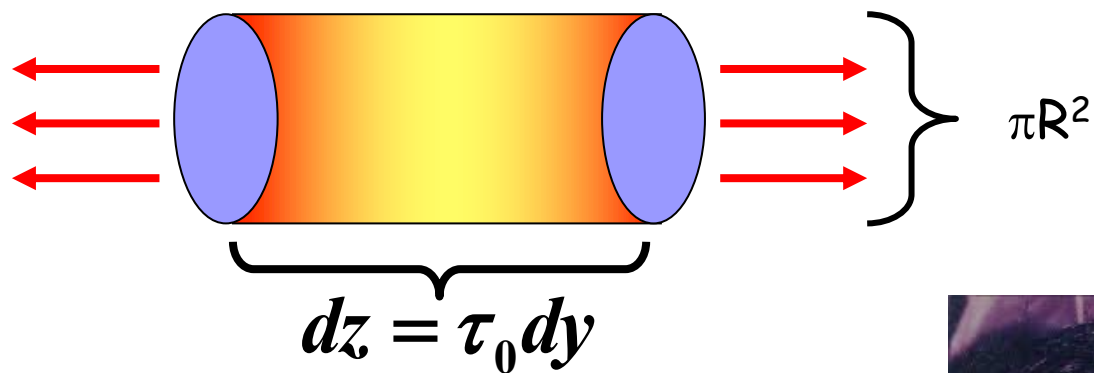
**VERY LARGE NUMBER OF PRODUCED PARTICLES**





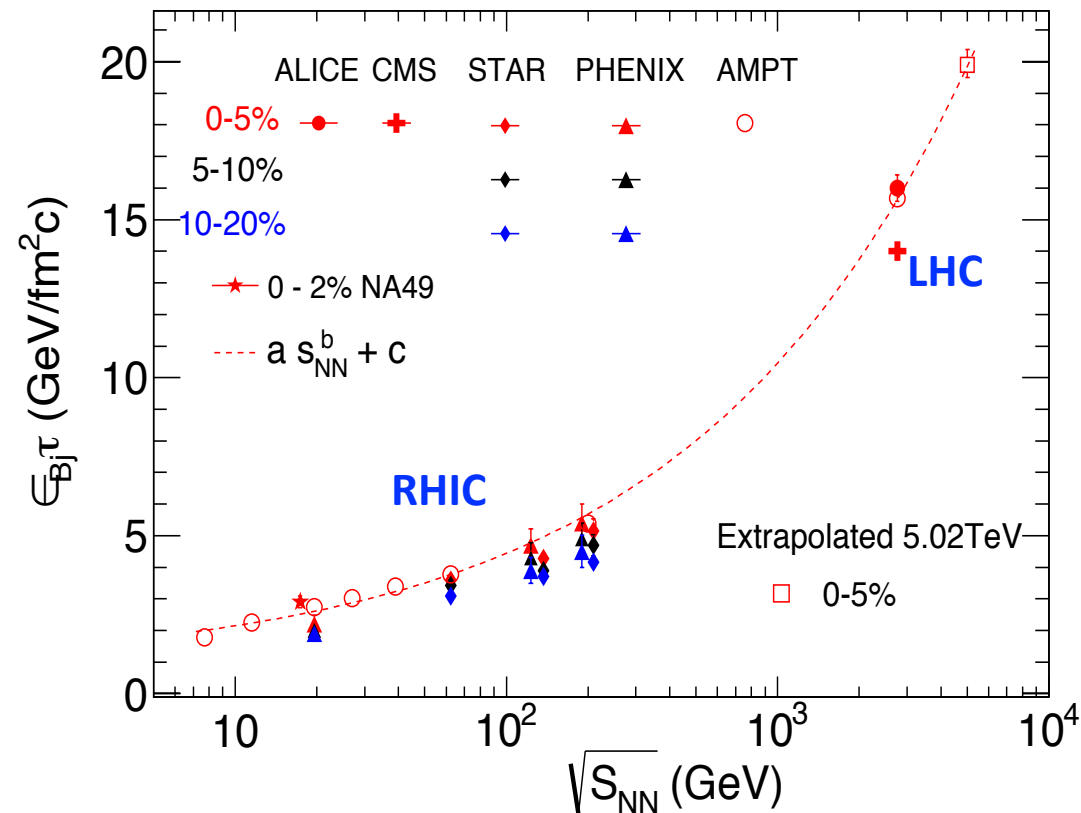
# Particle density & Energy density

J. D. Bjorken, Phys. Rev. D 27, 140 (1983).



$$\varepsilon_{Bj}(\tau) = \frac{1}{\pi R^2 \tau} \frac{dE_T}{dy}$$

$$\approx \frac{1}{\pi R^2 \tau} \langle m_T \rangle \frac{3}{2} \frac{dN_{ch}}{d\eta}$$

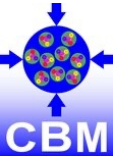


**$\varepsilon \cdot \tau \sim 16 \text{ GeV/fm}^2 c$**

**LARGEST ENERGY DENSITIES  
EVER ACHIEVED ....**

S. Basu et al. PRC 93 (2016) 064902

R. Sahoo et al. Adv. in HEP, Vol. 2015

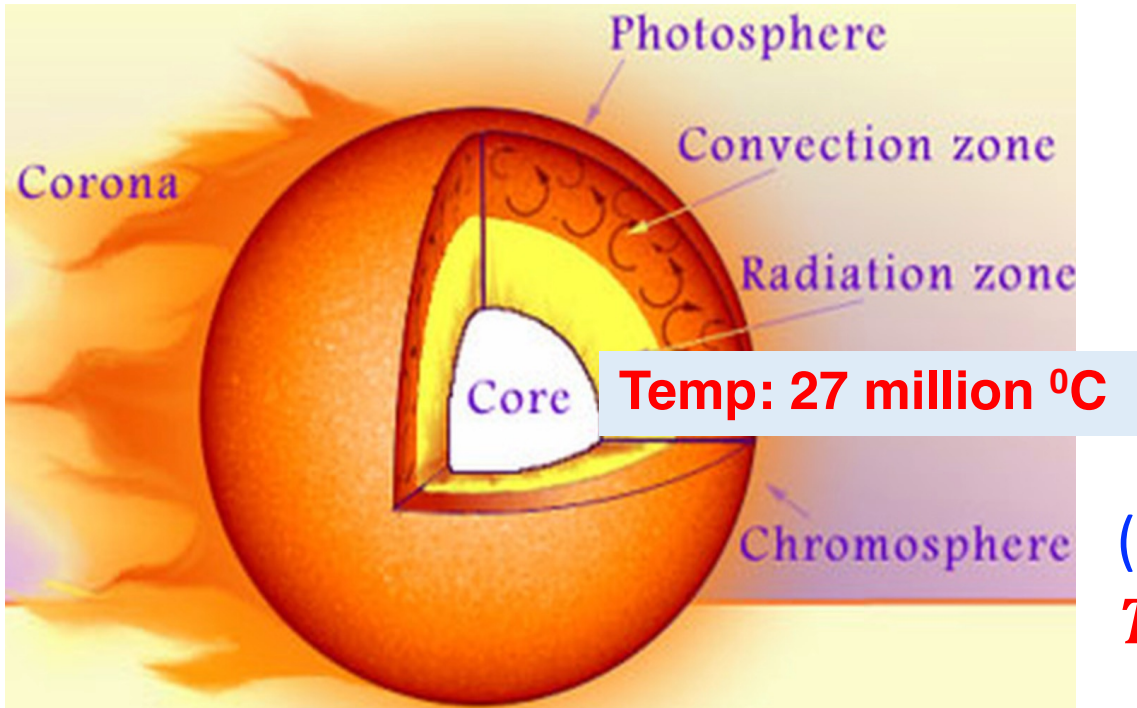


# Photon Spectra and QGP temperature

Phys. Lett. B 754 (2016) 235-248

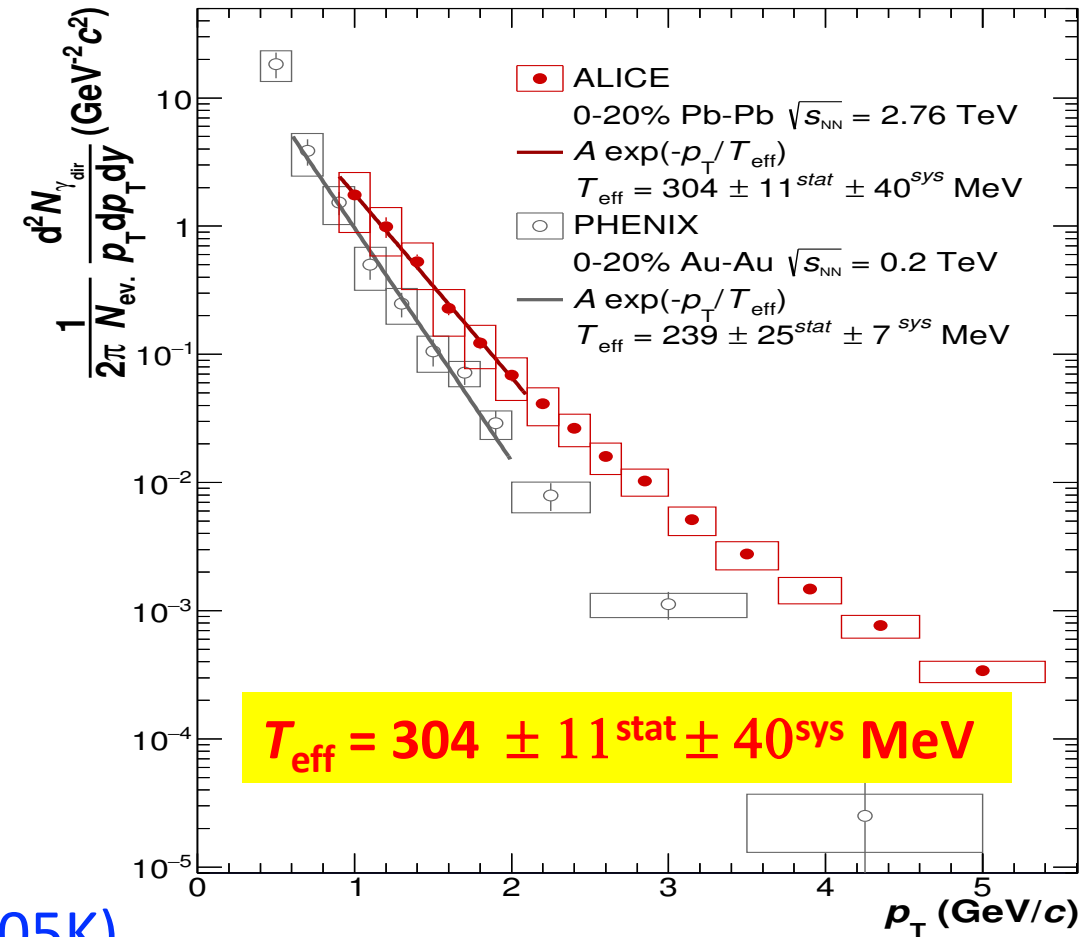
- Photons do not interact via the nuclear force → transparent to the medium
- Photons are emitted in all stages and are unaffected by the medium.

## Core of the Sun:



(1eV=11605K)

$T_{\text{eff}} = 3,527,920$  million deg

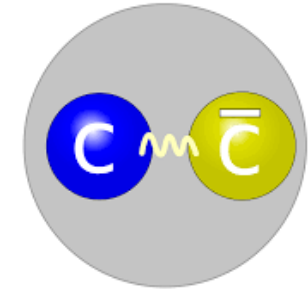
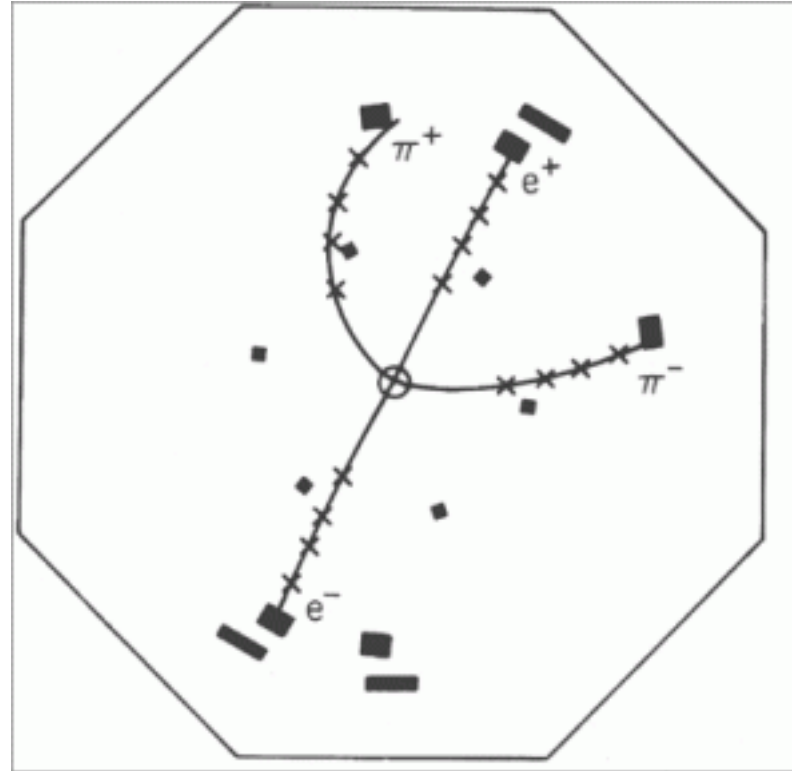
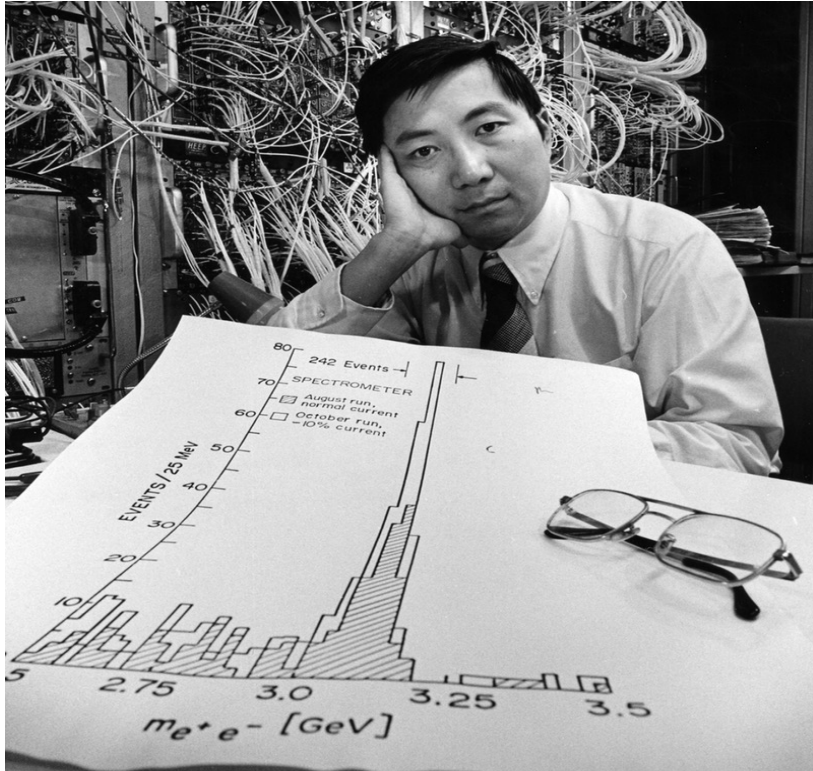


**LARGEST EVER TEMPERATURE REACHED IN THE LAB ...**



# Charmonia, Machine Learning and QGP

# The November Revolution: 1974



Crosses: spark chamber hits  
Dark rectangles: ToF counters

$$\psi' \rightarrow \psi \pi^+ \pi^-$$

Griffiths

- 1.14. Using four quarks ( $u, d, s$ , and  $c$ ), construct a table of all the possible baryon species. How many combinations carry a charm of +1? How many carry charm +2, and +3?



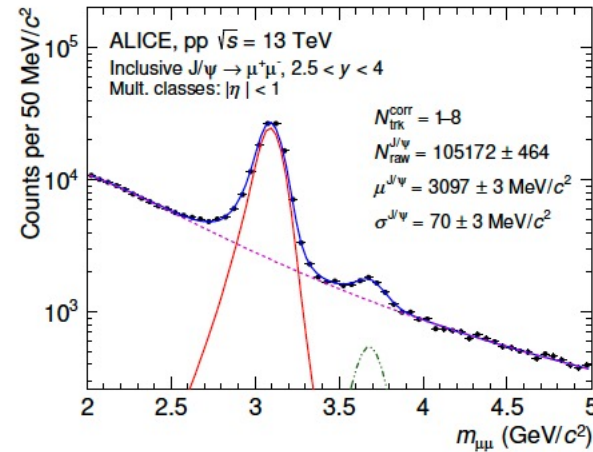
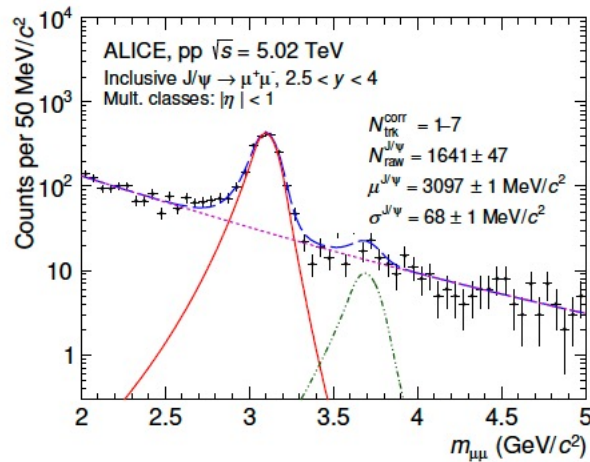
The Nobel Prize in Physics 1976



Burton Richter@SLAC:  $e^+e^-$   
Sam Ting@BNL:  $pp$



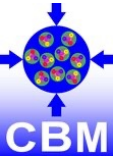
# Our discovery (measurement) of $J/\psi$



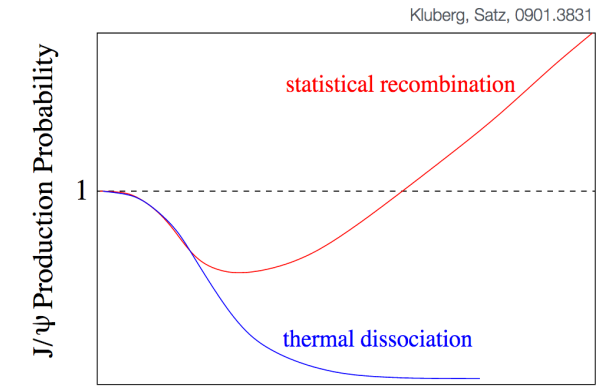
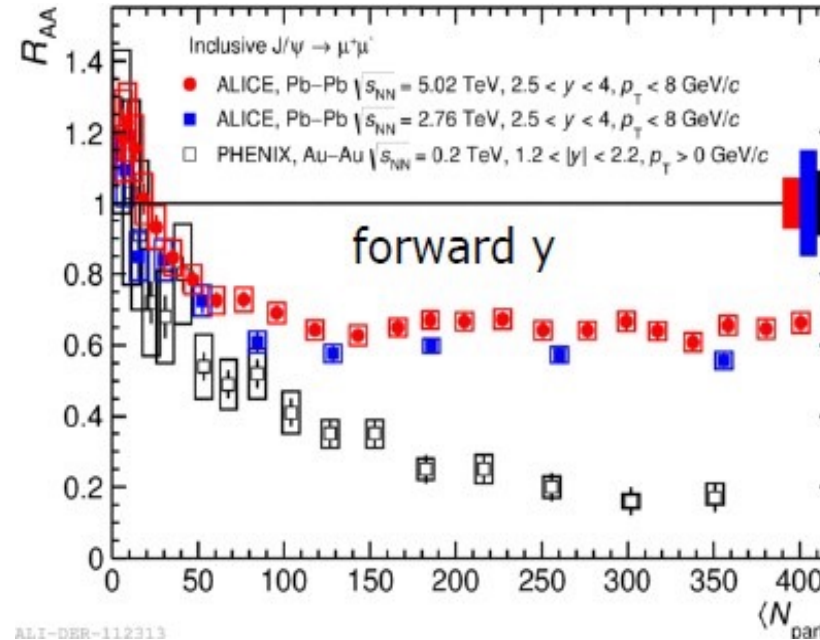
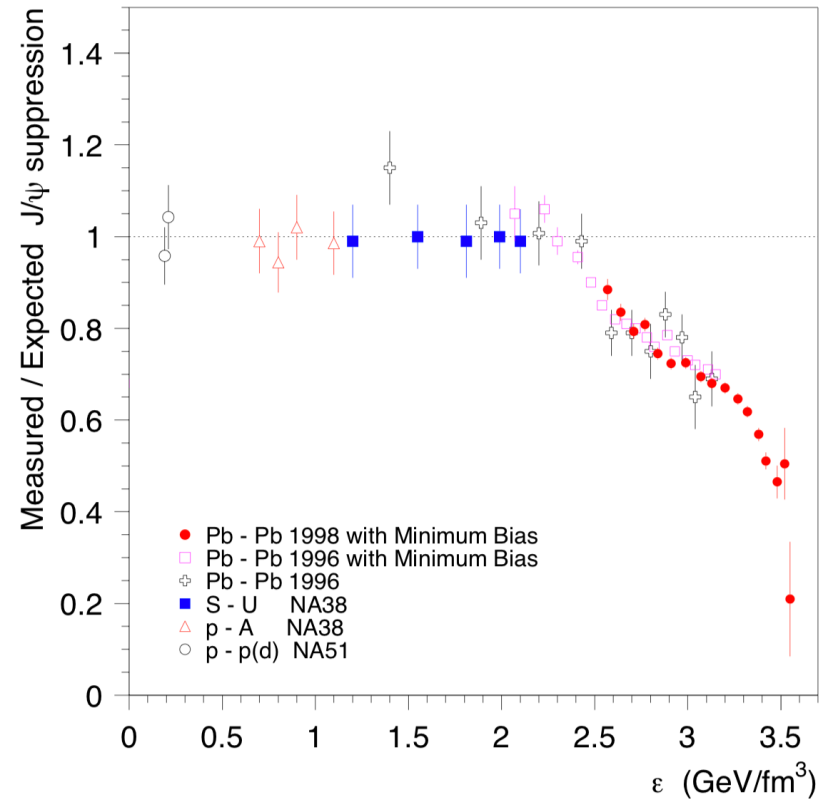
D. Thakur, R. Sahoo et al. ALICE Collaboration JHEP06(2022)015

<https://alice-notes.web.cern.ch/node/734>, ANA-734, D. Thakur and R. Sahoo

<https://alice-publications.web.cern.ch/node/5122>, D. Thakur, R. Sahoo et al.



# Experimental observation of J/ψ Suppression



$$R_{AA}(p_T) = \frac{d N_{AA}/dp_T}{\langle T_{AA} \rangle \times d\sigma_{pp}/dp_T}$$

$R_{AA} < 1$  : Suppression of yield due to presence of medium

$R_{AA} > 1$  : No suppression and hence no medium

( Physics Letters B 766 (2017) 212–224 )

<http://alice.web.cern.ch/content/mystery-jpsi>

➡ **Big question:** use of pp as reference at LHC

➡ **Need :** pp should be investigated properly

CERN SPS (NA50): observed J/ψ suppression as a function of energy density for various collision species. Note that the **critical energy density** for a partonic medium is **1 GeV/fm³**.

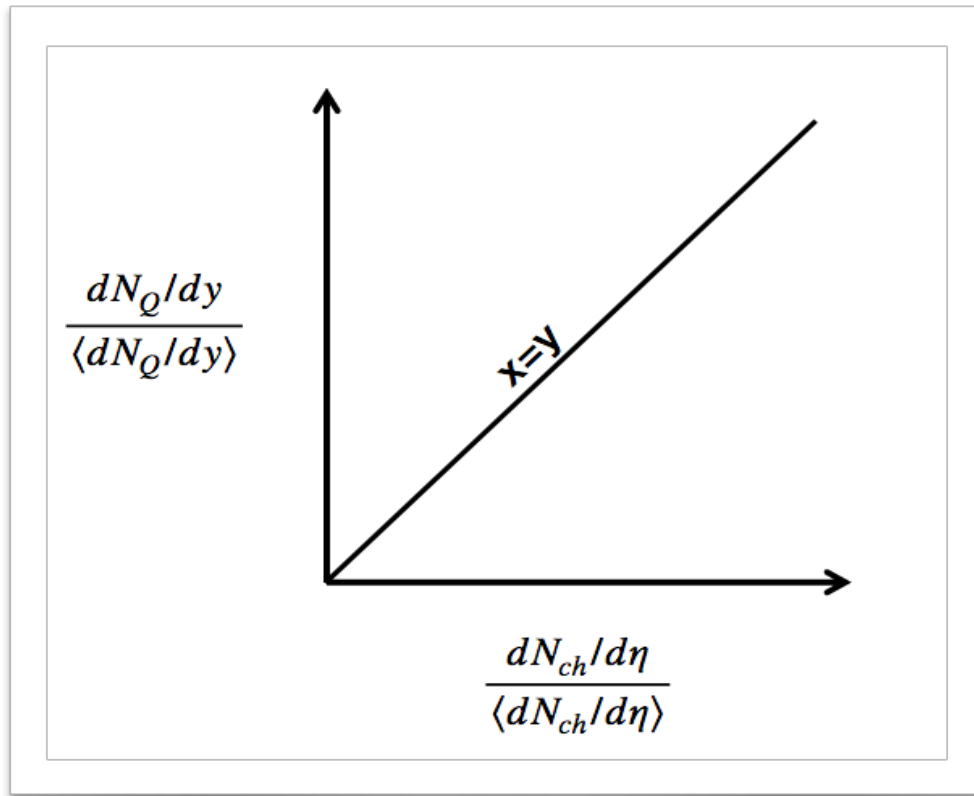


# Study of J/ψ production in pp collisions

→ Investigate charmonium production in pp as a function of multiplicity

## Observables:

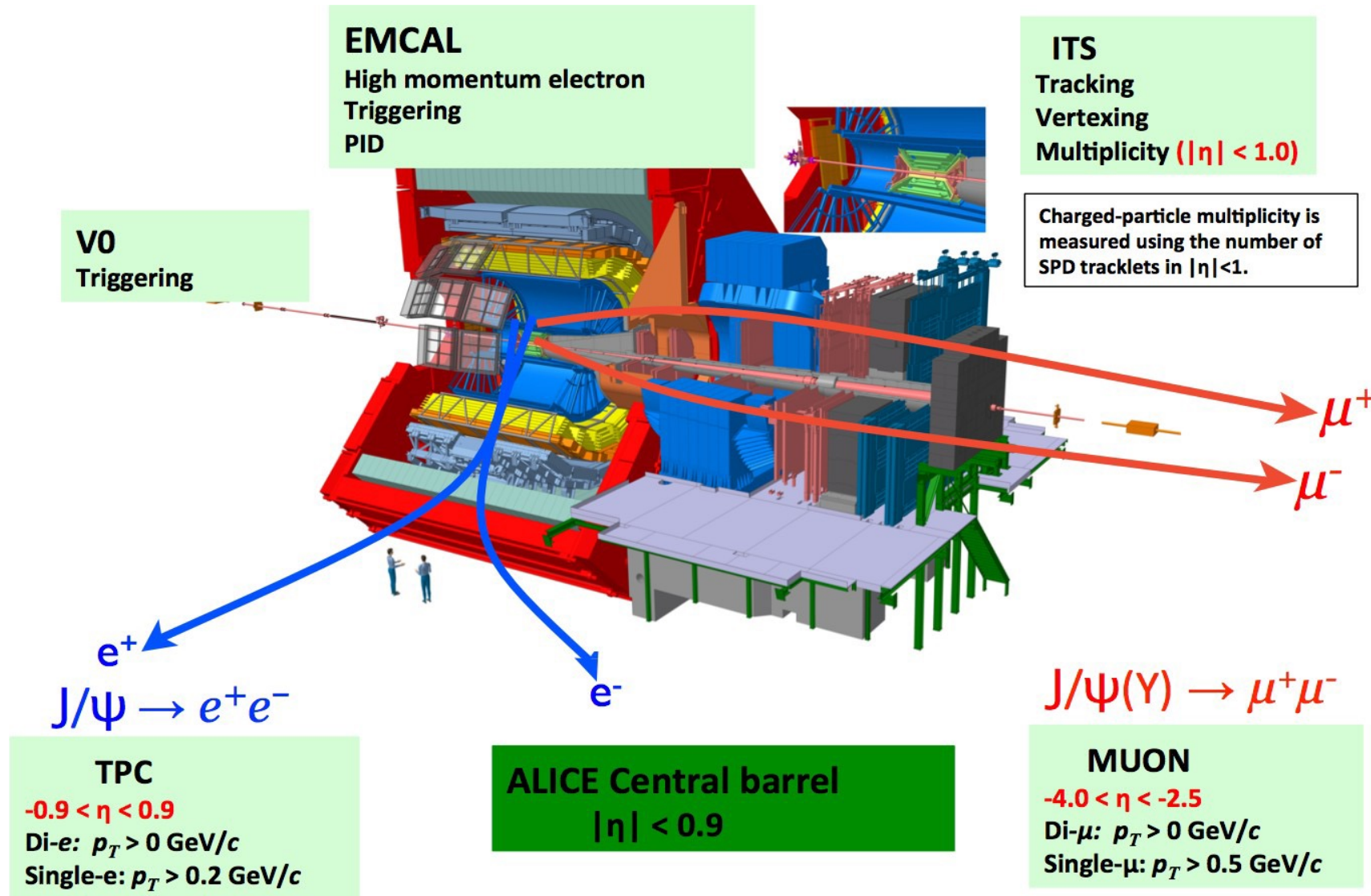
- X axis: relative charged-particle density
- Y axis: relative quarkonium yield (w.r.t. minimum bias)



## Advantages:

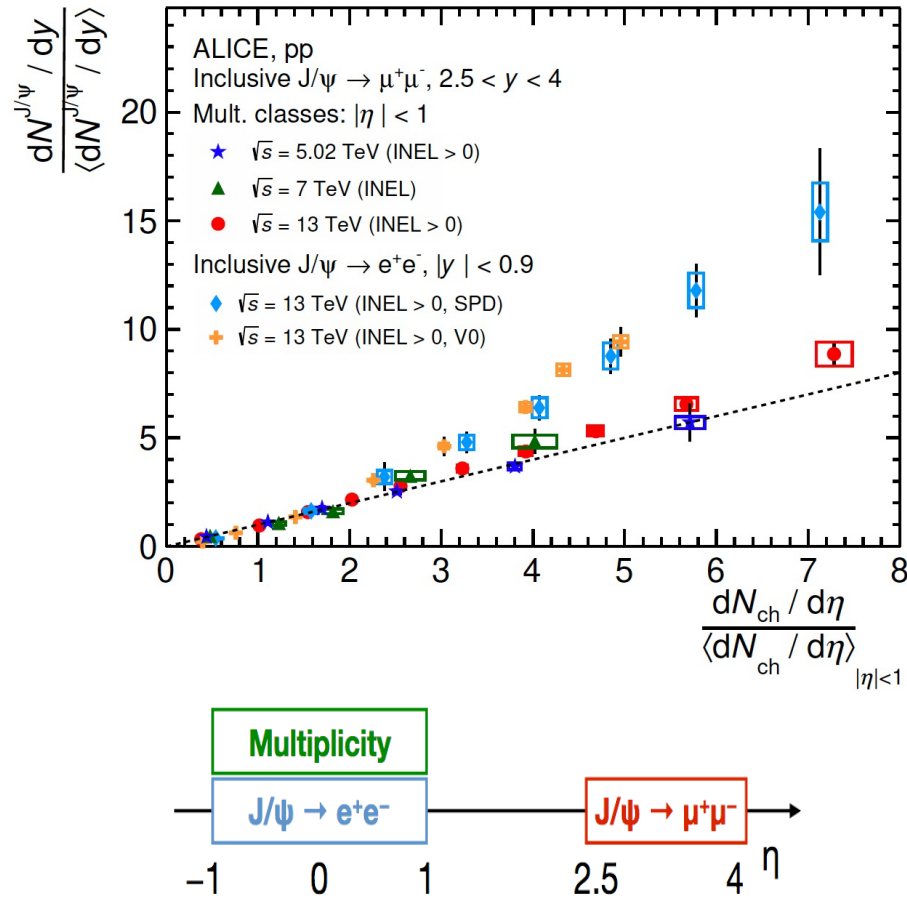
- Several correction factors cancel out in relative yields
- Easy to compare the results across collision systems and energies

# Study of $J/\psi$ production in ALICE





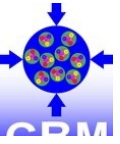
# Study of $J/\psi$ production in ALICE pp collisions



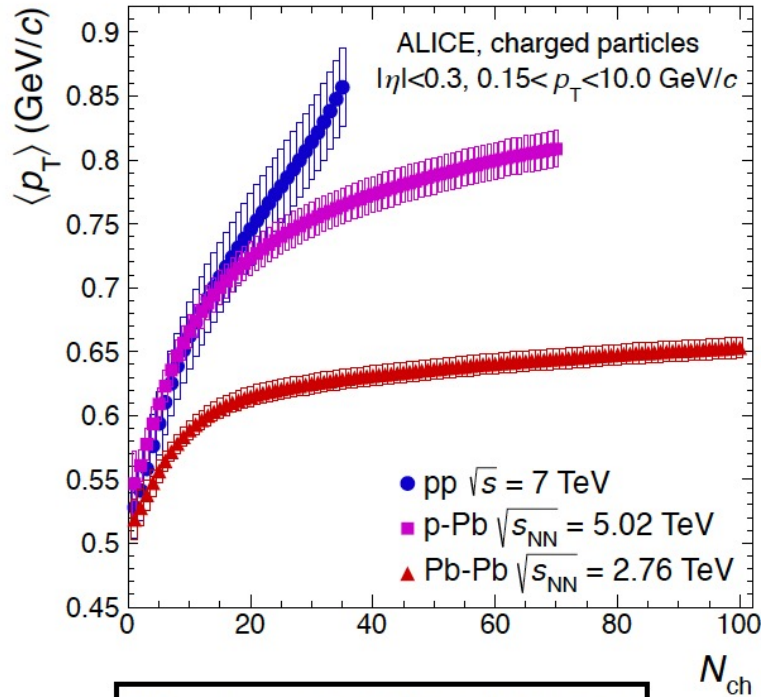
ALICE: JHEP06(2022)015

<https://alice-notes.web.cern.ch/node/734>, ANA-734, D. Thakur and R. Sahoo  
<https://alice-publications.web.cern.ch/node/5122>, D. Thakur, R. Sahoo et al.

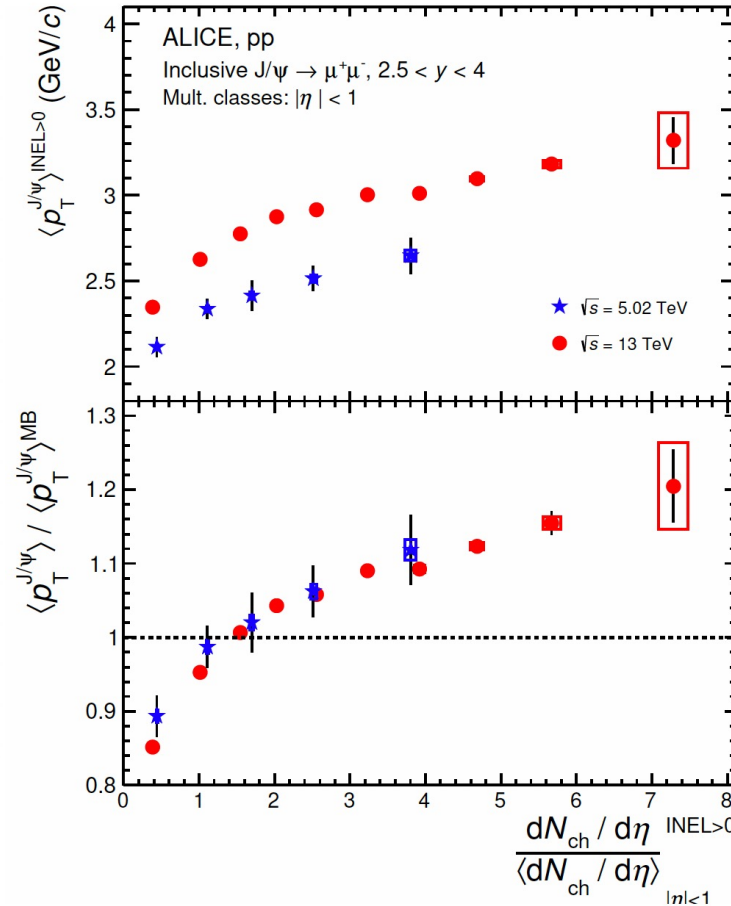
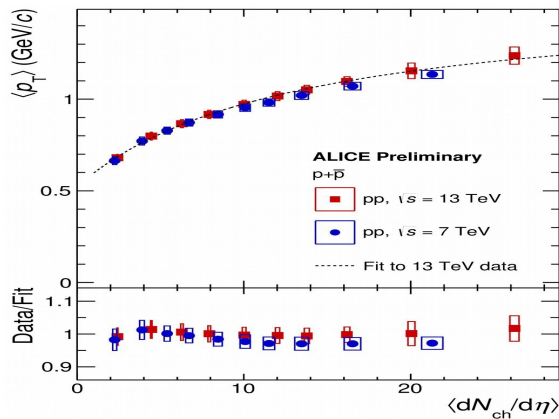
- Relative  $J/\psi$  yield at **midrapidity** is compared to the forward rapidity yield as a function of **midrapidity** relative charged-particle multiplicity
- Midrapidity yields exhibit **faster than linear** increase
- The results using midrapidity multiplicity selection based on the SPD detector ( $|\eta| < 1$ ) and forward-rapidity multiplicity selection based on the V0 detector ( $-3.7 < \eta < -1.7$  and  $2.8 < \eta < 5.1$ ) are found to be compatible within the uncertainties
- Therefore, the different trends in the multiplicity dependence of the  $J/\psi$  production observed at midrapidity and forward rapidity are **not** due to a possible **auto-correlation bias**



# $\langle p_T \rangle$ of $J/\psi$ vs. multiplicity in pp collisions



Phys. Lett. B 727 (2013) 371-380



❖  $\langle p_T \rangle$  of  $J/\psi$  increases with increasing multiplicity with a little saturation towards higher multiplicities

► collectivity? (Phys. Lett. B 727 (2013) 371-380)

❖ Possible explanation of MPI prospect: the high multiplicity events are produced by MPIs and in the absence of CR, incoherent superposition of MPIs would lead to constant  $\langle p_T \rangle$  at high multiplicity.

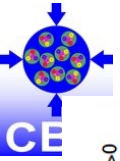
❖  $\langle p_T \rangle$  of  $J/\psi$  vs multiplicity trend is energy-independent

❖ The multiplicity dependent trend is the same for light-flavor and heavy-flavor particles

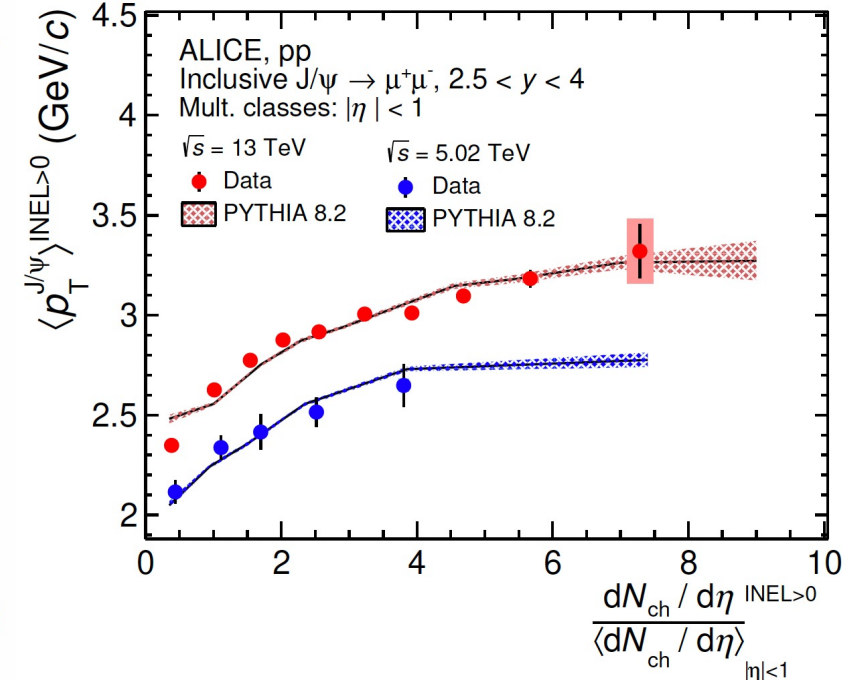
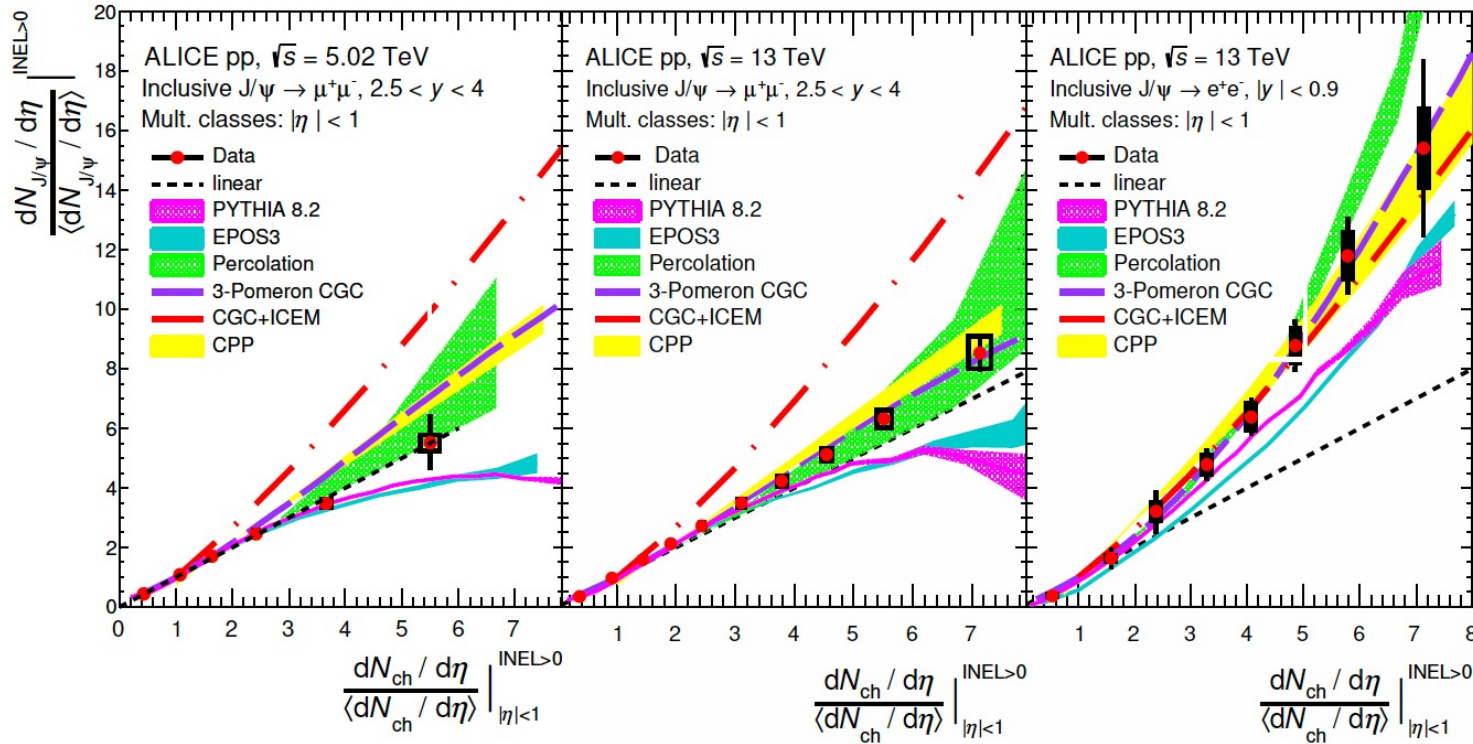
<https://alice-notes.web.cern.ch/node/734>, ANA-734, D. Thakur and R. Sahoo

<https://alice-publications.web.cern.ch/node/5122>, D. Thakur, R. Sahoo et al.





# Theoretical model comparison: J/ψ production



None of the theoretical models give a complete picture of the J/ψ production dynamics in pp collisions

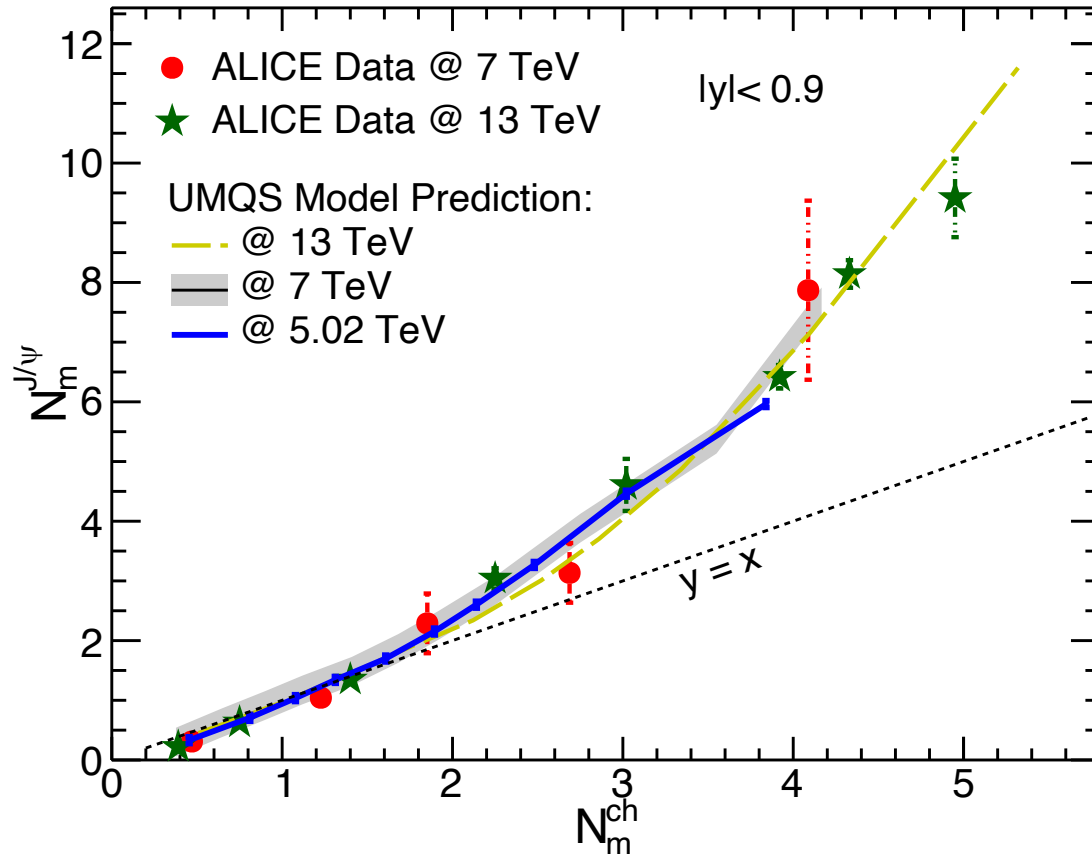
PYTHIA8 with CR gives a reasonable description of the multiplicity dependence of J/ψ  $\langle p_T \rangle$  in pp collisions

<https://alice-notes.web.cern.ch/node/734>, ANA-734, D. Thakur and R. Sahoo

<https://alice-publications.web.cern.ch/node/5122>, D. Thakur, R. Sahoo et al.

A lot of room for theory/phenomenology!

# UMQS model explains ALICE J/ψ production



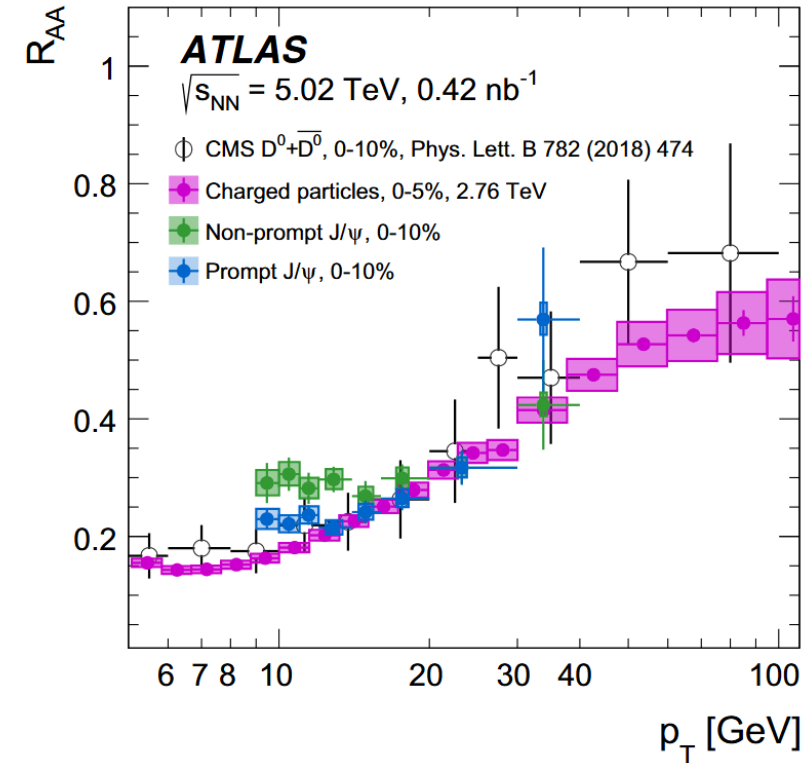
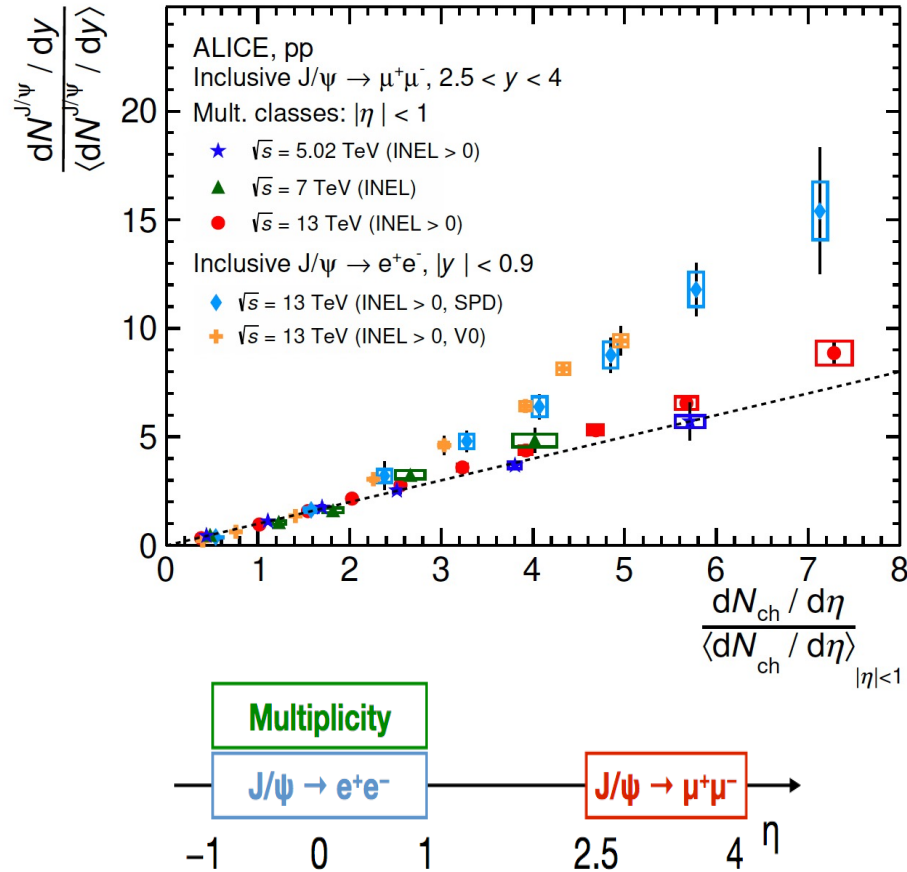
- ✓ J/ψ self-normalized yield as a function of self-normalized multiplicity follows a **scaling across collision energies**.
- ✓ Unified Model of Quarkonia Suppression (UMQS) model which incorporates the **suppression** of J/ψ through **color screening**, **gluonic dissociation**, and **collision damping** and **regeneration of charmonium** due to correlated  $c - \bar{c}$  pairs.

C.R. Singh, S. Deb, R. Sahoo, J. Alam, Eur. Phys. J. C, 82, 542 (2022)



# Need of ML: Separating prompt from nonprompt

Inclusive

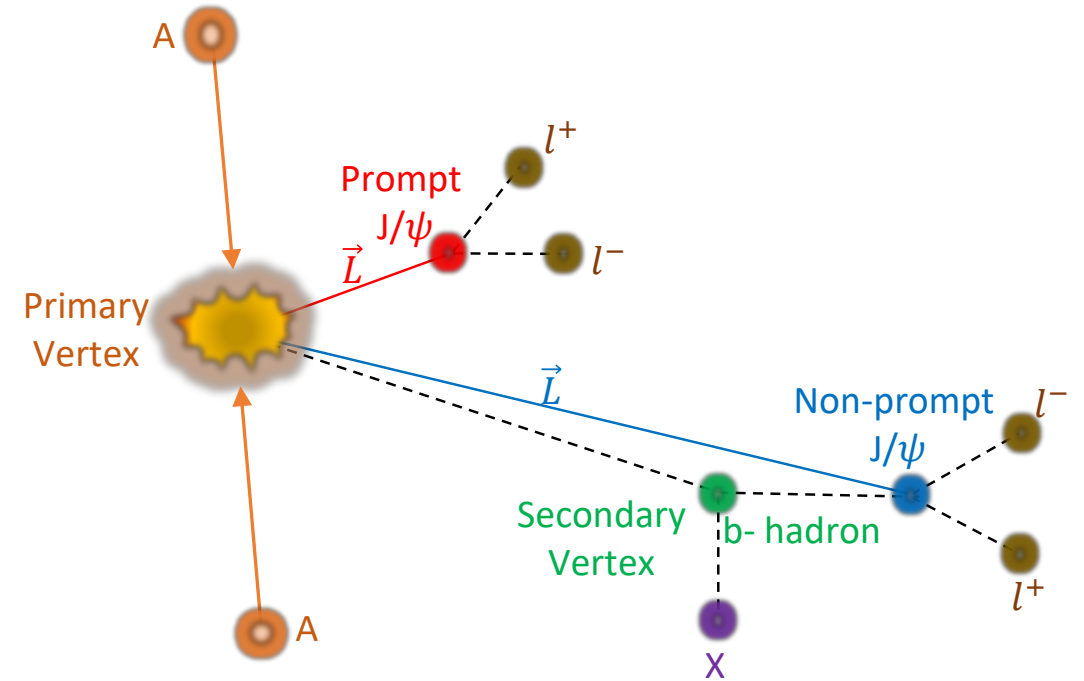


Nuclear modification factor for prompt and non-prompt  $J/\psi$  are different.

D. Thakur, R. Sahoo et al (ALICE), JHEP (2022)

# ML: Separating prompt and non-prompt $J/\psi$ @LHC

- $J/\psi$  ( $3.096 \text{ GeV}/c^2$ )
- In experiments,  $J/\psi \rightarrow \mu^+ + \mu^-$  or  $J/\psi \rightarrow e^+ + e^-$
- **Prompt Production:** Direct production/ decay of heavier charmonia states
- **Non-prompt Production:** Products of beauty hadron weak decays
- Prompt and non-prompt  $J/\psi$  are **topologically different**



S. Prasad, N. Mallick and R. Sahoo, *Phys. Rev. D* 109, 014005 (2024)



# ML to separate prompt and non-prompt $J/\psi$ @LHC

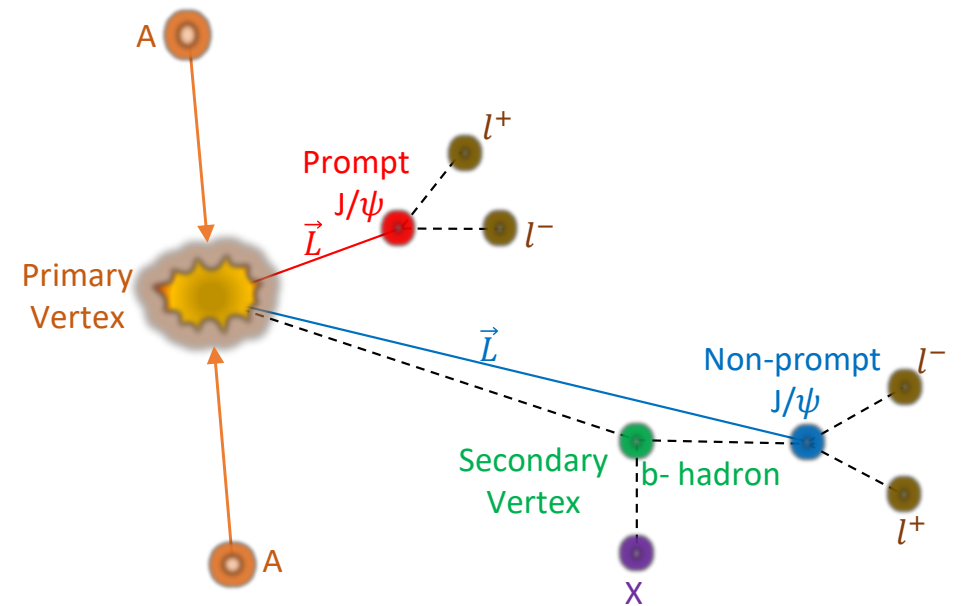
Simulating pp collisions at  $\sqrt{s} = 13$  TeV using PYTHIA8

Training machine-learning models

Using the machine-learning models to predict prompt and non-prompt yields at different energies

Results

- PYTHIA8 (4C-tune) 20 billion minimum bias events for pp  $\sqrt{s} = 13$  TeV
- The coordinates of the primary vertex are randomised following a Gaussian distribution: [experiment-like scenario](#)
- $J/\psi \rightarrow \mu^+ + \mu^-$  channel is used to reconstruct invariant mass ( $m_{\mu\mu}$ ), transverse momentum ( $p_{T,\mu\mu}$ ), pseudorapidity ( $\eta_{\mu\mu}$ ) and rapidity ( $y_{\mu\mu}$ ) of the dimuons
- Pseudoproper decay length ( $c\tau$ ) of the reconstructed dimuon pairs along with  $m_{\mu\mu}$ ,  $p_{T,\mu\mu}$ , and  $\eta_{\mu\mu}$  are taken as inputs



$$c\tau = \frac{c m_{J/\psi} \vec{L} \cdot \vec{p}_T}{|\vec{p}_T|^2}$$

# ML parameters to separate prompt and non-prompt $J/\psi$ @LHC

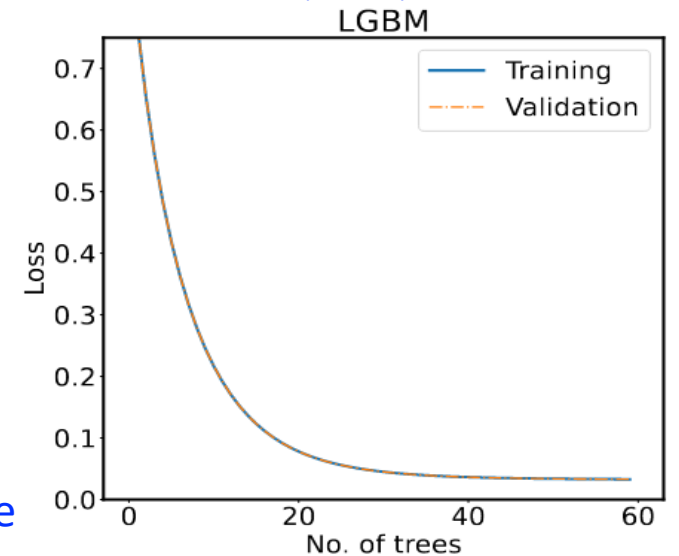
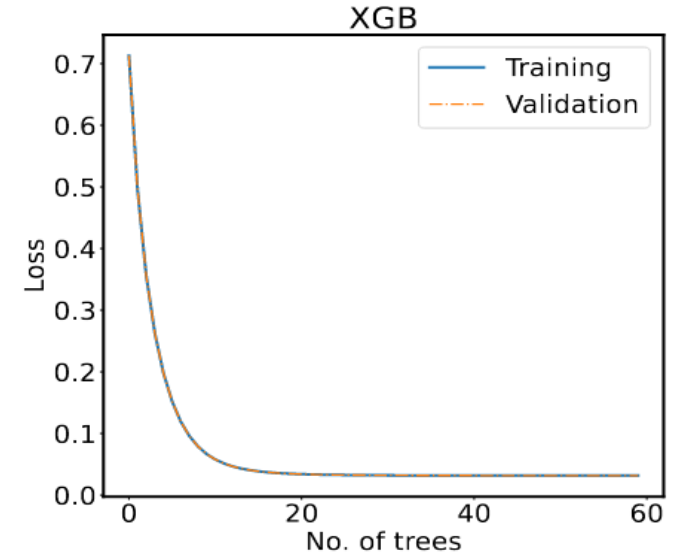
- Background : Prompt : Non-prompt = 20 : 10 : 1
- Classification models required to be trained on similar number of training instances  $\rightarrow$  oversampling of data is done
- Dataset for Training : Testing : Validation = 81 : 10 : 9
- Parameters are chosen through a grid search method (Making an array of all possible parameters and training to find the parameter values for minimum loss)
- Grid Search Method to find best parameters

	XGB	LGBM
Learning rate	0.3	0.1
Sub-sample	1.0	1.0
No. of trees	60	60
Maximum depth	3	3
Objective	<i>softmax</i>	<i>softmax</i>
Metric	<i>mlogloss</i>	<i>multilogloss</i>

S. Prasad, N. Mallick and R. Sahoo, *Phys. Rev. D* 109, 014005 (2024)

- Loss saturates around 25 and 45 trees for XGB and LGBM
- Training and validation curves are on top of each other  $\rightarrow$  No overfitting/underfitting

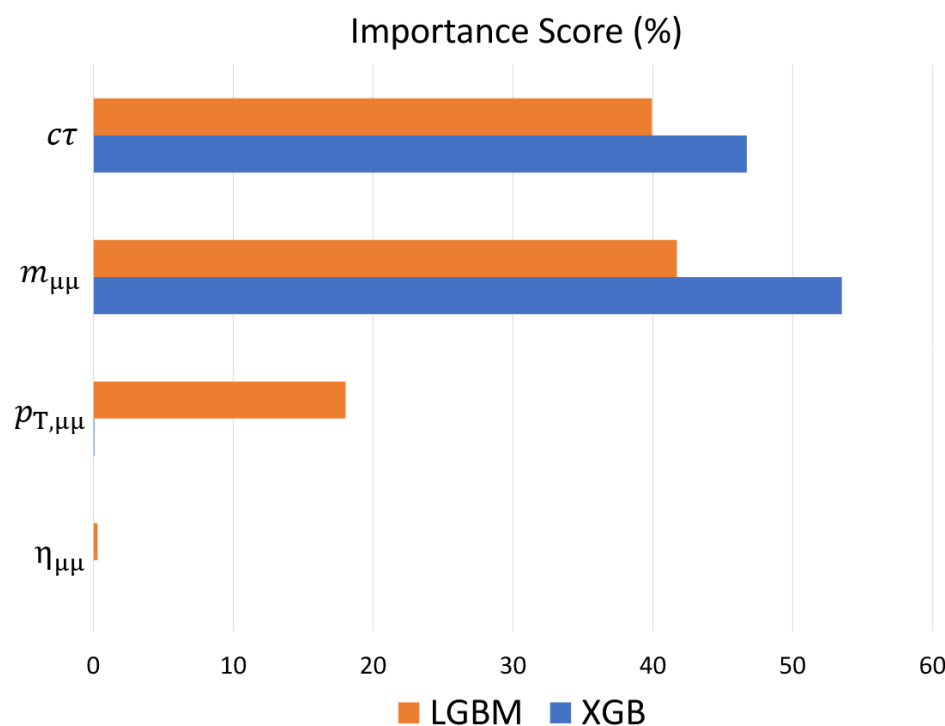
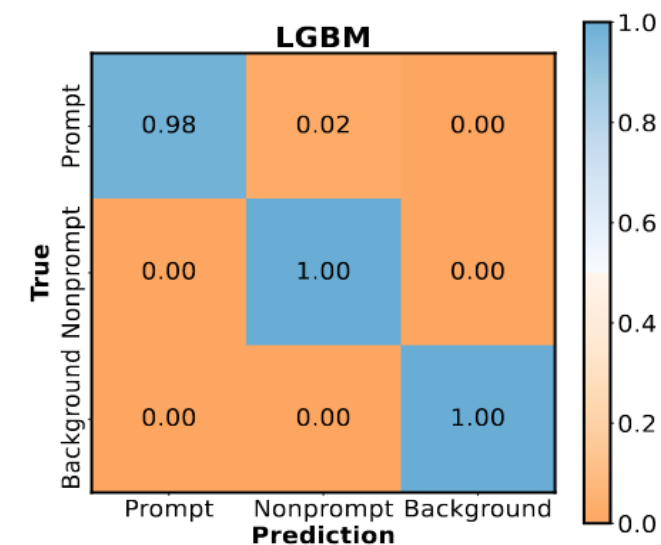
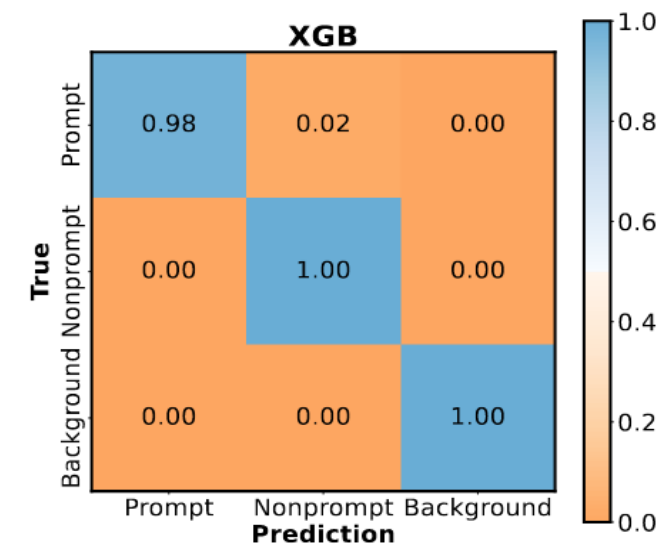
LGBM: Light Gradient Boosting Machine  
XGB: Extreme Gradient Boosting





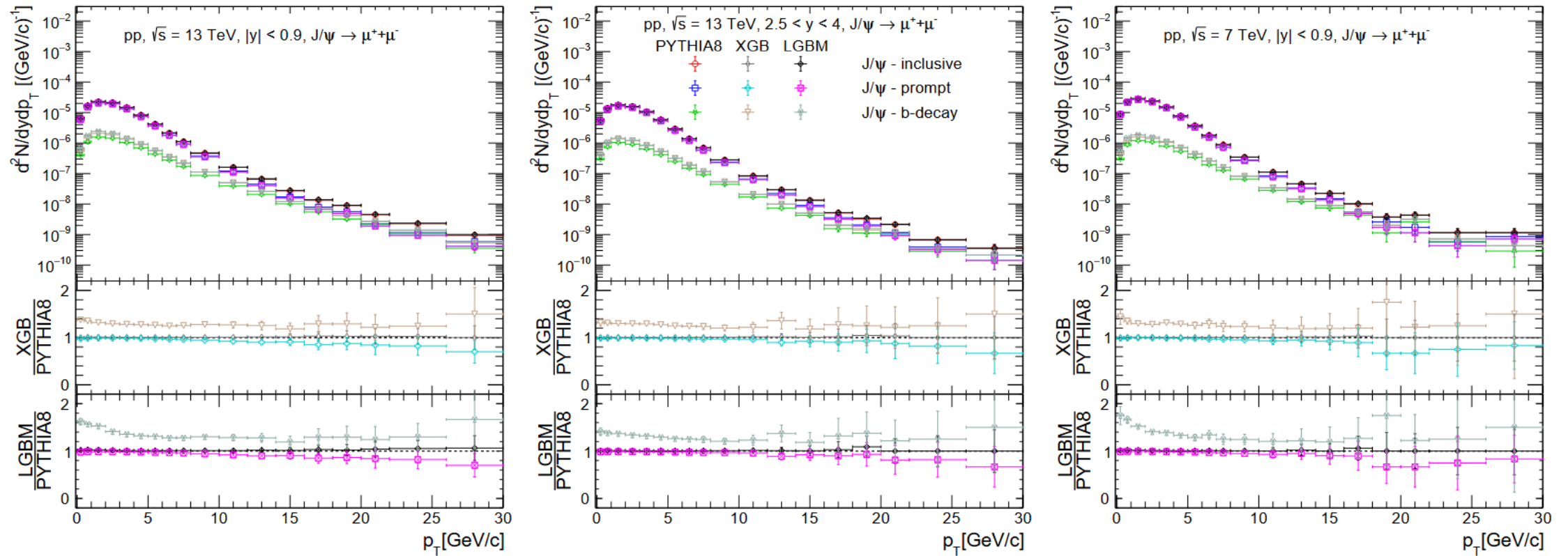
# ML Model performance to separate prompt and non-prompt $J/\psi$ @LHC

- Confusion Matrix talks about the mispredictions given by the model for each class
- Both XGB and LGBM perfectly separate the inclusive  $J/\psi$  from the uncorrelated background pairs
- Both models mispredict 2% of prompt  $J/\psi$  as the non-prompt  $\rightarrow$  Raises non-prompt yield



- The importance score tells how important a feature is for the decision-making of the models
- The importance score of the invariant mass of dimuons is highest for both models
- $c\tau$  contributes to decision making of the models significantly

# ML Results: Transverse momentum spectra

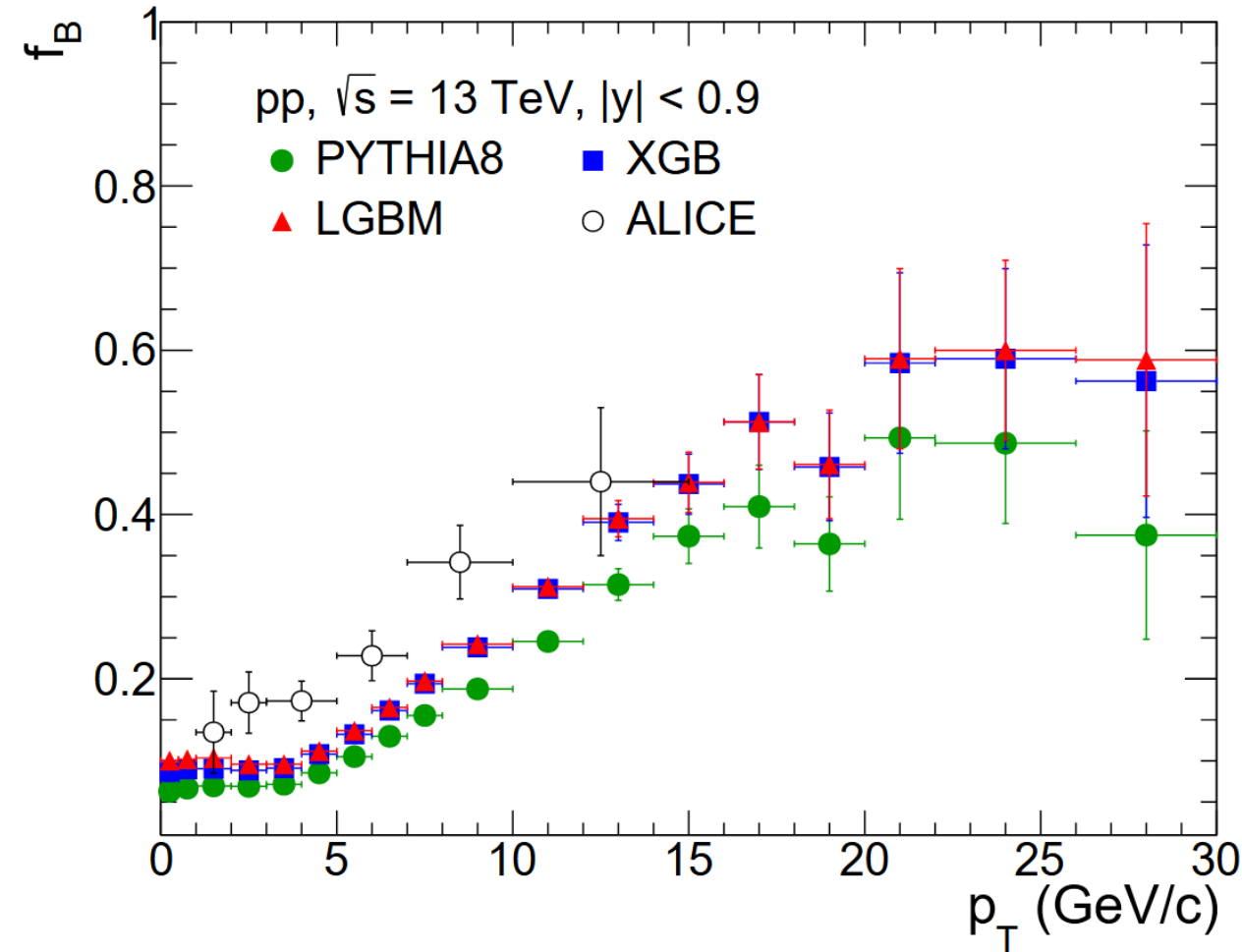


- Both XGB and LGBM give accurate predictions for  $p_T$ -spectra for inclusive and prompt- $J/\psi$  both in mid and forward rapidity in pp collisions at  $\sqrt{s} = 13$  TeV and 7 TeV
- The ML models overpredict the non-prompt  $J/\psi$  throughout the  $p_T$  spectra for both the collision energy and rapidity  
 → Expected from the confusion matrix

S. Prasad, N. Mallick and R. Sahoo, *Phys. Rev. D* 109, 014005 (2024)



# ML Results: Fraction of non-prompt J/ψ yield



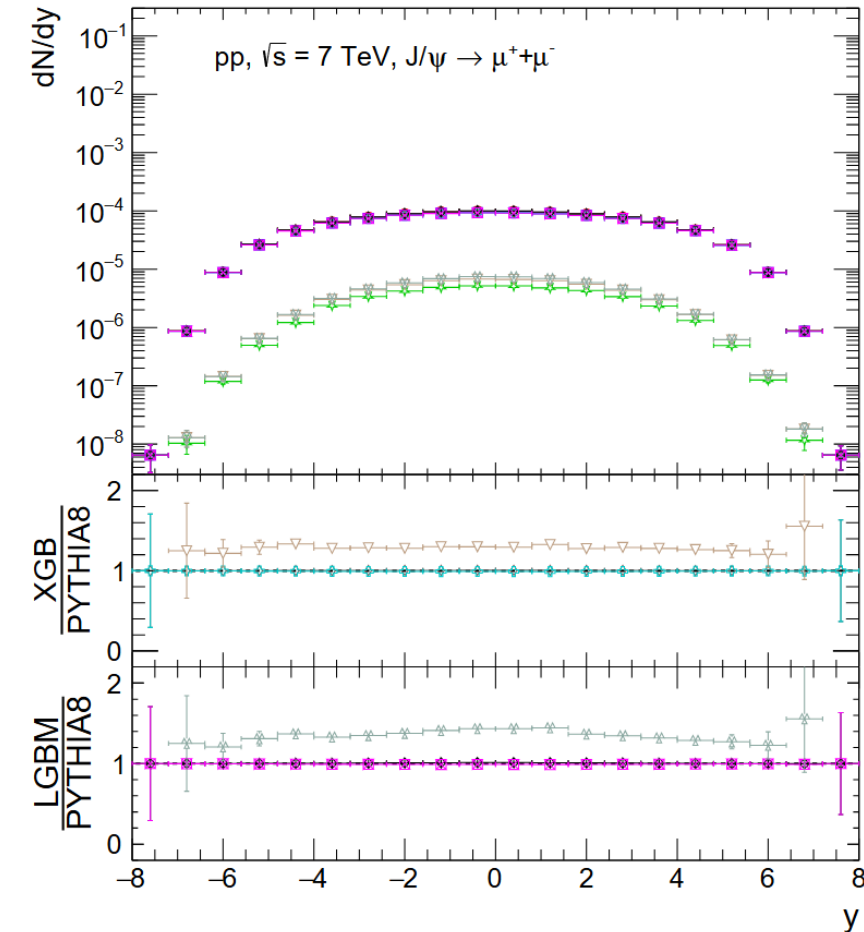
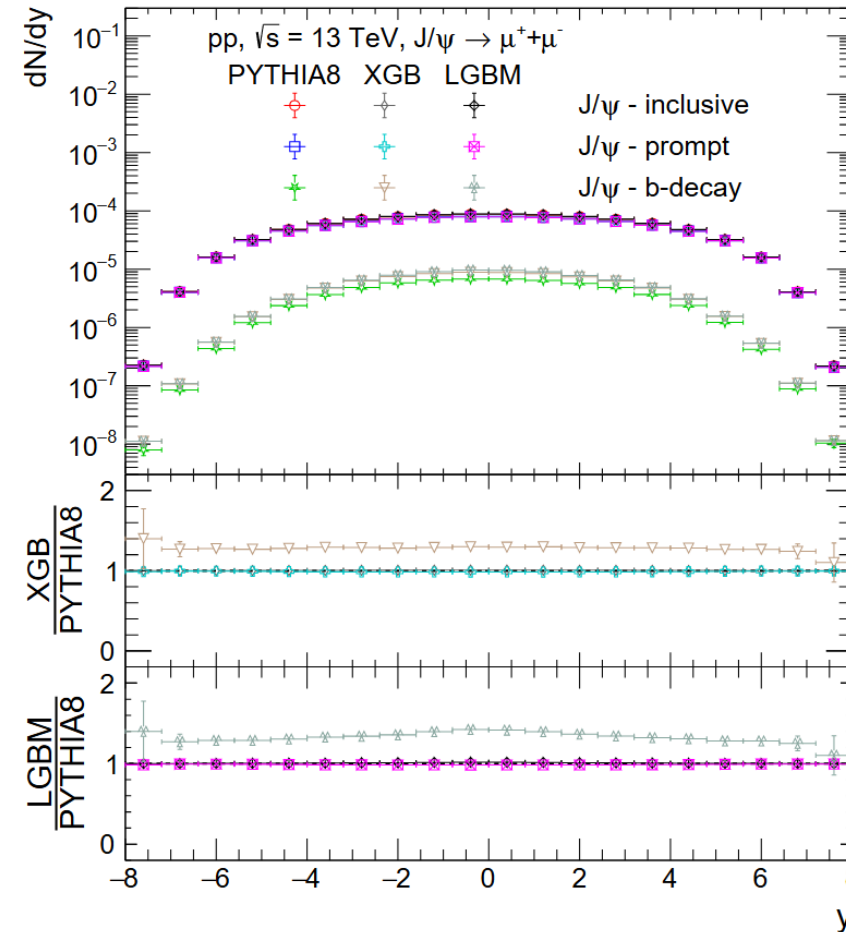
$$\sigma_{\text{nonprompt J}/\psi} = f_B \cdot \sigma_{\text{J}/\psi},$$

$$\sigma_{\text{prompt J}/\psi} = (1 - f_B) \cdot \sigma_{\text{J}/\psi}.$$

- $f_B$  is the fraction of the non-prompt production (b-hadron decays)
- $f_B$  increases with increase in  $p_T \rightarrow$  The b-hadron production is favoured towards higher  $p_T$
- PYTHIA8 underestimates the experimental data following a similar trend
- Both XGB and LGBM overestimate PYTHIA8
- As this method does not require fitting, it can be used in both low and high statistics without affecting its efficiency

S. Prasad, N. Mallick and R. Sahoo, *Phys. Rev. D* 109, 014005 (2024)

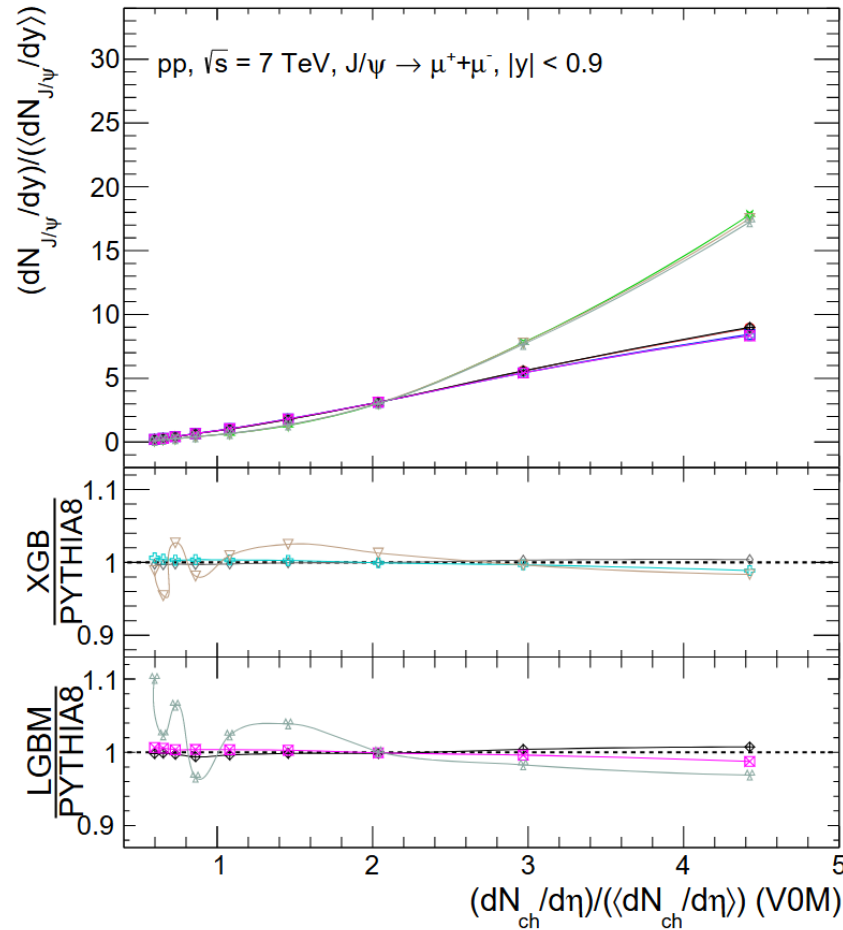
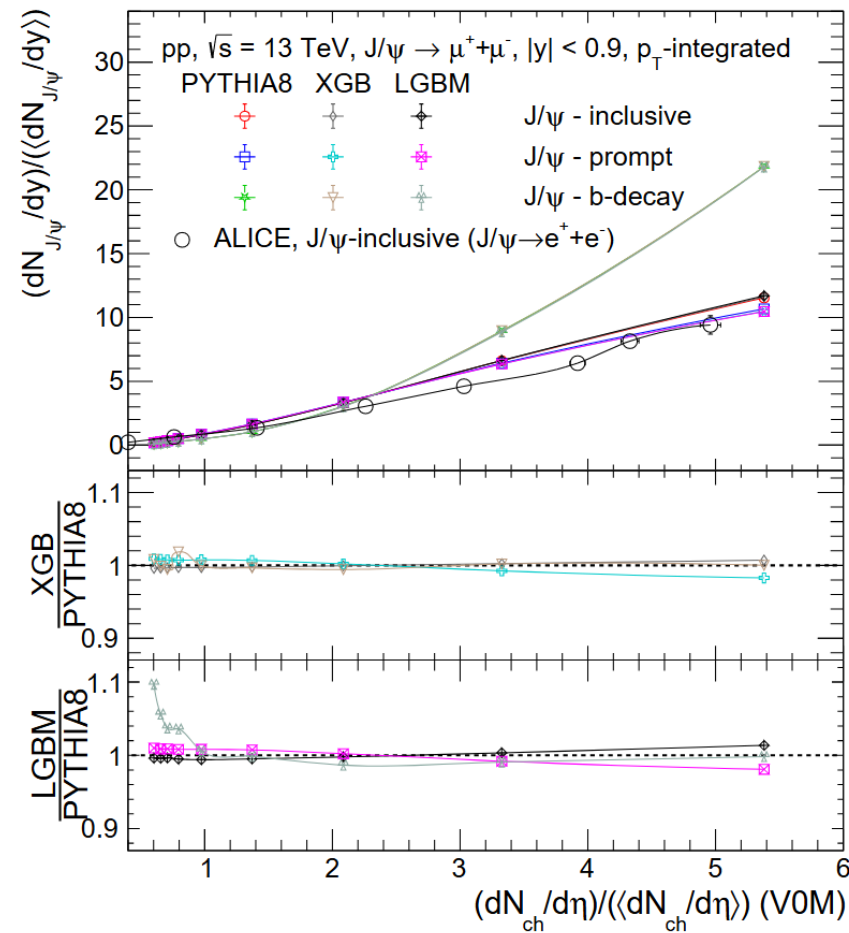
- Both XGB and LGBM give accurate predictions for rapidity spectra for inclusive and prompt- $J/\psi$  in pp collisions at  $\sqrt{s} = 13$  TeV and 7 TeV
- The ML models **overpredict the non-prompt  $J/\psi$**  throughout rapidity region for both the collision energies



S. Prasad, N. Mallick and R. Sahoo, *Phys. Rev. D* 109, 014005 (2024)



# ML Results: Normalized $J/\psi$ Yields



- The normalised yield for inclusive  $J/\psi$  from PYTHIA8 matches qualitatively with the ALICE results
- Both XGB and LGBM reproduce the PYTHIA8 results very precisely for inclusive and prompt  $J/\psi$
- The predictions for non-prompt  $J/\psi$  from both XGB and LGBM matches PYTHIA8 findings within 10% uncertainty

S. Prasad, N. Mallick and R. Sahoo, *Phys. Rev. D* 109, 014005 (2024)

## ML Results $J/\psi$ : Summary

- We have used **BDT based ML models** such as **XGBoost** and **LGBM** to segregate the prompt, non-prompt and inclusive  $J/\psi$  production in pp collisions at  $\sqrt{s} = 13$  TeV
- The models the parameters such as, pseudo-proper decay length ( $c\tau$ ), invariant mass ( $m_{\mu\mu}$ ), transverse momentum ( $p_{T,\mu\mu}$ ), pseudorapidity ( $\eta_{\mu\mu}$ ) of the dimuons as the input, which are accessible in the experiments
- The model almost achieves **99% overall accuracy**
- The estimations for the prompt and inclusive  $J/\psi$  from the ML models match with the PYTHIA8 for the inclusive and non-prompt  $J/\psi$
- Using these models, track label identification is possible, and it avoids the necessity of fit for the identification



# Open Charms: $D^0$

PHYSICAL REVIEW D VOL..XX, 000000 (XXXX)

## Machine learning-based study of open-charm hadrons in proton-proton collisions at the Large Hadron Collider

Kangkan Goswami<sup>✉</sup>, Suraj Prasad<sup>✉</sup>, Neelkamal Mallick<sup>✉</sup>, and Raghunath Sahoo<sup>✉\*</sup>  
Department of Physics, Indian Institute of Technology Indore, Simrol, Indore 453552, India

Gagan B. Mohanty<sup>✉</sup>

Tata Institute of Fundamental Research, Homi Bhabha Road, Mumbai 400005, India

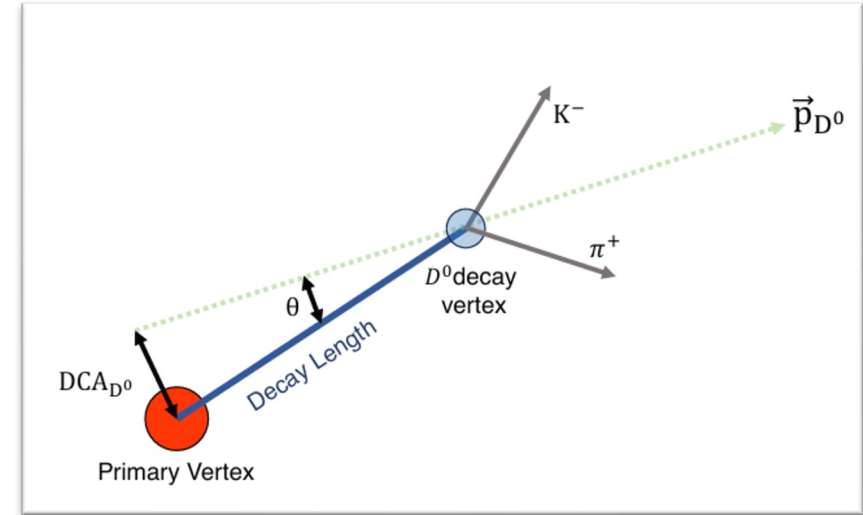
(Received 16 April 2024; accepted 2 July 2024)

In proton-proton and heavy-ion collisions, the study of charm hadrons plays a pivotal role in understanding the QCD medium and provides an undisputed testing ground for the theory of strong interaction, as they are mostly produced in the early stages of collisions via hard partonic interactions. The lightest open charm,  $D^0$  meson ( $c\bar{u}$ ), can originate from two separate sources. The prompt  $D^0$  originates from either direct charm production or the decay of excited open charm states, while the nonprompt stems from the decay of beauty hadrons. In this paper, using different machine learning (ML) algorithms such as XGBoost, CatBoost, and Random Forest, an attempt has been made to segregate the prompt and nonprompt production modes of the  $D^0$  meson signal from its background. The ML models are trained using the invariant mass through its hadronic decay channel, i.e.,  $D^0 \rightarrow \pi^+ K^-$ , pseudoproper time, pseudoproper decay length, and distance of closest approach of  $D^0$  meson, using PYTHIA8 simulated  $pp$  collisions at  $\sqrt{s} = 13$  TeV. The ML models used in this analysis are found to retain the pseudorapidity, transverse momentum, and collision energy dependence. In addition, we report the ratio of nonprompt to prompt  $D^0$  yield, the self-normalized yield of prompt and nonprompt  $D^0$ , and explore the charmonium,  $J/\psi$  to open charm,  $D^0$  yield ratio as a function of transverse momenta and normalized multiplicity. The observables studied in this paper are well predicted by all the ML models compared to the simulation.

DOI:

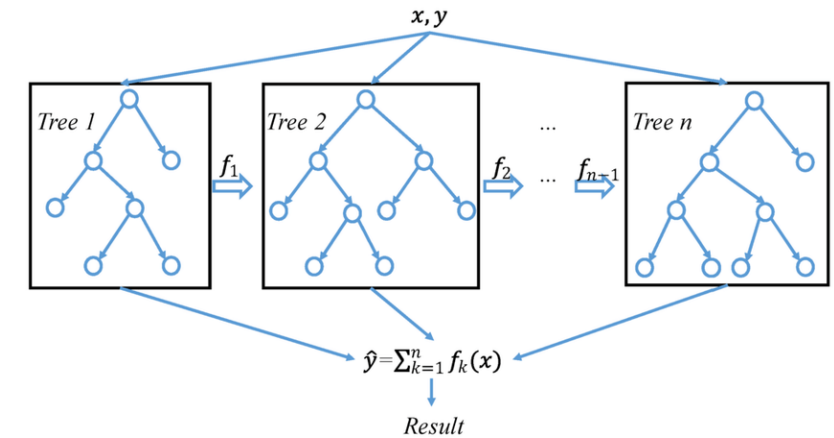
Phys. Rev. D (2024: In Press)

arXiv: 2404.09839

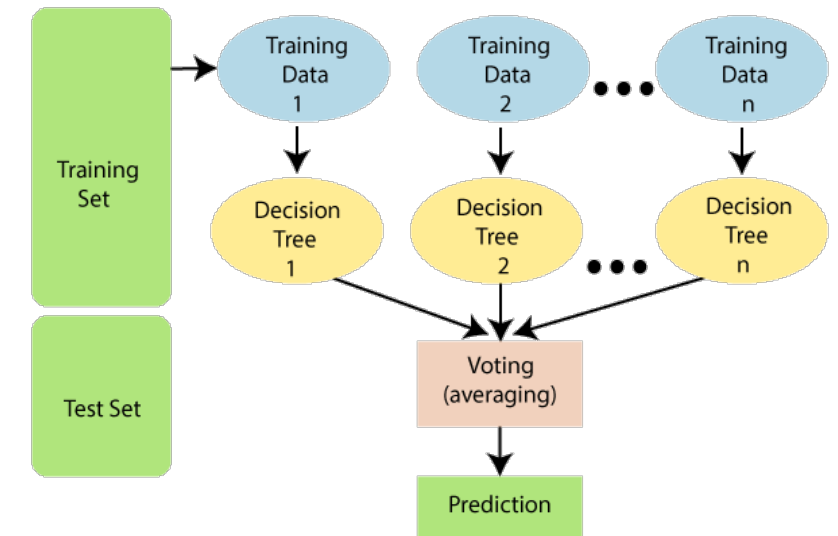


# ML Techniques

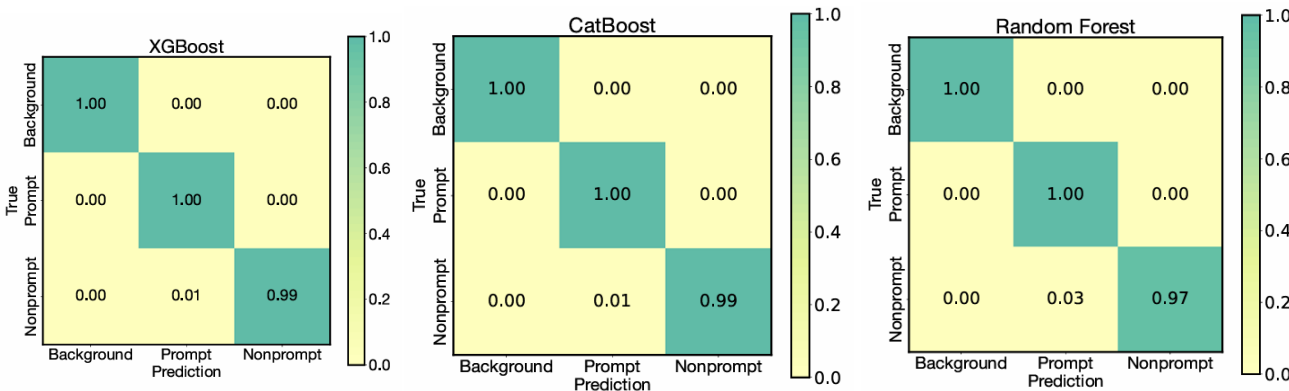
- Extreme Gradient Boost (XGBoost): Combines the predictions of multiple weak models to produce a stronger model.
- Categorical Boosting (CatBoost): Similar working principle as XGBoost but faster and more efficient when working with categorical data.
- Random Forest: In a Random Forest classifier, multiple decision trees are created, each on a different subset of the data. Each tree gets a vote on the class label for a new instance. The class that gets the most votes is chosen as the final prediction.



XGBoost and CatBoost Architecture



Random Forest Classifier Architecture





# Training ML Models

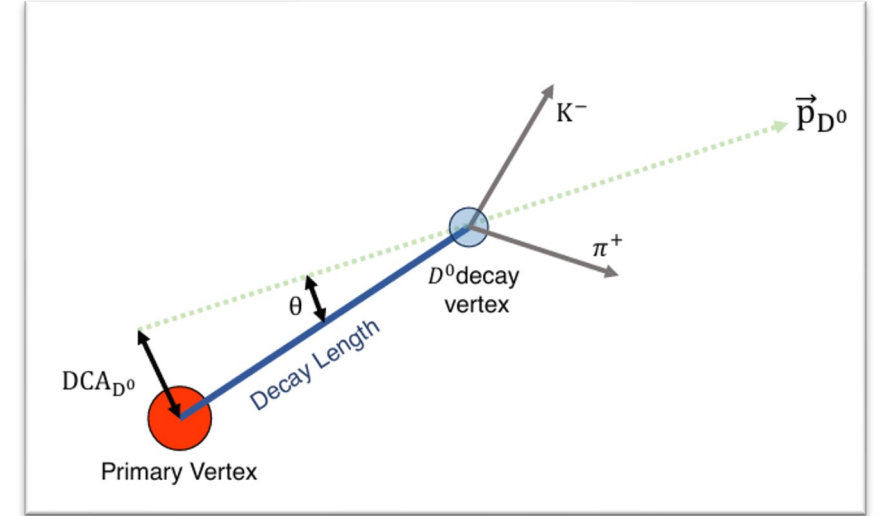
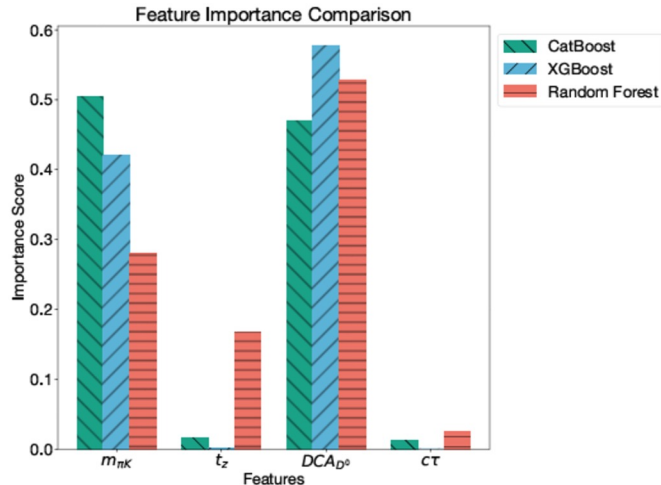
## Input Variables

1. Invariant Mass
2. The pseudo-proper time:
3. Pseudo-proper decay length:
4. Distance of closest approach:

$$t_z = \frac{(z_{D^0} - z_{PV}) \times m_{D^0}}{p_z}$$

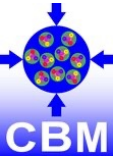
$$c\tau = \frac{cm_{D^0} \vec{L} \cdot \vec{p}_T}{p_T^2}$$

$$DCA_{D^0} = L \times \sin \theta$$



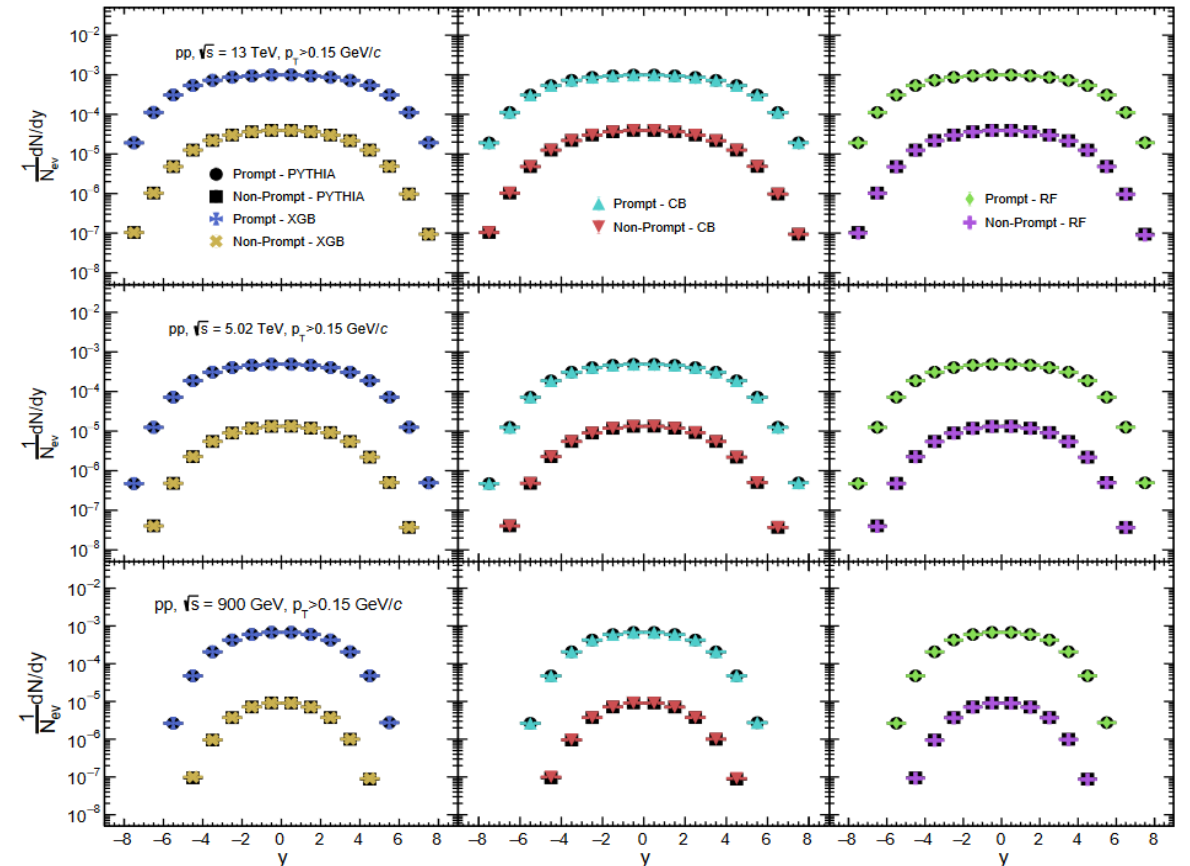
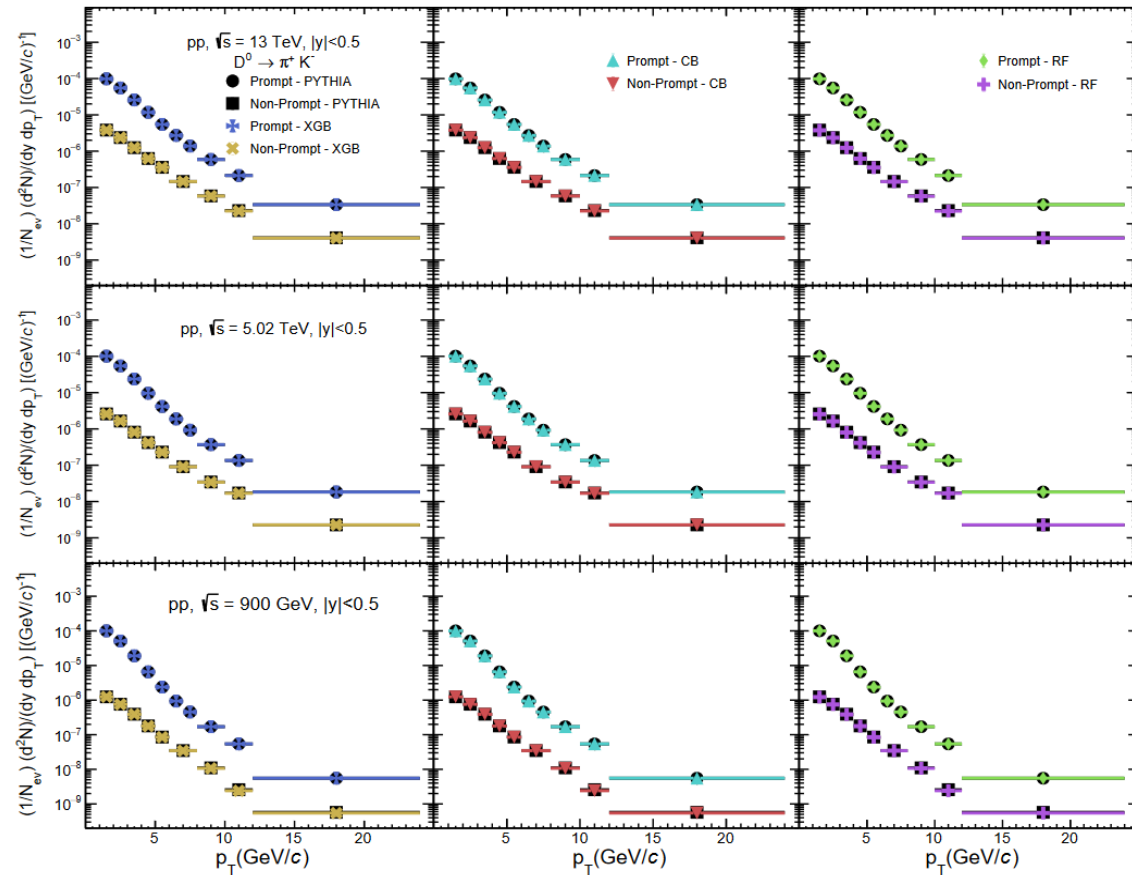
$\vec{L}$  is the vector pointing from the primary vertex towards  $D^0$  decay vertex, i.e.  $\vec{L} = \vec{V} - \vec{S}$ .  $\vec{V}$  is the position of the primary vertex and  $\vec{S}$  is the position of the  $D^0$  decay vertex given by,

$$S_i = \frac{(t_1 + d_{i,1}m_1/p_{i,1}) - (t_2 + d_{i,2}m_2/p_{i,2})}{m_1/p_{i,1} - m_2/p_{i,2}}$$



# Results

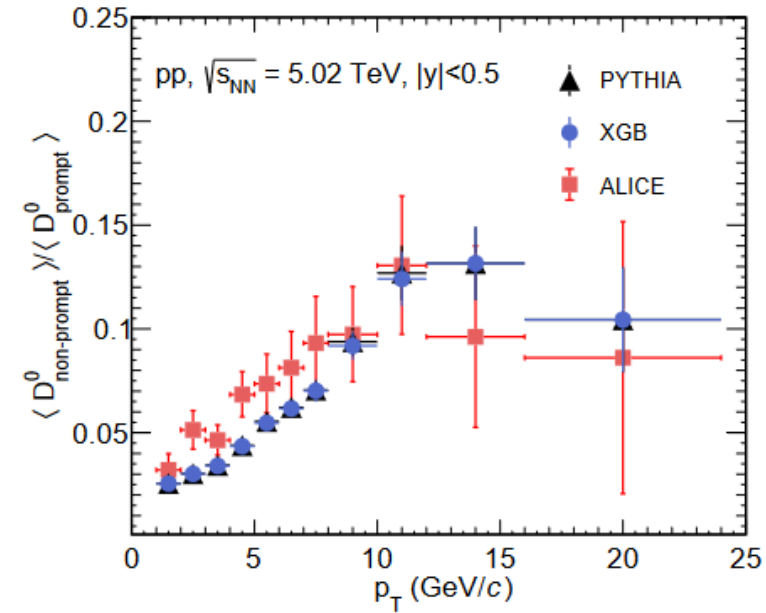
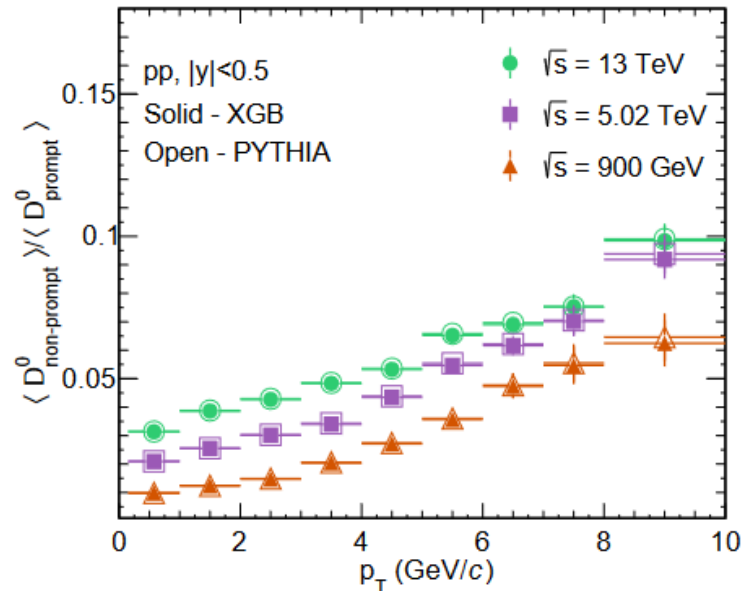
- Transverse momenta and rapidity spectra
- Trained the ML models only at one centre-of-mass energy:  $\sqrt{s} = 13$  TeV
- Predicted normalized  $D^0$  meson yield at  $\sqrt{s} = 13$  TeV, 5.02 TeV and 900 GeV





# Results

- ❖ Predicted the non-prompt to prompt ratio at 5.02 TeV and compared with ALICE data
- ❖ We observe a linear increase in the ratio with  $p_T$ . However, the **linear trend** holds true only up to a certain  $p_T$  range.

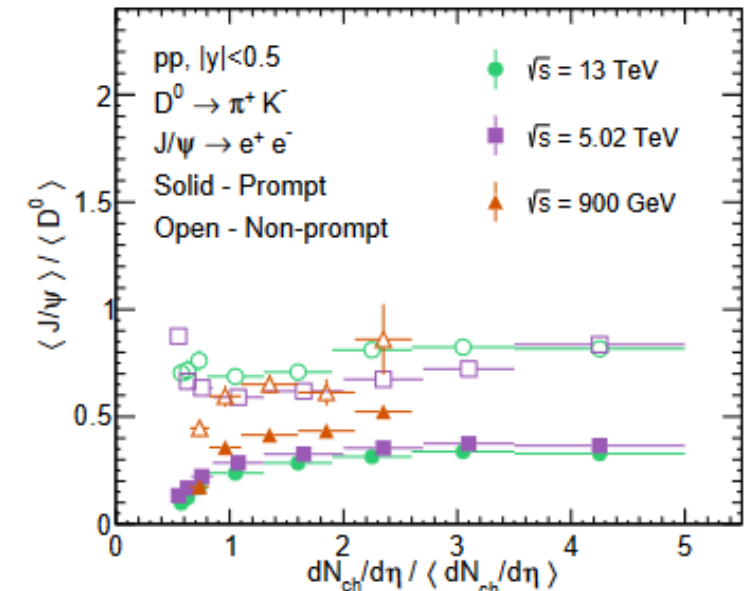
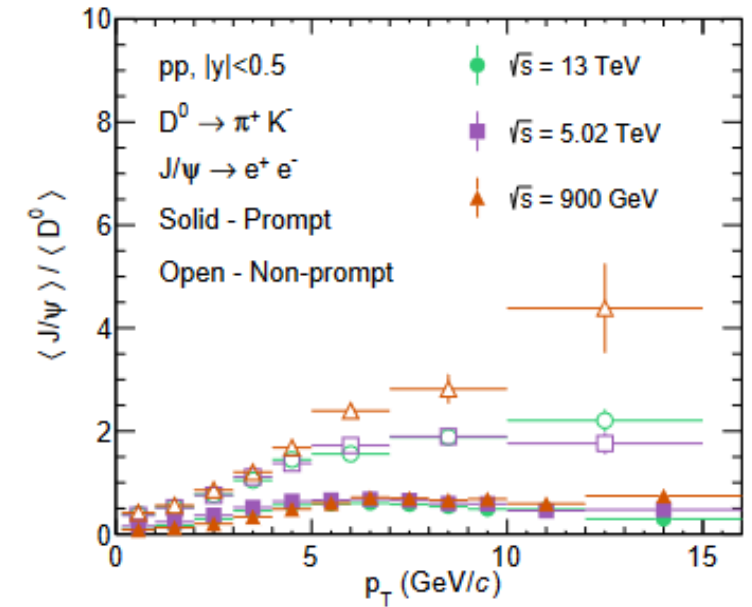


- One can clearly notice the increase in the ratio with increasing  $p_T$  across all the collision energies.
- We observe an **energy-dependent hierarchy** in the ratio.

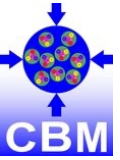
# Results

This ratio tells us about the production dynamics of charmonium state wrt open-charmed hadrons.

- The ratio shows a similar rising trend as a function of  $p_T$ , upto 5 GeV.
- The prompt  $J/\psi$  to  $D^0$  ratio is always less than 1. However, the non-prompt ratio rises above 1, indicating a higher contribution of beauty hadrons towards  $J/\psi$  states.
- For the prompt ratio, there is a slight increase and then it follows a flat trend.
- However, the non-prompt ratio is independent of the charged particle multiplicity.

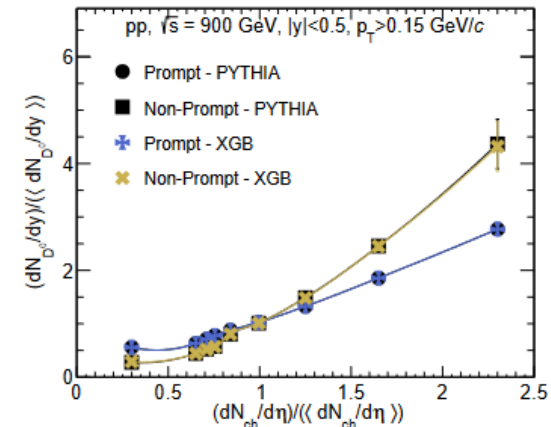
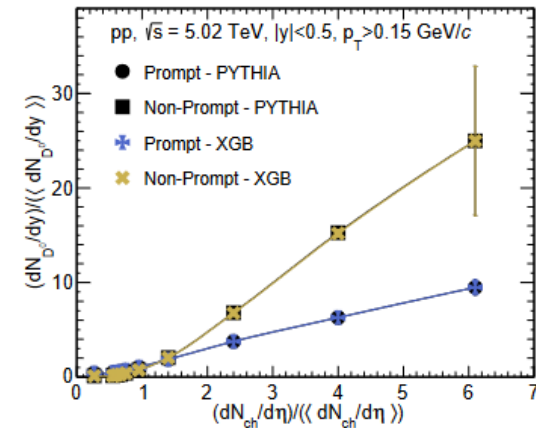
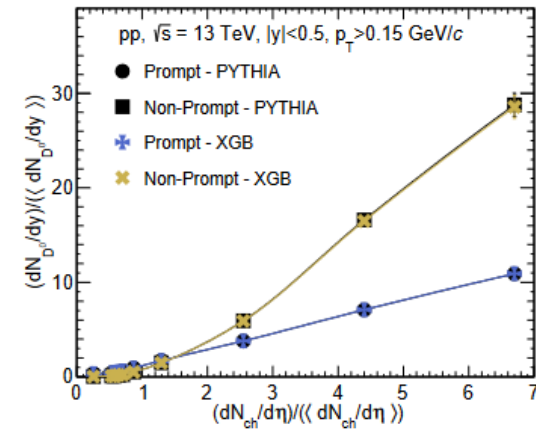






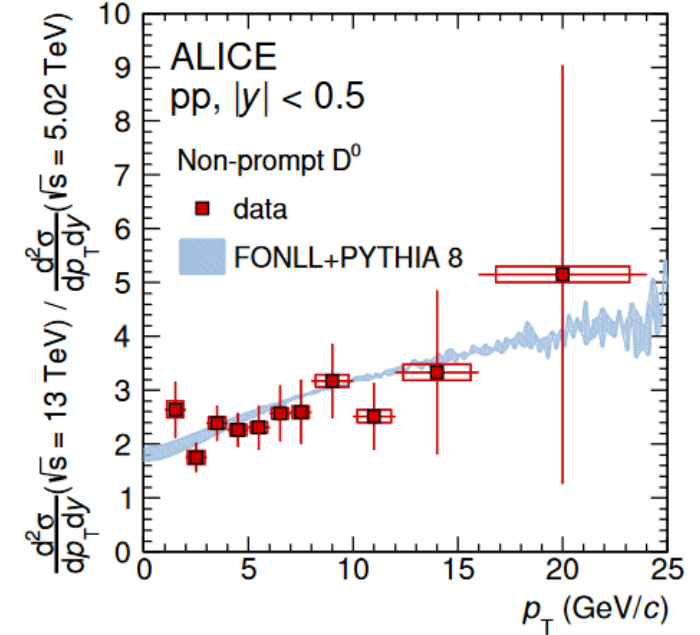
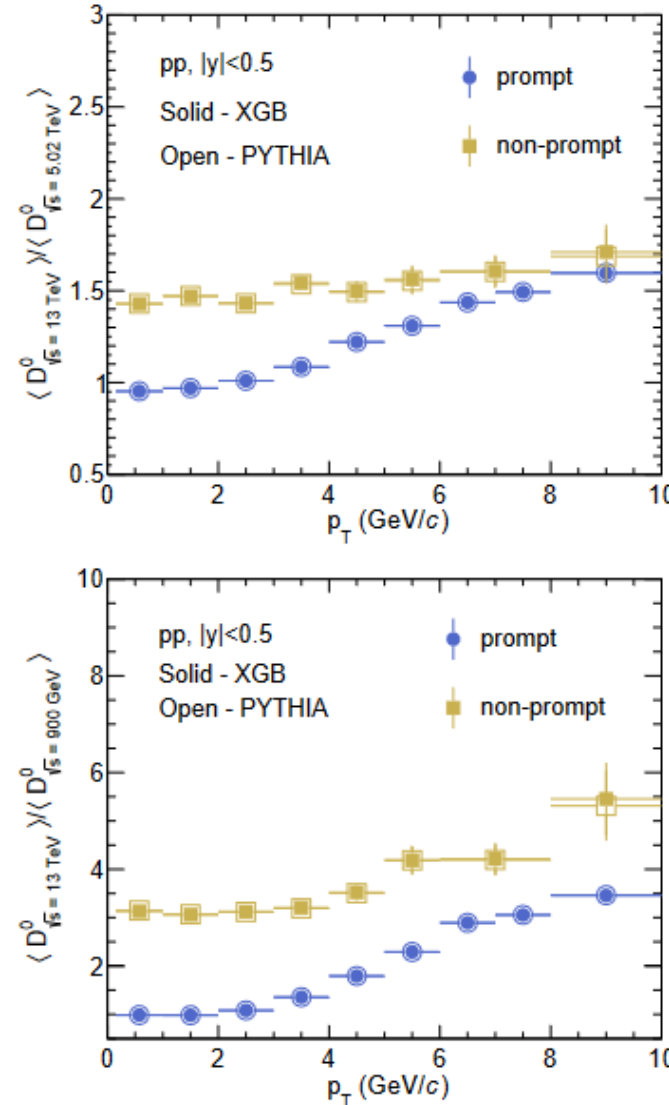
# Results

- Self-normalized yield of prompt and non-prompt  $D^0$  meson as a function of charged particle multiplicity.
- A linear rise can be seen for the prompt  $D^0$  meson.
- A non-linear rise is observed for non-prompt  $D^0$  meson.



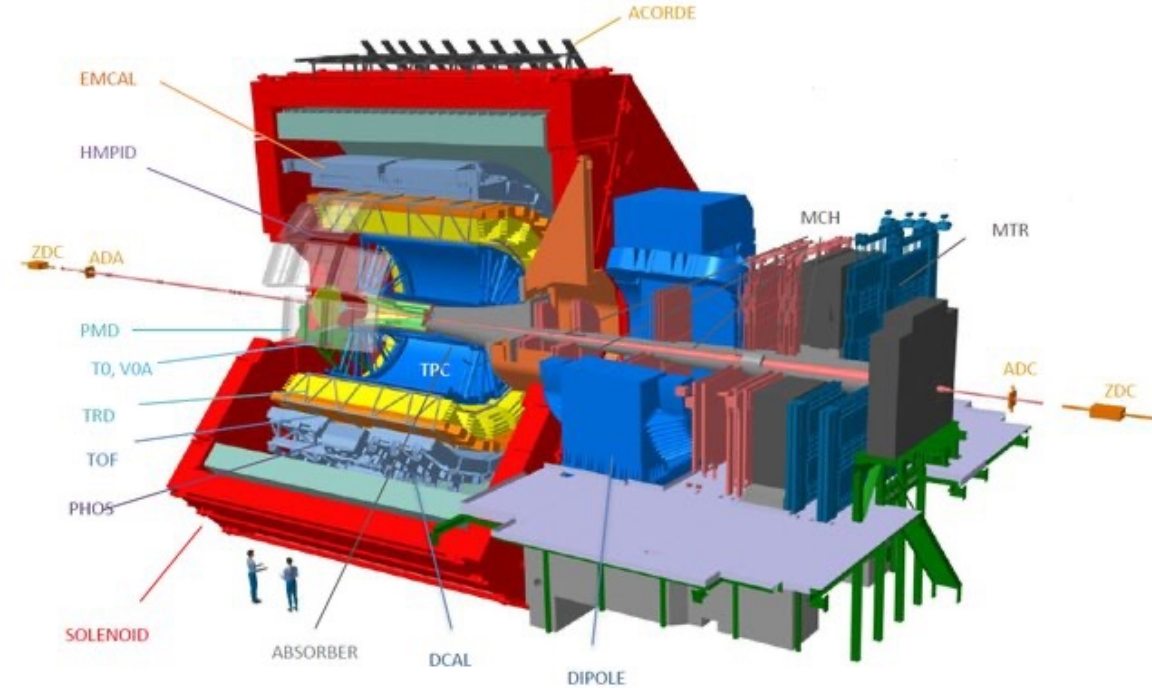
# Results

- ❖ Role of centre-of-mass energy in  $D^0$  meson production.
- ❖ In both plots, a clear increase in the ratio for prompt  $D^0$  meson can be observed.
- In the top panel, a flat trend can be seen for the non-prompt case. Similar results have been observed in ALICE.
- In the bottom panel, the same ratio tends to increase slightly due to the significant difference in energies.
- A higher value of non-prompt ratio indicates more abundant production of beauty hadrons at higher  $\sqrt{s}$ .

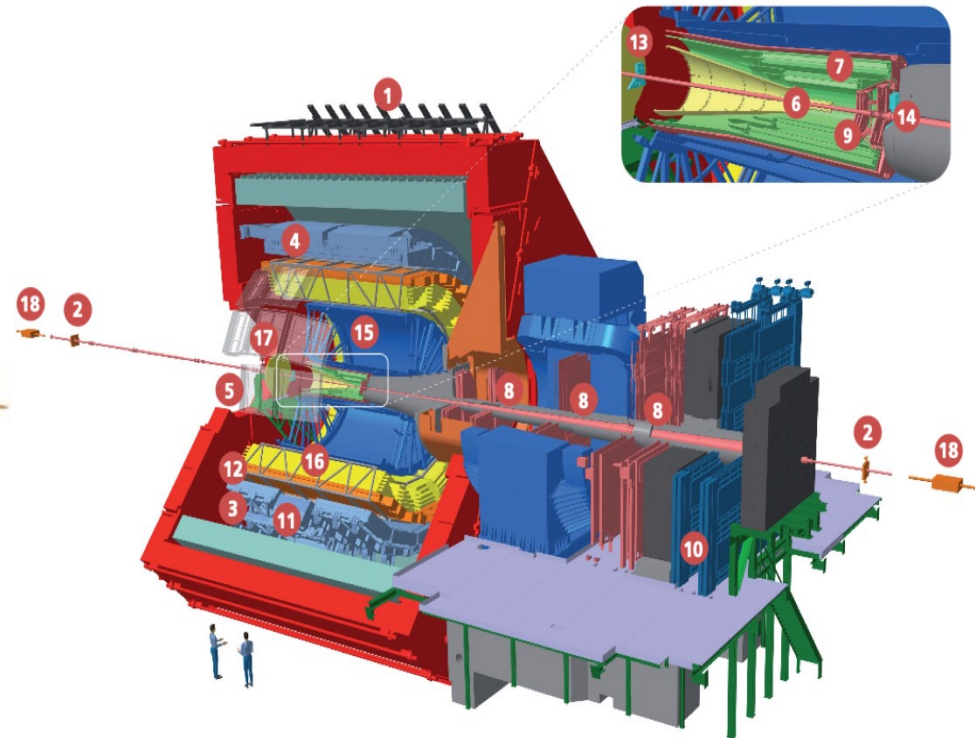


Source: ALICE Collaboration,  
arXiv:2402.16417

ALICE in RUN 3 with Muon Forward Tracker (MFT) will enhance the charmonia measurement Capability while distinguishing prompt vs non-prompt  $J/\psi$ .



ALICE RUN 2 Setup

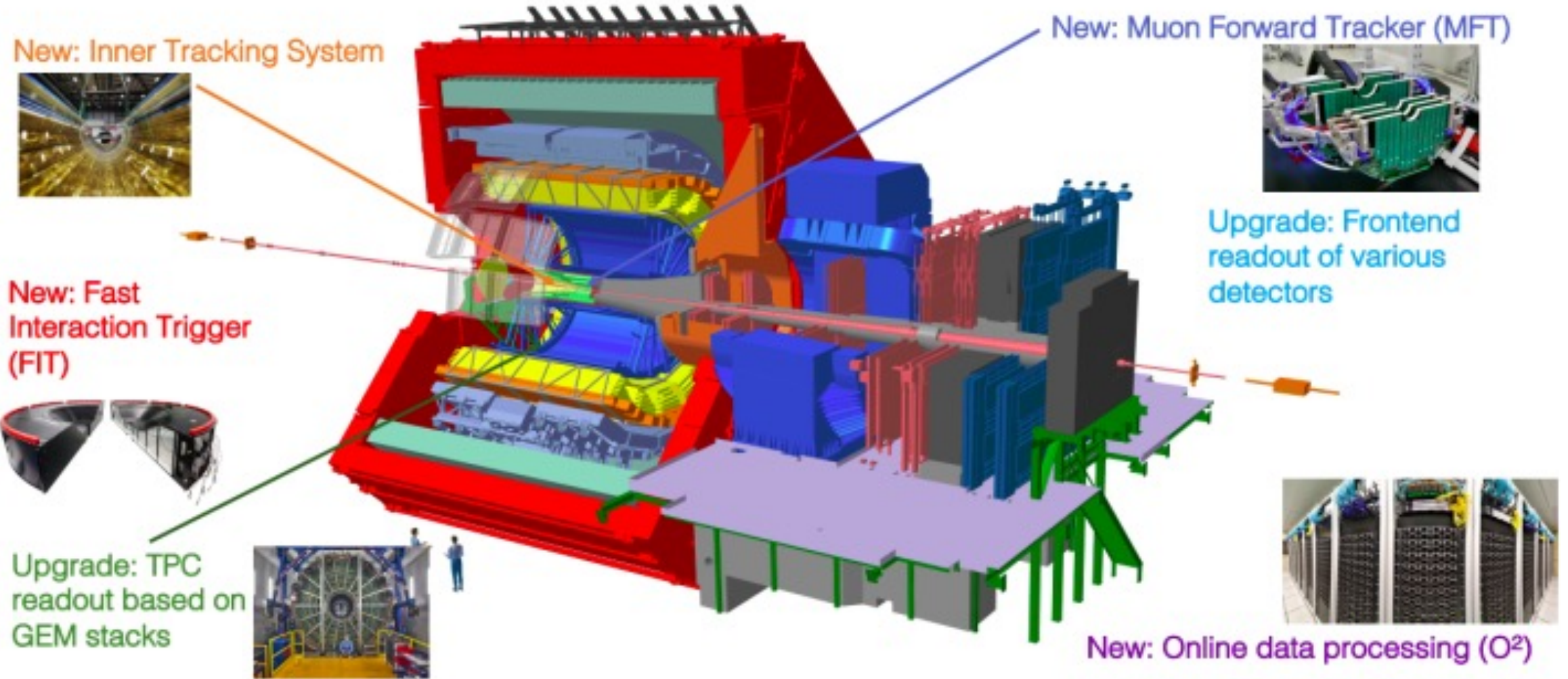


ALICE RUN 3 Setup

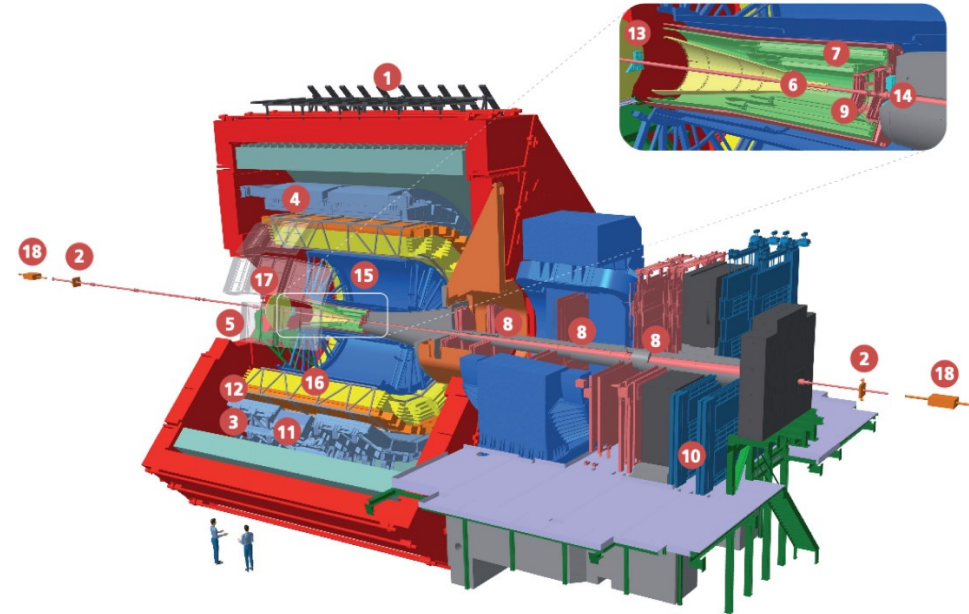
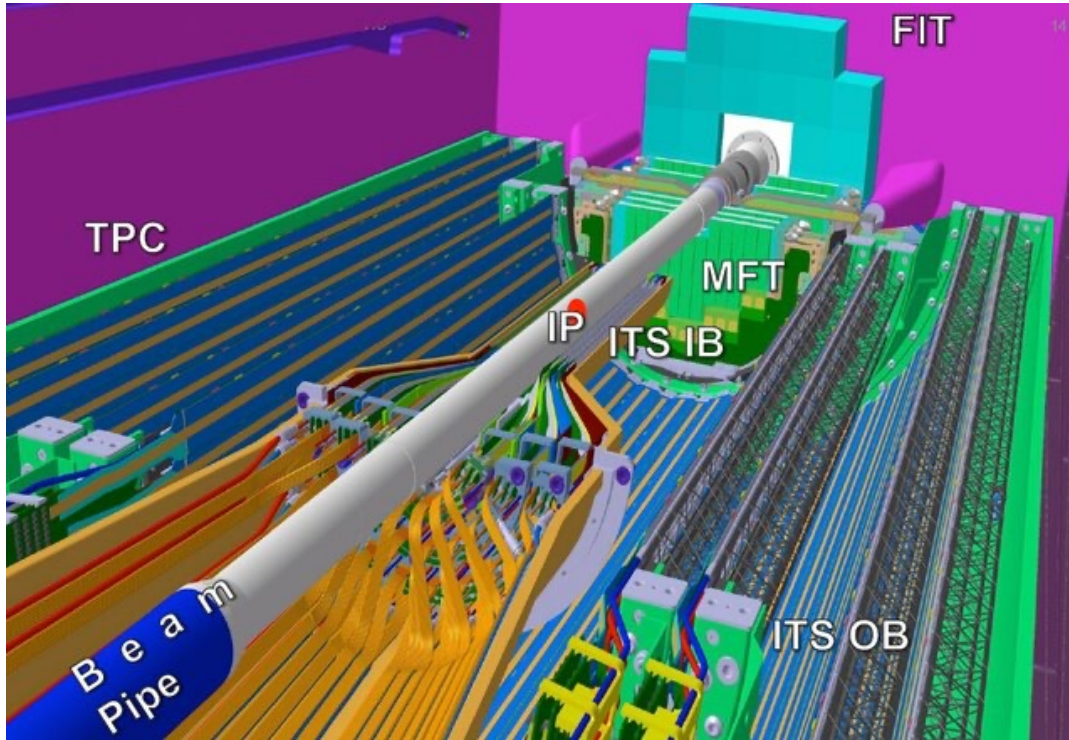
- 1 ACORDE | ALICE Cosmic Rays Detector
- 2 AD | ALICE Diffractive Detector
- 3 DCal | Di-jet Calorimeter
- 4 EMCal | Electromagnetic Calorimeter
- 5 HMPID | High Momentum Particle Identification Detector
- 6 ITS-IB | Inner Tracking System - Inner Barrel
- 7 ITS-OB | Inner Tracking System - Outer Barrel
- 8 MCH | Muon Tracking Chambers
- 9 MFT | Muon Forward Tracker
- 10 MID | Muon Identifier
- 11 PHOS / CPV | Photon Spectrometer
- 12 TOF | Time Of Flight
- 13 T0+A | Tzero + A
- 14 T0+C | Tzero + C
- 15 TPC | Time Projection Chamber
- 16 TRD | Transition Radiation Detector
- 17 V0+ | Vzero + Detector
- 18 ZDC | Zero Degree Calorimeter



# ALICE RUN 3 Upgrades



ALICE in RUN 3 with Muon Forward Tracker (MFT) will enhance the charmonia measurement Capability while distinguishing prompt vs non-prompt  $J/\psi$ .



- 1 ACORDE | ALICE Cosmic Rays Detector
- 2 AD | ALICE Diffractive Detector
- 3 DCal | Di-jet Calorimeter
- 4 EMCal | Electromagnetic Calorimeter
- 5 HMPID | High Momentum Particle Identification Detector
- 6 ITS-IB | Inner Tracking System - Inner Barrel
- 7 ITS-OB | Inner Tracking System - Outer Barrel
- 8 MCH | Muon Tracking Chambers
- 9 MFT | Muon Forward Tracker
- 10 MID | Muon Identifier
- 11 PHOS / CPV | Photon Spectrometer
- 12 TOF | Time Of Flight
- 13 T0+A | Tzero + A
- 14 T0+C | Tzero + C
- 15 TPC | Time Projection Chamber
- 16 TRD | Transition Radiation Detector
- 17 V0+ | Vzero + Detector
- 18 ZDC | Zero Degree Calorimeter

ALICE RUN 3 Setup showing MFT

ALICE RUN 3 and beyond stays interesting given HF measurements at the LHC!



Bon Voyage

Accelerating Science

Accélérateur

*Thank you*